THE HYPERSONIC SHOCK TUBE

Thesis by

Yusuf A. Yoler

In Partial Fulfillment of the Requirements

For the Degree of

Doctor of Philosophy

California Institute of Technology

Pasadena, California

1954

ACKNOWLEDGMENTS

The author wishes to express his sincere appreciation to Dr. H. T. Nagamatsu for his help and encouragement in all phases of the project, and to Prof. L. Lees whose interest and suggestions have been so valuable throughout the course of the research reported in this thesis.

Thanks are due to Mr. C. Bartsch for his help in the construction of the shock tube, to Mr. M. Jessey who designed and built most of the electronic equipment, and to Mr. J. Rabinovicz for his assistance during the experimental phase of the work.

Appreciation is also expressed to Miss N. Waldron for her aid in preparing the manuscript, to Mrs. H. Van Gieson for typing the thesis, and to Miss F. Scheinis and Mrs. M. Wood for preparing the figures.

ABSTRACT

The feasibility of using a shock tube for quantitative investigations of hypersonic flow phenomena at temperatures simulating free flight conditions is studied theoretically and experimentally. In the theoretical part, various aspects of the hypersonic shock tube problem are treated in logical order. Methods of producing high Mach numbers, limitations on the test section Mach number, methods of generating strong shock waves, flows with variable specific heats and dissociation, types of problems amenable to study with the hypersonic shock tube are discussed.

To verify and supplement some of the theoretical results, a shock tube of a somewhat unconventional design has been built. The bulk of the experimental investigations undertaken to date have dealt with pressure studies using piezoelectric gages, and schlieren studies of the flow. The results obtained so far with flow Mach numbers in excess of six, stagnation temperatures up to 9000°R and stagnation pressures up to 200 psi, have not only contributed to a much greater understanding of this relatively new field of application of the shock tube, but have indicated a well defined course along which future investigations will continue.

TABLE OF CONTENTS

LIST OF FIGURES

LIST OF PLATES

SYMBOLS

a	speed of sound, ft./sec.
A	cross sectional area
A_c	cross sectional area of the compression chamber
A_E	cross sectional area of the uniform expansion tube
A_T	cross sectional area at the test section
A^*	cross sectional area at the throat corresponding to M = 1
B	rear of the rarefaction wave
C	mixing zone in the uniform expansion tube
C'	interface in the diverging section
C_I	mixing zone in the intermediate chamber
C_p	specific heat at constant pressure, BTU/lb.-^oR
C_v	specific heat at constant volume, BTU/lb.-^oR
γ	ratio of specific heats, C_p/C_v
e	overall error, per cent
ϵ	experimental error, per cent
F	front of the rarefaction wave
F'	reflected front of the rarefaction wave
G	gain factor
M	Mach number
$M_{(\ )}$	flow Mach number with respect to the <u>local</u> speed of sound
$M_{s(\ )}$	shock wave propagation Mach number with respect to the speed of sound in the flow <u>ahead</u> of the shock front
p	pressure, psi or mm. Hg.
ρ	density, lb./cu. ft.

Re	Reynolds number
R	the shock reflected at the end of the uniform expansion tube
r	the shock reflected from the second diaphragm
s	shock propagating into the intermediate chamber
S	shock wave propagating in the uniform expansion tube
S_1	first shock in the diverging section
S_2	second shock in the diverging section
T	absolute temperature, ^{o}R
t	time, seconds or micro-seconds
u	velocity, ft./sec.
x	space variable along the tube, with origin at the diaphragm section
t_{sc}	duration of flow at the inlet to the diverging section between the shock S and the mixing zone C, μsecs.
$t_{F's}$	duration of flow between the shock S and the reflected front F' of the rarefaction wave, μsecs.
t_{Bs}	duration of flow between the shock S and the rear B of the rarefaction wave, μsecs.

Superscripts

$( )^{*}$	conditions at the throat, corresponding to M = 1

Subscripts

$( )_o$	stagnation conditions
$( )_1$	initial conditions in the expansion chamber (except for S_1)
$( )_2$	properties of the flow between the shock wave S and the mixing zone C (except for S_2)

$( )_{2'}$ properties of the flow behind the reflected shock R before interaction with C

$( )_3$ properties of the uniform flow behind the mixing zone C

$( )_4$ initial conditions in the compression chamber

$( )_I$ initial conditions in the intermediate chamber (except for C_I)

$( )_{II}$ properties of the flow between s and C_I

$( )_{III}$ properties of the uniform flow behind C_I

$( )_{IV}$ properties of the flow behind r before interaction with C_I

$( )_{( )_\infty}$ limiting conditions corresponding to $p_4/p_1 \Rightarrow \infty$

$( )_c$ conditions at the mixing zone c (except for A_c)

$( )_{c'}$ conditions at the interface c'

$( )_{c_I}$ conditions at the mixing zone c_I

$( )_T$ conditions at the test section

$( )_{( )_o}$ optimum conditions

$( )_s$ conditions at the shock front S

$( )_{s_1}$ conditions at the shock front S_1

$( )_{s_2}$ conditions at the shock front S_2

$( )_s$ conditions at the shock front s

$( )_R$ conditions at the reflected shock front R

$( )_r$ conditions at the reflected shock front r

I. INTRODUCTION

The theoretical and experimental work reported herein deals with the feasibility of the use of shock tubes for quantitative investigations of aerodynamic phenomena associated with hypersonic flows at stagnation temperatures simulating the conditions encountered in free flight.

When a body is flying through air at a Mach number of six, the temperatures on some parts of the body may reach three or four thousand degrees Rankine. At these temperatures, air can no longer be treated as a gas with constant specific heats. At even greater speeds, temperatures will be such as to cause dissociation and, later, ionization of air. Scarcely anything more than speculative remarks can be put forth yet as to the possible effects of these conditions on the forces exerted on a body. Other aspects of aerodynamics gaining rapidly in importance are concerned with viscous interaction problems at low Reynolds numbers and rarefied gas flow phenomena.

Although continuous wind tunnels producing highly-uniform flows within a wide range of hypersonic Mach numbers are in existence, one with a stagnation temperature in excess of 1700°R does not exist. For hypersonic flow investigations at low stagnation temperatures, the wind tunnel has no equal. For high stagnation temperatures, however, other techniques must be explored. To date, three methods suggest possibilities:

(1) The ballistic-range (Cf. Refs. 30 and 43)

(2) The free flight of missiles

(3) The shock tube

In the first method, since the model is not stationary, little if any instrumentation can be attached to the model. The measurements are mostly external, and the duration of each test is of the order of a few milliseconds. Although the data and information obtained by the second method are very realistic, the expense involved in this type of experimental work puts it beyond the reach of all but a few investigators.

In view of the serious drawbacks associated with the first two methods, the third, the shock tube, holds encouraging possibilities. As with the ballistic range, the great disadvantage of the shock tube is the extremely-short duration of uniform flow. Unlike in the ballistic range, however, the model is at rest with respect to the earth, and the necessary instrumentation can be attached to it. Another important advantage is the flexibility with which it can be used for studying many types of problems.

Shock tubes have, in the past few years, gained immensely in popularity and importance for studying many special problems arising in diverse fields such as chemistry, physics, fluid dynamics, structures, and cosmology.* For the particular application with which this investigation is concerned, it has become popular to describe the shock tube as "an intermittent wind tunnel of very short duration". This application of the shock tube has been utilized by a number of investigators** in studies which have dealt primarily with unsteady flow phenomena in channels and around models. However, the shock tube has not yet been given the attention it deserves for the quantitative study of aeronautical

---

* Refs. 5, 6, 10, 11, 13, 15, 17, 25, 27, 29, 30, and 32.

** Refs. 5, 6, 11, 12, 13, and a number of U.T.I.A. reports on wave interactions.

problems, and particularly so in the generation of hypersonic flows and studies in this field.

The problem is very challenging: it is proposed to measure a quantity of pressure with sufficient accuracy to distinguish the deviations caused by incremental contributions resulting from viscous effects and/or non-ideal gas conditions, as compared with the corresponding results (theoretical and/or experimental) in flows in which these conditions cannot be produced.

The work reported herein has not answered the problem completely. However, it has not only led to a much better understanding of this relatively new field of application of the shock tube but has shed much valuable light on the course along which future work in this field at GALCIT will continue.

The theoretical and experimental studies undertaken to date are presented in the following four sections in a rather condensed form, in order to prevent the main results and important concepts from getting obscured by a bulk of details. Electronic circuit diagrams, simple equations derivable from well-known relations of fluid dynamics, etc. are omitted. In many instances, the results of the analyses are given with only a brief mention of the method of treatment. The works of other investigators are indicated by references to published papers except in those cases where a brief survey of certain studies reported in the literature has been considered necessary for an understanding of the contents of this thesis.

Following a brief review of the well known ideal theory of uniform shock tubes, Section II presents a study of the methods of producing uniform hypersonic flows in shock tubes with diverging sections. A

comparative analysis of the flows produced by different types of nozzles and the maximum test section Mach numbers associated with each type indicates the necessity for generating strong shock waves. This leads to a study of the various methods of producing strong shock waves. The high temperatures produced in the flow behind a strong shock wave lead, in turn, to the analysis of the effects of variable specific heats, dissociation, and deviations from thermal equilibrium.

It is a well-confirmed fact that the quantitative agreement between theoretical and experimental results becomes increasingly poor for shock tube flows produced by strong shock waves. A survey of the magnitudes and the probable causes of these deviations has led to the conclusion reached in Section III: namely, for hypersonic flow studies of a quantitative nature with a shock tube, the quantities of interest must be measured directly whenever possible. Theory is useful only for rough analyses and for comparative studies between gross effects.

In line with this assertion, the remainder of Section III is devoted to a brief study of the possible types of instrumentation which can be used for studies with a hypersonic shock tube. It is concluded that pressure measurements hold the greatest possibility for fairly accurate quantitative investigations. Finally, in the light of this conclusion, the types of problems which are of current interest and are amenable to study with hypersonic shock tubes are summarized.

The hypersonic shock tube with which the experimental investigations have been carried out is described in Section IV. Since this tube has been constructed for basic studies of an exploratory nature, simplicity and economy in both the structural features and the electronic instrumentation have been a major consideration.

Section V contains outlines of the method of calibration of the various pieces of instrumentation and of the main topics of investigations undertaken to date with the GALCIT hypersonic shock tube. The bulk of the experimental work consists of pressure studies with piezoelectric gages and flow studies by shadow and schlieren techniques.

Finally, the important conclusions drawn from the results of the investigations reported in this thesis are summarized in Section VI.

II. IDEAL SHOCK TUBE THEORY

A. The Uniform Shock Tube

The ideal theory of the uniform shock tube has been treated in great detail by a number of authors (Refs. 2, 3, 4, 5, and 10). This theory, worked out on the basis of experimentally-observed facts, assumes that upon completely and instantaneously removing a diaphragm separating two uniform chambers which may hold, in general, different gases at different temperatures and pressures, a shock wave propagates into the expansion chamber (Cf. Fig. 2) initially at pressure p_1 and a centered rarefaction wave into the compression chamber at pressure p_4, $(p_4/p_1 > 1)$.

The shock wave propagates with the speed $M_s = \frac{u_s}{a_1}$, and behind it starts a flow at Mach number $M_2 = \frac{u_2}{a_2}$, temperature T_2, $(T_2/T_1 > 1)$, and pressure p_2, $(p_2/p_1 > 1)$. The flow behind the shock wave is assumed isentropic.

At the instant of the diaphragm removal, the centered rarefaction wave moves towards the compression chamber at the local speed of sound with respect to the flow. Hence, the front of the wave F moves at the speed a_4 with respect to the fluid at rest, and the rear wave B travels with the speed a_3 with respect to the gas which, at that point, the wave has cooled down to the temperature $T_3 < T_4$ and expanded to the pressure $p_3 < p_4$.

Since, in the one-dimensional flow between the rarefaction wave and the shock wave, there is no mechanism which can support a pressure gradient, $p_2 = p_3$ = constant throughout. Then, assuming that no mixing

takes place at the interface "C", $u_2 = u_3$. All the particles originally in the expansion chamber are heated by the shock wave from T_1 to T_2 whereas the particles originally in the compression chamber are cooled by the expansion wave from T_4 down to T_3. Thus, the plane "C", which originally separated the two chambers and which, after the diaphragm removal, propagates behind the shock wave with particle velocity $u_3 = u_2$, represents a "contact surface", in other words, a temperature and an entropy discontinuity.

It has already been mentioned that the rear, "B", of the rarefaction wave (Cf. Fig. 1) propagates upstream with the local speed of sound a_3 with respect to the flow propagating downstream with particle velocity u_3. Hence, depending on whether $M_3 = u_3/a_3 > 1$ or $M_3 < 1$, the rear of the rarefaction wave moves into the expansion chamber or the compression chamber, respectively.

Now, to formulate the model thus set up, the usual procedure is as follows: although in general the energy equation is not invariant under a Galilean transformation, for particular cases, such as the one-dimensional propagation of a shock wave, the energy equation, as well as the equations of continuity and momentum, is invariant (Ref. 1). Hence, M_S, p_1, and T_1 being given, the stationary shock wave relations, the perfect gas law, and a simple Galilean transformation to let $u_1 = 0$ determine u_2, T_2, p_2 as a function of M_S. Similarly, for a given p_4/p_2, and T_4, the well known relations for an unsteady isentropic expansion wave (Ref. 1) determine the variables in Region 3. Finally, to get a unique relation between p_4/p_1 and M_S, the condition $u_3 = u_2$ and $p_3 = p_2$ is used. Then all other quantities of interest are easily derivable.

For a given gas combination and an initial temperature ratio T_4/T_1, the strength of the shock wave (M_S or p_2/p_1) reaches a finite limit as the initial pressure ratio p_4/p_1 tends to infinity. This limit is

$$M_{s_\infty} = \frac{\gamma_1 + 1}{\gamma_4 - 1} \cdot \frac{a_4}{a_1}$$

For example, if $T_4/T_1 = 1.0$, for N_2 - Air this limit is six; for He - Air it is very close to ten. The Mach number M_2 of the flow in Region 2 similarly tends to a finite value given by

$$M_{2_\infty} = \left[\frac{2}{\gamma_1(\gamma_1 - 1)} \right]^{1/2}$$

independent of M_S. For $\gamma_1 = 7/5$, with air or nitrogen in the expansion chamber, $M_{2_\infty} = 1.89$. For monatomic gases $\gamma_1 = 5/3$, with helium or argon in the expansion chamber, this limit is $M_{2_\infty} = 1.34$. Contrary to the rather severe limitations on the Mach numbers in Region 2, $M_3 = M_2 (a_2/a_3)$ can grow indefinitely, since a_3/a_2 tends to zero as p_4/p_1 tends to infinity.

A real shock tube is necessarily finite; hence, the rarefaction wave and the shock wave eventually get reflected from the two ends of the tube. The duration of testing time is determined by the appearance of such effects in the flow. Most tubes are designed in such a way that the duration of steady flow test time for Region 2 is ended by the arrival of the contact surface at the test section and for Region 3 by the arrival at the test section of either the rear B or the reflected front F' of the rarefaction wave.*

Hence, there are two regions of uniform flow, in either one of

---

* A detailed treatment of this problem can be found in Ref. 7.

which aerodynamic studies can be made. The particular problem under consideration is the generation of hypersonic flows at high stagnation temperatures. The flow behind the shock wave has the desired property of high stagnation temperatures, but in a uniform tube the maximum Mach number which can be obtained in this flow is, for most gases, limited to a rather low supersonic value.

Theoretically, the Mach number of the flow in Region 3 can be made as high as necessary. Whether this is possible to achieve experimentally is still a controversial point (Cf. Refs. 6, 14, and 24). Furthermore, the stagnation temperatures in present day hypersonic wind tunnels are higher than those which could be obtained in this flow unless the gas in the compression chamber is preheated. Moreover, not only is it necessary to preheat the gas in the compression chamber to very high temperatures, but it is an experimental fact that the flow in this region is extremely turbulent and not suited for even qualitative studies at high initial pressure ratios. This subject will be considered in more detail in Section III. The flow in Region 2 suffers from no such drawbacks.

The main reason for the limitation on the Mach number attainable in the flow behind the shock wave in Region 2 is the high speed of sound (i.e., high static temperature). Hence, the Mach number of the flow in Region 2 can be increased if, with a relatively small or no change in the stagnation temperature, some of the thermal energy is converted into kinetic energy. The well known method of accomplishing this is to expand the flow in a nozzle. This leads to the topic treated in the next section.

B. Hypersonic Shock Tubes (Tubes with Diverging Sections)

By expanding the flow in Region 2 in a suitable nozzle, the flow Mach number can be increased. Hence, in this approach, a steady flow of reasonable duration is accumulated in a uniform expansion chamber and then fed into a nozzle. If the flow behind the shock S is supersonic, then a divergent nozzle is necessary. If, however, this flow is subsonic, a convergent-divergent nozzle is required.*

The problem of the establishment of flow following the propagation of a non-stationary shock wave down the nozzle is complicated due to the shock-diffraction at the inlet, the appearance of a second shock wave behind the first, and a region containing both entropy discontinuities and smooth gradients in between. Finally, depending on the type of nozzle design, the steady flow at the test section is either a source flow, as in a simple double wedge nozzle, or uniform parallel flow, as in a Busemann-type nozzle. With each type is associated a maximum test section Mach number which depends on p_o/p_1 (or M_s).

In the following three sections these topics will be treated separately. The general pictures and the notations are illustrated in Figs. 2, 3, and 4.

1. The D-Nozzle Vs. the CD-Nozzle

In Section II.B.3 it is shown that the maximum test section Mach number which can be obtained in the nozzle is determined by the magnitude of p_o/p_1, where p_o is the stagnation pressure of the flow. Hence, a

---

* For convenience, a divergent nozzle will be referred to as a D-nozzle, and a convergent-divergent nozzle as a CD-nozzle (Cf. Figs. 2 and 3).

comparative study of the stagnation conditions produced by a D-nozzle and a CD-nozzle, for identical initial conditions, will now be undertaken.

a. The D-Nozzle

For $M_2 > 1$ the flow in Region 2 is fed into a diverging nozzle for further expansion (Cf. Fig. 2). The duration of steady flow at the test section is determined by the arrival at the test section of the contact surface C. The stagnation conditions of the flow in Region 2 are also the stagnation conditions of the steady flow at the test section if isentropic expansion is assumed. This assumption is probably very closely realized in view of the very great speed of the gas in the nozzle, and the relatively short distance between the inlet to the nozzle and the test section.

b. The CD-Nozzle

If the flow in Region 2 is subsonic, then a CD-nozzle must be used (Cf. Fig. 3). However, the pressure ratio p_o/p_1 in such cases is too low to attain high Mach numbers at the test section (see Section II.B.3). The CD-nozzle can be used to advantage with strong shocks S and $M_2 > 1$ if the subsonic flow behind the reflected shock R is used. For a given set of initial conditions, the stagnation quantities in the Region 2 depend on the area ratio A_E/A^* of the expansion chamber to the throat. However, it is possible to draw upper and lower bounds to the problem. Clearly, the upper bound corresponds to the condition $A_E/A^* = \infty$. Then the problem is essentially that of a normal reflection of a shock wave, and the static conditions in Region 2 are the stagnation

conditions. The lower limit is reached when $M_R = M_2$, since then the reflected shock becomes a stationary shock, and a smaller area ratio makes it move downstream toward the throat.

For these upper and lower limits, the comparisons between a D-nozzle and a CD-nozzle for the stagnation conditions p_o/p_1 and T_o/T_1 and the strength M_{S_1} of the shock* at the inlet to the diverging section are given in Figs. 5 and 6. The interesting result is that at the lower limit, the stagnation conditions produced by the CD-nozzle are almost identical to those for a D-nozzle. At the upper limit, the CD-nozzle produces somewhat larger stagnation conditions, and the gain factor is almost constant for a wide range of M_S.

If the length of the uniform expansion chamber is much greater than the length of the nozzle, then the duration of flow for the two cases is almost the same.

Hence, in view of this analysis, a CD-nozzle seems to be the preferable type. However, certain practical considerations may overbalance the theoretical advantages of the CD-nozzle in favor of the D-nozzle:

(1) If the area ratio A_E/A^* is too small, then considerable time may be required for the formation of the reflected shock R, during which period the flow conditions at the test section will not remain constant.

(2) For large area ratios A_E/A^*, a large uniform expansion chamber is required for a reasonable-sized section at the throat.

(3) Broken diaphragm particles will tend to collect ahead of the throat and may have to be removed before every shot.

---

* For a D-nozzle, at the inlet $M_S = M_{S_1}$.

2. Establishment of the Flow

a. The D-Nozzle

In the uniform expansion chamber the gas in Region 2 flows with the velocity u_2 behind the shock wave S of strength M_S. As the shock wave enters into the diverging section, it is cancelled gradually by expansion waves initiating at the walls. The velocity immediately behind the decaying shock must be less than u_2; but if isentropic supersonic flow in the nozzle is to be ultimately established, then the particle velocity in the nozzle must increase and will tend, in the limit, to $\sqrt{2\, C_p\, T_o}$. The decay of the shock wave and the increase of particle velocity in the isentropic flow behind it are incompatible unless some phenomenon takes place to remove the discrepancy. A study of the static pressures will reveal a similar incompatibility.

It has been observed experimentally, and shown theoretically, that the compatibility is achieved by the appearance of a second shock wave S_2 which "splits" from S_1 at the inlet to the nozzle and faces upstream. Its strength is such as to bring the velocities and pressures in Region T into an agreement with those behind S_1 (Fig. 2).

If there is no discontinuity in the slope of the walls at the inlet, then clearly this second shock will start as an acoustic wave propagating upstream with respect to the flow. Since the flow itself is supersonic, however, this wave will be swept downstream with respect to the walls. As the expansion waves from the walls continuously cancel S_1, the signals reflected from the shock wave form an envelope, the result of which is a gradually-strengthening second shock S_2. If the

walls have a discontinuous slope at the inlet, there will be a Prandtl-Meyer expansion at the corner. Hence, in the close vicinity of the corner, the strength of S_1 must jump discontinuously. The result is that adjacent to the wall, immediately downstream of the expansion fan, there will form a second shock S_2 of finite strength, which will decay to an acoustic wave at the centerline. The necessary consequence of this is the appearance of a contact discontinuity right next to the wall, between S_1 and S_2, and propagating downstream with particle velocity. It is important to note that this contact discontinuity will diffuse out to become a smooth entropy gradient away from the wall and that, in the case of an inlet with no discontinuities in slope, there will be no entropy discontinuities but entropy gradients between the two shocks, the strengths of which are changing continuously.

The cancellation of the first shock wave starts near the walls, where the second shock is the strongest. Hence, the establishment of the flow is described qualitatively, as shown in Fig. 2, with the central portions bulging out. This picture is in agreement with experimentally-observed facts (Cf. Ref. 11).

b. The CD-Nozzle

The qualitative picture for the CD-nozzle is very much the same as that discussed in the previous section, with one exception: when the area ratio A_E/A^* is large, and if it is assumed that a reflected, one-dimensional shock wave R is formed instantaneously, then the strength of S propagating downstream as S_1 will increase discontinuously. Simple calculations will also show that there may be an unsteady expansion (rarefaction) wave starting at the throat, which will interact in some

complicated manner with the steady expansion waves issuing from the walls of the divergent section. Ultimately, however, the picture will be very much the same as before.

3. Maximum Test Section Mach Number

It is clear that as the flow keeps on expanding, S_1 will continuously lose its strength and tend, in the limit, to become an acoustic wave. The second shock S_2, on the other hand, will gain in strength until a point is reached at which $M_T = M_{S_2} = (u_{S_2}/a_T)$. At this point, the second shock will become stationary with respect to the walls, and the test section Mach number will reach a limit. The analytical treatment of this nonlinear, two-dimensional, unsteady flow problem with two shock waves separated by a region of non-isentropic flow is impossible, and its numerical solution impractical.* The flow some distance away from the immediate vicinity of the nozzle inlet may be assumed to be one-dimensional. Even then, the non-isentropic region between the two shocks requires simultaneous analysis in the r-t plane as well as the u-a plane. If, at the expense of much time and labor, an approximate solution is obtained, this may not shed much light on the general problem. Furthermore, for real, viscous flows, it has been observed that the flow separates at the inlet upstream of S_2, and this region is later swept downstream. Steady flow is established only after the two shock waves and the region of separation are swept past the test section (Refs. 11 and 12).

It was felt that considerably more insight into the problem would be gained if, instead of following it in all its details, the

---

* Cf. Refs. 33, 34, 35, 36, 37, and 39.

problem was treated in the limit.

a. The Double-Wedge Nozzle

It is assumed that the simple double-wedge nozzle expands to a very large area ratio or that the nozzle is attached to a huge settling chamber in which the state of the gas is initially identical with that in the expansion chamber. This settling chamber is so large that not only does the inflow of gas through the nozzle cause a negligible change in its pressure and temperature, but it is brought to rest isentropically. Hence, if the flow in Region 2 is of a sufficiently-long duration, the ultimate steady flow will be that of an underexpanded flow in a channel and, beyond a certain expansion ratio, a standing shock must form. The value of the Mach number just ahead of this shock is a function of p_o/p_1. In Fig. 7 the maximum test section Mach number is shown plotted as a function of M_S for air in the expansion chamber.

b. The Busemann Nozzle

In the analysis discussed in the previous section, a great deal of information has been sacrificed. The first shock was completely ignored and assumed to have decayed to an acoustic wave. The second shock S_2 then became the standing shock which determined the maximum test section Mach number attainable for a given p_o/p_1.

To get a rough idea as to the manner in which the transfer of strength from S_1 to S_2 takes place, it is supposed that the flow is finally made parallel by expanding isentropically through a Busemann-type nozzle (Cf. Fig. 4). In the final uniform channel the pressure between the shocks must be constant. Since the strengths M_{S_1} and M_{S_2}

of the two shocks will eventually have reached a constant value, the particle velocity between the two shocks will also have become constant. Then, given the state of the gas in Region 1 and in Region T (from isentropic channel flow relations), the Rankine-Hugoniot relations across the two shocks, and the condition of identical pressure and velocity for the region in between, a system of equations may be set up to determine uniquely M_{S_1} and M_{S_2}. Note that the results are not affected by the manner in which the entropy varies in a small non-isentropic region in the flow between the two shocks; hence, the M_{S_1} and M_{S_2} thus determined must be very realistic. Of course, ignoring the entropy variation makes it impossible to determine the distance between the two shocks, even though their strengths can be accurately predicted. This approach yields more information than the one undertaken in the previous section, but at the expense of increased labor. A complete set of calculations must be carried out for each M_S.

Figure 8 presents the results of calculations for $T_4/T_1 = 1$ and $p_4/p_1 = \infty$ for the two cases He - Air and N_2 - Air. It is seen that with increasing M_T the strength of S_2 is increased until a point is reached where $M_T = M_{S_2}$. The analysis cannot be carried further, since at that point there will ultimately be a standing shock and the maximum value of M_T is reached. Figure 8 indicates that this occurs at $M_T = 6.5$ for N_2 - Air and at $M_T = 7.0$ for He - Air.

For N_2 - Air at $p_4/p_1 = \infty$, $M_{S_\infty} = 6.0$. For He - Air, $M_{S_\infty} = 10.0$. Now, comparing the maximum M_T corresponding to these two values of M_S for a Busemann nozzle with those attainable for the same M_S in a double-wedge nozzle, one important conclusion derivable from the foregoing simple analyses is that the maximum M_T which can be obtained in a double

wedge nozzle is considerably higher than that which can be obtained in a Busemann nozzle. That this is so is evident from the fact that for a given M_T and p_o the pressure behind the standing shock in the double wedge nozzle is less than p_1, since p_1 is the stagnation pressure of the flow behind S_2. On the other hand, for the Busemann nozzle, the pressure behind S_2 must be higher than p_1 since S_1 is finite in strength and the pressure between S_1 and S_2 is constant.

Thus, for a given set of initial conditions the strength of S_2 versus expansion ratio increases faster in a Busemann nozzle. However, the test section flow has the advantage of being parallel instead of source flow. It is important to note that the degree to which the maximum M_T discussed in the last two sections can be realized depends on whether or not the two shocks and the region of separation are swept down the test section before the contact surface C' arrives. This question has been one of the main topics of study in the experimental program reported in Section V. The signals which are reflected from the first shock and which form an envelope at the second shock take a finite amount of time to travel between these shocks. Hence, another interesting question is whether or not the second shock "overshoots" the maximum test section Mach number position and then gradually approaches it from the other side. It is not impossible for a considerable overshoot to take place, allowing, for a short duration, the attainment of Mach numbers higher than the ultimate limiting values.

The foregoing analyses have also made clear the importance of a high p_o/p_1 in obtaining high Mach numbers. An equally important point which makes it desirable to have p_o/p_1 as high as possible is the criterion for accurate pressure measurements, to be treated in detail in Section III.B.2. Since p_o/p_1 is closely related to M_S, it becomes

necessary to consider next the methods of producing strong shock waves.

C. Methods of Producing Strong Shock Waves

A great many methods of producing strong shock waves have been and are still being analyzed and tried experimentally.* This section presents a very brief discussion of the known methods of producing strong shock waves and also suggests a few possibilities not so far treated in the literature.

The methods of producing strong shock waves are the following:

(1) High pressure ratios across the diapgragm

(2) Gas combinations

(3) Mechanical or electrical heating of the compression chamber gas

(4) Combustion or explosion processes

(5) High voltage discharge techniques

(6) Non-uniform tubes

(7) Multiple diaphragms

1. High Pressure Ratios

The use of high pressure ratios across the diaphragm has been the most commonly used method for producing strong shocks. Unfortunately, as the pressure ratio p_4/p_1 is increased, M_s tends asymptotically to a finite value so that beyond a certain range little can be gained by increasing the pressure ratios. Furthermore, the limitations on the sensitivity of the optical apparatus and the pressure gages used for studying the flow make it desirable to operate at high expansion chamber pressures at hypersonic Mach numbers. Hence, the pressure of the compression

* Refs. 10, 22, 25, 28, 29, and 38.

chamber becomes uneconomically and undesirably large.

2. Gas Combinations

For a given initial pressure and temperature ratio across the diaphragm, from the point of view of producing strong shock waves it is desirable to have $a_4/a_1 >> 1$ and $\gamma_4/\gamma_1 < 1$. The influence of the last parameter is of much less importance than the first. It follows that for a uniform tube the main requirement is to have a light gas in the compression chamber and a gas as heavy as possible in the expansion chamber. In this respect hydrogen, helium, and nitrogen have been the most popularly used compression chamber gases. For the expansion chamber many complex gases of high molecular weights have been suggested and tried. Figures 9 to 12 give the comparative studies for a number of gas combinations.

For hypersonic shock tubes, however, the basis on which the merits of performance of expansion chamber gases must be judged is quite different. The value of γ_1, of little consequence in the uniform tube, assumes a great importance. A small change in the value of γ_1 leads to a large change in the amount of expansion required to attain a certain Mach number. Hence, gases with complex molecules are undesirable, unless the phenomenon of dissociation is the main topic of investigation. In the order of desirability, monatomic and diatomic gases are the best. These facts are strikingly illustrated in Fig. 13.

Unfortunately, the most common monatomic gas, helium, when used in the expansion chamber, is too light for the production of strong shock waves. In the order of increasing desirability follow neon, argon,

krypton, and xenon. However, unless the gas is indispensable for the outcome of a certain project, the economical limitations alone rule out the use of all but argon. Argon seems to be an excellent gas for both the uniform and the diverging tube for high temperature, high Mach number work. However, aerodynamics is ultimately interested in air more than in any other gas. If used with a light gas such as helium in the compression chamber, the He - Air combination appears to be quite satisfactory for hypersonic flow applications. Unfortunately, at relatively low temperatures the specific heat of air undergoes marked changes, and at higher temperatures dissociation sets in. Under these extreme conditions it becomes necessary to study the deviations from ideal shock tube flow assumptions. The possibility of a violent reaction has so far made the hydrogen-air combination unpopular, unless the explosion method is utilized on purpose to produce the shock wave.

3. Mechanical or Electrical Heating

The main consequence of this method is to increase a_4/a_1. The relative complexity of the mechanical details and the relatively long heating time which would be required have led to the almost complete abandonment of this method. However, an interesting method of compression and heating which is being planned for an intermittent tunnel is worthy of note (Cf. Ref. 20).

4. Combustion or Explosion Processes

This technique and the method of high voltage discharge are relatively recent in application. Indeed, these are as yet pioneering

projects. The meager data so far published on the shocks produced by the ignition of a combustible mixture in the compression chamber show that very strong shock waves can be produced, but the uncertainty of the initial conditions may cause poor reproducibility. In any case, a decision on the suitability of this technique for a quantitative, reproducible type of studies must wait for further confirmation. The explosion of solid detonants has been tried and recommended for the production of strong shocks in large shock tubes (Cf. Ref. 28). Interesting observations have been reported in Ref. 42.

5. High Voltage Discharge

Among the methods of increasing the internal energy of the compression chamber gas to produce strong shocks, this method holds great promise. The initial conditions are believed to be highly controllable, and hence the flow conditions reproducible. However, the data and information published so far in the literature are extremely meager (Cf. Ref. 22).

6. Non-Uniform Tubes (Refs. 3 and 10)

In a uniform tube the gas in the compression chamber is accelerated from a state of rest to u_3 through an unsteady expansion (rarefaction) wave. If the cross sectional areas of the two uniform chambers are different, then the acceleration will take place partly through a steady isentropic expansion and partly through a rarefaction wave. Since a steady expansion is somewhat more efficient than the expansion through a rarefaction wave, stronger shocks can be produced for a given initial pressure ratio p_4/p_1 when $A_c/A_E > 1$. The "Gain Factor", denoted

by G, will be defined by

$$G = (p_{4_u}/p_{4_N})_{p_1}$$

namely, the compression chamber pressure for a uniform tube divided by that for a non-uniform tube at a given value of p_1. If $A_c/A_E \geq 1$, then $G \geq 1$, and to produce a given M_S, the p_4/p_1 for the uniform tube will be larger than that for a non-uniform tube. Beyond a certain pressure ratio and area ratio, the Mach number at the diaphragm section is unity ($M_3 \geq 1$) and G remains constant. Otherwise ($M_3 < 1$) it varies with p_4/p_1.

Figure 14 shows the values of G as a function of M_S when M_3 is supersonic. In Fig. 15 G is shown plotted versus p_4/p_1 for $M_3 < 1$ for the case $A_c/A_E = 2.80$. A tube of this type with $A_c/A_E = 2.80$ has been used in the experiments to be discussed later in this report.

7. The Multiple-Diaphragm Method

Consider the shock tube shown in Fig. 16. The over-all pressure ratio between the compression and the expansion chambers is p_4/p_1. However, an intermediate chamber at pressure p_I has been inserted between the two. The gases in the three chambers are initially separated by two diaphragms.

When the first diaphragm is exploded, a shock wave of strength M_δ propagates into the intermediate chamber, heating and compressing the gas from state I to state II. The shock wave δ hits the second diaphragm and gets reflected normally. The gas in state II is further heated and compressed to state IV behind the reflected shock "r". The second diaphragm may be exploded by some mechanism which is triggered by δ and after a suitable delay actuates a mechanical, electrical, or

spark discharge unit when the reflected wave "r" reaches a predetermined point. Thus, the final shock S propagating into the expansion chamber is now produced by a shock tube with initial conditions p_{IV}/p_1 and T_{IV}/T_1.

The flow in Region IV is subsonic relative to "r"; hence, following the bursting of the second diaphragm, the rarefaction wave will eventually catch up with "r". As "r" is canceled, the reflections of the rarefaction wave will propagate downstream with the local speeds of sound and will catch up with C, and later with S. The "delay time" for the bursting of the second diaphragm is determined by the desired duration of uniform flow at the test section before the reflected waves arrive. On the other hand, following the break of the first diaphragm, a contact surface C_I propagates downstream and must eventually interact with "r". Depending on the initial conditions, either a shock wave or a rarefaction wave propagates downstream following the interaction. Again, these waves eventually appear at the test section, and this condition determines the necessary length of the intermediate chamber.

Equivalent conditions may be achieved if, instead of delaying the breaking of the second diaphragm, the shock impact is made to break the second diaphragm as soon as the shock hits it, <u>provided</u> that there is a large contraction of area from the intermediate chamber to the expansion chamber. Otherwise, assuming S to be stronger than δ, there will be a simple rarefaction wave issuing from the break of the second diaphragm.

In the following section, only the method in which there is a delay in the breaking of the second diaphragm (or a large contraction

following the automatic break by the impact of δ) will be treated in some detail for the following two reasons:

(1) At high pressure ratios for a given T_4/T_1, M_S tends asymptotically to a limiting value. Hence, at high pressure ratios, large increases in p_4/p_1 produce little gain in M_S. Under these conditions a small increase in T_4/T_1 is advantageous even if a considerable sacrifice is made in p_4/p_1 (Cf. Figs. 17 and 18). For a given p_4/p_1 and T_4/T_1, the double-diaphragm method essentially sacrifices pressure ratio in favor of increased temperature ratio. If $T_4/T_1 = 1$ and if the gases in the three chambers are identical, then always $p_{IV}/p_1 \leq p_4/p_1$ and $T_{IV}/T_1 \geq T_4/T_1$. The net result is that for a given gas combination and over-all initial conditions p_4/p_1 and T_4/T_1 it is possible to produce stronger shocks in the expansion chamber with the double-diaphragm method than with the usual single-diaphragm technique. The results are presented in Figs. 19 to 22, for various gas combinations. In all cases $T_4/T_1 = 1.0$, p_4/p_1 has a given value for each figure, while the variations of M_S with respect to p_I/p_1 are studied. Of course, the case $p_I/p_1 = p_4/p_1$ would correspond to the usual single-diaphragm method. It is interesting to note that for each gas combination and over-all pressure ratio there is an optimum value of p_I/p_1 which will produce the strongest shock "S". For the case Air - Air - Air, this condition occurs when $p_4/p_I = p_I/p_1$ is roughly satisfied.

Another advantage of the method is that since the pressure ratio across each diaphragm is smaller than the over-all pressure ratio, the temperatures behind the contact surfaces may be prevented from reaching the extremely-low theoretical temperatures which are expected in a simple diaphragm tube with the same over-all conditions.* As a matter of fact, these temperatures can be made as high as those behind the shock wave S. This point is considered in the following section.

(2) It has been mentioned previously that, given T_4 and T_1, the rarefaction wave cools the compression chamber gas from T_4 to T_3 in Region 3, whereas the shock wave heats the expansion chamber gas from T_1 to T_2 in Region 2. Furthermore, in Regions 2 and 3 the velocities are identical. Hence, it should be possible to choose T_4 and T_1 so that $T_3 = T_2$, and if the two gases are the same, then $M_2 = M_3$ and $Re_2 = Re_3$. In short, the state of the gas remains uniform throughout the region between the shock front S and the rarefaction wave and, theoretically, no discontinuity appears at the contact zone. Theoretically, this method may be used to increase the duration of test flow with a given length of tube. For air, the initial conditions on T_4/T_1 vs. p_4/p_1 which satisfy the condition $M_2 = M_3$ are shown on Fig. 23.

---

* These very low temperatures behind the contact surface at high pressure ratios with the single-diaphragm tube are reported to have a negligible effect on the flow ahead of the contact surface, (Cf. Ref. 14).

Unfortunately, it is seen that it is necessary to heat the compression chamber gas (or cool the expansion chamber) to a very high value in order to produce strong shocks. To achieve this heating externally is a very difficult problem. The double-diaphragm method, however, accomplishes this heating as a part of the shock tube flow process, and strong shocks can be produced which satisfy the conditions $M_2 = M_3$, $Re_2 = Re_3$. In Figs. 19 to 22, the points indicated by P on each curve give the necessary initial conditions and the strength M_S of the resulting shock wave which will make the states of flow in the Regions 2 and 3 identical, when air is the test medium. The interesting result is that, for all the cases considered, this condition is realized when p_I/p_1 is very nearly equal to 1.0. Hence, for practical purposes it is sufficient to insert a second diaphragm into the expansion chamber and evacuate both sections to the same pressure without detailed calculation. It may be argued that this suggestion is in contradiction to a discussion given earlier, namely, the unsuitability of the highly turbulent flow behind a diaphragm for testing purposes. The double diaphragm method which matches the flows in the Regions 2 and 3 certainly does not eliminate the turbulence in Region 3. However, in hypersonic flow applications, this flow is eventually expanded in a nozzle. It is felt that when the flow is expanded through an area ratio of fifty or more, the existing turbulent fluctuations may tend to decrease to a low level. Although this argument is not conclusive, the method suggested is believed to be worthwhile investigating experimentally.

The very high temperatures which can be produced behind a strong shock wave necessarily lead to the subject treated in the following section.

D. Hypersonic Shock Tube Flow with Variable Specific Heats

1. The Uniform Shock Tube

The shock wave relations for gases with temperature dependent specific heats have undergone considerable theoretical treatment following the fundamental work of Bethe and Teller (Ref. 21).* These relations, as worked out originally, were for a frame of reference stationary with respect to the shock wave. The shock tube relations for a gas with variable specific heats can then be derived by a simple Galilean transformation to make $U_1 = 0$ (Cf. Refs. 8 and 24). Figures 24 to 27 show the state of flow behind the shock wave vs. p_4/p_1 for He - Air and Air - Air with and without the variations in specific heats and dissociation.

For a diatomic gas, or a fluid made up mostly of diatomic gases (such as air), the rotational energy of the molecules is very small compared with the energy required to excite the vibrational modes. Furthermore, the rotational mode can be assumed to have reached thermal equilibrium instantaneously. The vibrational mode, however, requires a much larger number of collisions to reach thermal equilibrium. Hence, for air, the state of the fluid immediately behind the shock wave is very nearly that calculated by assuming $\gamma = 1.4$. As thermal equilibrium is gradually established, the flow variables tend in an exponential manner to the values shown by the dotted curves (Figs. 24 to 27).

For air, dissociation is not important below 5500°R. Furthermore, even for relatively strong shocks ($M_s \approx 7.0$), the relaxation time is of the order of a few milliseconds. Hence, for low hypersonic Mach numbers simulating free flight stagnation temperatures, and for all the experiments that have been undertaken so far on this project,

---

* Considerable data and valuable references on the subject may be found in Ref. 41.

dissociation is not very important. However, because of the high sensitivity of isentropic channel flow conditions to changes in γ_1, the variations of the specific heats must be carefully considered.

In the uniform tube, the pressure ratio and the speed of propagation of the shock wave are little affected by temperature. On the other hand, for strong shock waves, the temperature and density ratios across, and the Mach number in the flow behind, the shock wave deviate considerably from the constant specific heat results.

2. Relaxation Time

The time which it takes for thermal equilibrium to be established in the flow behind the shock wave is known as the relaxation time. The magnitude of this duration can be estimated theoretically, but with the exception of a very few gases, such as oxygen, little accuracy can be expected from the results. This is due to the lack of experimental data on the values of certain parameters (such as the mean free paths). In general, the relaxation time is fairly long at low temperatures but rapidly decreases with increasing temperature.

3. Diverging Section

In view of the uncertainties concerning the relaxation time, one cannot be very sure of the value of γ unless the relaxation time is either very long or very short compared with the duration of uniform flow in the tube. In the diverging nozzle, the decay of the shock wave and the expansion of the flow to lower temperatures take place smoothly and gradually. Hence, it may be reasonable to assume zero relaxation time for this phase of the flow. In other words, the gas is in thermal

equilibrium at all points of the expansion. If this assumption is made, then the nozzle can be divided into a number of sections, and the expansion through each section may be assumed to take place isentropically, with the local value of γ remaining constant within the strip. The procedure in this simple step-by-step numerical method is as follows: Given the state of the fluid at the beginning of a strip, the variables at the end of the strip are calculated by assuming that the γ at the beginning of the strip remains constant. Then, corresponding to the temperature calculated at the end of the strip, a new γ is found. If necessary, an iteration is carried out by assuming the average of the two values of γ. It is found that if the strips are reasonably small, such an iteration is hardly necessary.*

Figures 29 to 31 illustrate the Mach number, pressure, and temperature vs. expansion area ratio for various inlet conditions, with air as the expansion chamber gas. (Note that on these logarithmic plots, all curves become parallel to the $\gamma = 1.4$ curves for temperatures below $500^{\circ}R$.) For conditions easily attainable in the shock tube with shock waves of moderate strength, the results show serious deviations from the corresponding values for $\gamma = 1.4$. For example, with an area ratio $A/A^* = 100$, isentropic expansion with $\gamma = 1.4$ would predict $M_T = 7$, $p^*/p = 2100$, $T^*/T = 9$. For the same inlet conditions, and for the flow initiated by a shock S of strength $M_S = 7.5$, the results with variable specific heats are $M_T = 6$, $p^*/p = 1300$, $T^*/T = 5.3$.

In general, for a given area ratio, the gas with variable specific heats is not cooled and not expanded as much as a gas with constant specific heats. Naturally, for monatomic gases below their ionization temperatures, no such problem exists.

---

* This is not the only method of treating the variable specific heat expansion in the nozzle. Enthalpy charts can be used to treat the problem with equal ease.

III. THE HYPERSONIC SHOCK TUBE PROBLEM

A. Deviations from the Ideal Shock Tube Theory

At low pressure ratios across the diaphragm, the agreement between the theoretical and the experimental results in shock tubes is, indeed, very remarkable. As the pressure ratio is increased and as stronger shock waves are produced, the correlation becomes increasingly poor. These deviations are, no doubt, caused by the violation of the assumptions under which the ideal shock tube theory has been worked out. By treating separately the effects of violating each of these assumptions, it should be possible to formulate theoretically the necessary corrections to the ideal theory when these assumptions are violated singularly or in combination (Cf. Refs. 8, 9, and 24).

Unfortunately, not only are the theories which are aimed at formulating corrections for the non-ideal conditions themselves necessarily idealized to a high degree, but most of the parameters which assume importance at high pressure ratios and with strong shock waves are random in nature. The influence of factors such as the dimensions of the tube, the surface roughness, the geometrical shape of the tube cross section, the diaphragm material, the stress on the diaphragm at the time of rupture, the manner in which it breaks, the initial mixing in the contact zone, separation at the inlet to the divergent section, the degree of realization of one-dimensional, isentropic channel flow in the nozzle, etc., are not amenable to theoretical analysis, even if qualitative estimates can be made concerning the possible effects of such factors.

For hypersonic shock tube applications, the desirability of

producing flows with high p_o/p_1 (hence, high M_s) has already been emphasized and will become more evident later. In order to produce uniform flows of reasonable duration at the test section with strong shocks and at static pressures high enough to permit flow studies, the uniform tube must be relatively long and small in cross section. These conditions aggravate the situation by giving rise to strong viscous effects, bad mixing, and shock wave attenuation.

The resulting deviations from the ideal shock tube flow model are almost too many to enumerate.* Some of the more important effects are the following:

(1) Non-instantaneous formation of the shock wave and the rarefaction wave at the time of diaphragm rupture

(2) A series of Mach reflections and weak rarefaction waves produced during the formation of the shock front

(3) A system of transverse waves trailing behind the shock wave

(4) Shock wave attenuation

(5) Pressure rise behind the shock wave following the sudden jump across it

(6) Luminescence at the shock front and at shock strengths below the theoretically-expected ionization temperatures

(7) Bad mixing at the contact zone, and the increase of the speed of the contact front beyond the theoretically expected values

(8) Sharp, monotonic increase of pressure behind the contact surface, instead of the constant state of pressure

(9) Condensation and the generally bad flow conditions behind the contact surface

---

* Refs. 6, 11, 15, 16, 19, 22, and 24.

(10) Uncertainties involved in the assumption of one-dimensional, isentropic expansion in the nozzle

The severity of the contributions due to such deviations from the ideal shock tube flow model is open to argument. It is felt that the results may vary a great deal from one tube to another. In any case, one cannot, for quantitative studies, assume that the conditions at the test section will be those calculated on the basis of the methods discussed in Part II, unless this fact is first verified experimentally. A pessimistic view is taken on the generality and the accuracy with which these theories can be used for quantitative purposes. Moreover, the very nature of the hypersonic flow problems which permit any justification for the use of the shock tube instead of the wind tunnel for quantitative investigations is such that theoretical analyses are usually very difficult. Hence, instrumentation must be developed which will make possible the direct measurement of the variables necessary for the study of such problems.

In this thesis, the stand taken on the hypersonic shock tube problem is the following: The shock tube theory is very valuable for the rough analysis of gross effects, for comparative purposes, and for rough calculations of the expected state of the flow in the various regions of the tube. Each tube must be calibrated individually. The important variables of a particular problem must be measured directly whenever possible or calculated from other quantities which have been measured directly.

With this approach to the problem, it becomes necessary to review the possible methods of measuring the flow variables in a shock tube.

B. Quantitative Investigations with a Hypersonic Shock Tube

In the hypersonic shock tube the ultimate interest lies in the study of a hypersonic flow problem associated with the flow around a model at the test section. Hence, the best approach to the problem would be to measure directly, if possible, the state of the free-stream flow at the test section and around the model. Unfortunately, the flow stagnation pressures which can be obtained in a shock tube have somewhat restricted practical and theoretical limits. Moreover, some of the instruments most suited for measurements in very highly transient flows depend not on absolute values but on their ratios for accurate measurements.

At high Mach numbers, with shock waves the strengths of which are limited to those which can be produced without great difficulty, the test section static free stream pressures and densities become very low. Although very small quantities can be measured in a wind tunnel or a blow-down tunnel, such is not the case for the highly-transient shock tubes flows. Fast response techniques such as interferometry, spectrophotography, ultrasonic waves, piezoelectric gages, and hot wires have definite lower limits below which they cannot be used to yield reliable data. At high Mach numbers these limits may be approached and surpassed. It then becomes necessary to look into the possibility of deriving the test section variables from measurements made elsewhere in the tube where conditions are more favorable.

The best place for such measurements is the immediate vicinity of the entrance into the diverging section. For most tubes the distance from the inlet to the test section in the nozzle will be very short, a

few feet at the most, certainly much smaller than the length of the uniform tube if a reasonably long duration of steady flow is to be produced. In the nozzle, because of the large expansion required to attain high Mach numbers, irregularities such as turbulence will smooth out, and the boundary layer effects will become less serious. Moreover, a simple method of bleeding the boundary layer at the inlet to the nozzle and starting a fresh flow at the throat has been tried and found successful.*

For strong shock waves, the quantities such as pressure, density, and temperature can be measured at the inlet to the divergent nozzle. Hence, if, in addition to there being a fairly-accurate knowledge of the inlet conditions, the performance of the nozzle is determined, the test section conditions may be calculated with a degree of accuracy sufficient for certain problems, which are to be discussed later.

Finally, it would be worthwhile to consider the existence of interesting hypersonic problems for which a very accurate knowledge of the free stream conditions is not absolutely necessary. These topics will now be treated in some detail in the following sections.

1. Instrumentation

In order to determine the state of the uniform flow at any point in the shock tube, it is necessary to determine, with the highest possible accuracy, two independent flow variables and the Mach number. In the following paragraphs, the possible methods of measurement are discussed very briefly for the following quantities:

---

* This method is discussed in detail in Sections V and IV.

(1) Temperature

(2) Density

(3) Pressure

(4) Velocity

(5) Speed of Sound

(6) Mach Number

It is by no means implied that the techniques considered below are the only possible ones, although it is believed that the list is fairly representative of the present field of shock tube instrumentation.

a. Temperature

The measurement of temperatures may be accomplished by the following devices:

(1) Thermocouples

(2) Spectrometers

(3) Radiation Transducers

Very fine thermocouples with response times below 100 microseconds can be developed.* Although the response time is fast enough for shock tube work, the temperature limitations on these instruments are as yet too low (below 1000°F) to make them useful for hypersonic shock tube work at high temperatures.

Temperature measurements with spectrophotometers of high resolution has been shown to be possible when the gas is highly luminescent (Refs. 29, 30, and 42). For temperatures at which the luminescence is faint, multiple exposures can be taken. For even lower

---

* Such thermocouples are reported to have been developed by the Midwest Research Institute in Kansas City, Missouri.

temperatures, it becomes necessary to use a foreign additive, such as iron carbonyl . A small film of this liquid spread on the wall of the tube becomes luminescent at much lower temperatures when the shock wave passes over it. Then the shift of the iron bands may be measured. However, because of the small shift, the accuracy becomes poor at low temperatures.

Shock waves of sufficient strength to cause intense luminescence in air are difficult to produce although the spectrometric method may be used to advantage with a gas such as argon in the expansion chamber. Ordinary glass absorbs considerable ultraviolet light, and it may be necessary to use quartz windows and quartz lenses.

The last method to be considered here consists simply of using a photomultiplier to sense the radiation from the flow. This method has been tried successfully for measuring the duration and the intensity of luminescence (Cf. Refs. 10 and 25).

For quantitative work, some method of calibration is necessary to correlate the intensity with the temperature. Again, for air the luminescence is too low for the successful application of this method. However, water vapor radiates considerable infrared light, and it may be possible to pick up the radiations by means of an infrared sensitive photomultiplier. Ordinary glass absorbs infrared radiation as well; hence, salt crystals, instead of plain glass windows, have been used for infrared transmission. Unfortunately, in all of the above methods, the measured temperature is an average value across the width of the tube.

b. Density

At the present time, the interferometer is believed to be the only instrument which is suitable for density studies in the shock tube. However, the measured density is again an average, rather than a local, quantity. Assuming the use of mercury green light, with the expansion chamber initially at room temperature and the density jump across the shock wave between four and six, the shift across the shock wave will be three to four fringes, per psi initial pressure in the expansion chamber, per inch of width of flow. Hence, for hypersonic shock tube work the usefulness of the interferometer at the test section is limited to very strong shock waves. At the entrance to the nozzle, however, the density may be measured to $\pm 10\%$ accuracy for shock waves which can be produced without difficulty. (For a new technique, see Ref. 46.)

c. Flow Velocity

Two methods have so far been reported in the literature. The first is the hot-wire (Cf. Ref. 23), which, although holding promise for weak shock waves and low pressure ratios across the diaphragm, is certainly out of question for hypersonic shock tube work. The high temperatures involved and the great damage done by broken diaphragm particles are alone sufficient reasons to justify this statement.

The second technique is the photographic determination of the streamwise speed of propagation of weak disturbances produced in the flow behind the shock wave. These sonic disturbances have, in the past, been produced by the following techniques:

(1) A piece of scotch tape or thin metallic foil spanning one wall of the tube (Ref. 13)

(2) A weak spark discharge from one wall (Ref. 9)

(3) A narrow stream of ultrasonic waves produced by a piezo-electric crystal spanning flush one wall of the tube (Ref. 31).

All of these methods depend on either schlieren or shadow photography of the weak disturbance, which limits their use to relatively-high densities. With the static pressures and temperatures encountered in hypersonic shock tube work, the chances of utilizing these techniques are slight. Moreover, three-dimensional effects, boundary layers, wave diffraction, turbulence, etc. have reportedly restricted the usefulness of these methods very seriously, even at high densities. In some cases, attempts have been reported as "singularly unsuccessful" (Ref. 9).

Finally, for the sake of completeness, glow anemometry may be mentioned (Ref. 44). Unfortunately, this technique is sensitive not only to velocity, but pressure, density, and other mechanical details as well. A practical method of calibrating the instrument for use in supersonic flows has not yet been developed. The usefulness of glow anemometry in hypersonic shock tube work is believed to be extremely limited.

d. Sound Velocity

One possible method of deducing the temperature is to measure the speed of propagation of a very weak disturbance normal to the direction of flow. However, the techniques used are identical to the ones considered in the previous section and suffer from the same limitations.

e. Mach Number

One of the two methods used so far for determining the flow Mach number in a shock tube is to measure the wave angle caused by a disturbance placed in the flow. In order that the wave be well defined and not distorted by turbulent fluctuations, it is desirable to make it relatively strong. The disturbances used are either wedges or cones of known geometry.

If a two-dimensional model (i.e., a wedge) is used, then it must span the tunnel with close tolerance since gaps at the ends may tend to change the wave angles considerably. The interaction of the boundary layers on the side walls with the shock wave from the leading edge may also introduce errors (Cf. Ref. 9). A simple method of eliminating this interaction is to use a cone instead of a wedge, with the base at sufficient clearance from the walls. The magnitude of the effects caused by the growth of boundary layer on the cone itself can be determined by using widely-different cone angles. It is believed that the boundary layer on the cone will change the wave angle by a negligible amount. The other method is to determine the angle of detachment of the shock wave and, for low supersonic flows, the distance from the tip of the model to the detached shock (Refs. 5 and 45).

Unfortunately, at high flow Mach numbers, the Mach number is extremely sensitive to small errors in either the angle of attack or the measured wave angles; hence, the accuracy of the Mach number measured by this method becomes very poor at hypersonic Mach numbers. The angle of detachment suffers from a similar drawback. Thus, the measurement of the Mach number by these methods must be limited to supersonic

regimes ($M \leq 4$). It is gratifying that the Mach number corresponding to a given wave angle is very insensitive to γ ; hence, supersonic Mach numbers can be measured with accuracy without a knowledge of the flow temperature, even for gases with variable specific heats. In fact, this suggests a possibility for determining the temperature in a gas with variable specific heats: The pressure ratio (the static pressure on a wedge divided by the free stream static pressure) is somewhat sensitive to γ, whereas the wave angle is not. Assuming that pressures can be measured with great accuracy, the simultaneous measurement of the pressure ratio and the wave angle determines γ , and hence the temperature. Practically, this method is almost impossible since a small change in γ (and consequently in the pressure ratio) corresponds to a relatively very large change in temperature. Thus, a small experimental error leads to a large error in temperature.

If nothing else, the brief survey given above has served to illustrate the difficulties associated with the use of any of the instruments listed so far in the test section of a hypersonic shock tube, although most of them should perform satisfactorily at the inlet to the nozzle. Hence, unless extremely strong shock waves are produced, these measurements can be made only at or near the inlet to the nozzle. It appears that the most feasible method of determining the test section conditions is to survey the nozzle performance to enable the extension of the measurements made at the nozzle inlet to the test section. Pressure is the one quantity which is sensitive enough to the changes in Mach number and which can be measured with sufficient accuracy to make the realization of such a program possible. The study presented in the next section will reveal some interesting and rather unexpected

criteria which must be satisfied if accurate pressure studies are hoped for. In view of the great importance of pressure studies, the problem will be considered at considerable length in the next section.

2. Pressure Studies

As a fair analysis of the experiments reported in Section IV is difficult without a clear understanding of the principles presented in this section, the problem of pressure measurement is treated here in considerable detail.

For shock tube work, the desirable properties of a pressure gage are as follows:

(1) Fast response

(2) High output

(3) Linearity

(4) Sufficient damping

Linearity is almost essential since otherwise the task of data reduction becomes unduly complicated. In general, the faster the response, the lower the output.* Damping further tends to reduce the sensitivity. For certain problems it may be sufficient to use a gage fast enough only with respect to the duration of test flow.

To date, the common types of pressure gages which satisfy these requirements are: (1) High-frequency metallic membranes stretched flush on a wall; (2) Metallic tubes constructed so as to twist when the pressure in the tube fluctuates by a small amount; (3) Piezoelectric gages.

The minute changes in the amplitudes, caused by small pressure

---

* It is assumed that the input is not a periodic function of high frequency, since such is rarely the case in the shock tube.

variations, of the metallic membranes or tubes are converted to electrical outputs by (1) Changes in resistance; (2) Changes in reactance; (3) Changes in inductance of a unit attached to the pressure sensing element. The most common example of the first type is a strain gage attached to a membrane (Ref. 28). Various companies have developed gages which make use of the last two methods. In all these cases, the output is amplified at a bridge circuit, then fed into a scope. The known voltage amplitudes on the scope can then be calibrated to yield the corresponding pressure differences on the gage.

In the case of piezoelectric gages, the charge put out by the crystal is proportional to the deformation of the crystal. If the load on the crystal has a very high input impedance, then the amplified voltage, which is eventually traced on the scope, gives a faithful reproduction of the deformation. Hence, the principle of measurement with all the gages is the same: A voltage proportional to a deformation is photographed on a scope. If the gage is linear, the deformation, hence the voltage, is proportional to the pressure difference on the gage.

In the shock tube, the "reference pressure" (the zero amplitude sweep on the scope) corresponds to p_1, the initial expansion chamber pressure. It is important to keep in mind the fact that all the other pressures in the transient shock tube flow are measured with respect to this pressure. With this assumption, a simple error analysis will now be made.

Consider an arbitrary trace on the scope corresponding to a proportional pressure fluctuation in the shock tube.

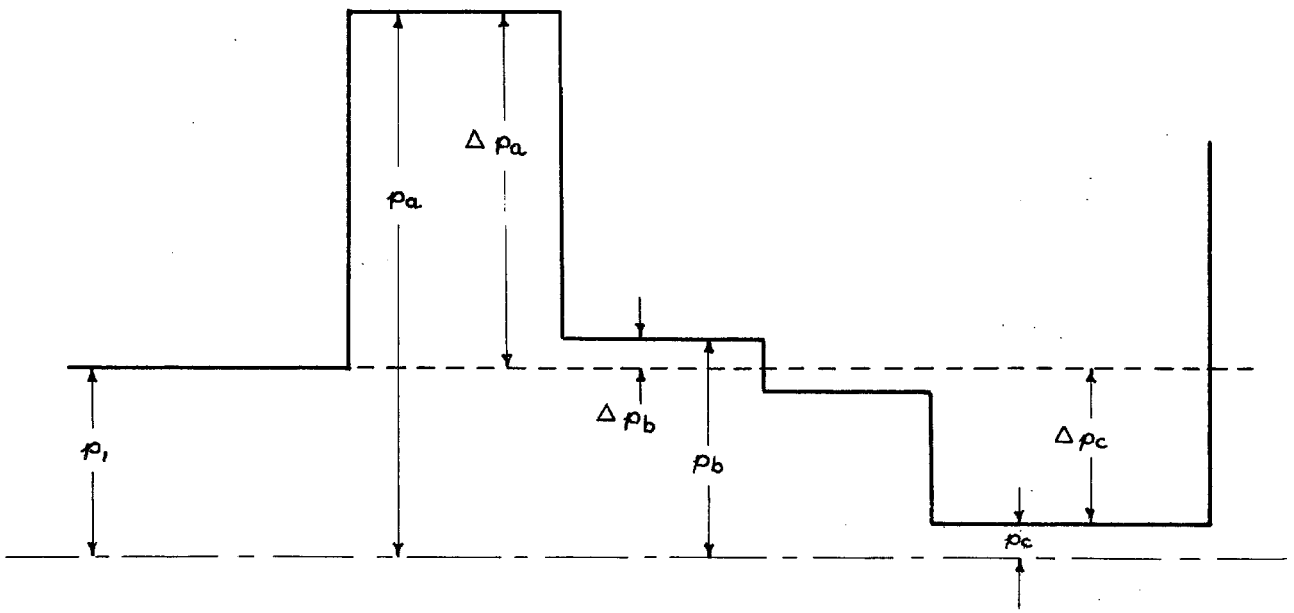

From the point of view of error analysis, the three conditions of interest are:*

(a) $\frac{\Delta p}{p_1} >> 1$

(b) $\frac{|\Delta p|}{p_1} << 1$

(c) $\frac{\Delta p}{p_1} = -1 + \alpha \qquad (\alpha \to 0)$

The first case occurs behind a strong shock in the uniform section. The last case occurs in the uniform flow at the test section at high Mach numbers.

The "experimental error" will be defined as the combined error due to the uncertainties in the calibration of the pressure gage, the scope

---

* Δp is assumed positive for $\frac{p}{p_1} \geq 1$

amplitude calibration, insufficient time constants or parasitic leaks in the electronic circuits, the errors in measuring the scope trace on the photographic film, noise, drift in the electronic apparatus, and similar effects. It is now proposed to show that the final over-all error "e" made in the determination of the quantity of interest, namely, p/p_1 or p_1/p, is not necessarily equal to the experimental error, "ϵ".

Let Δp = Actual pressure difference on the gage

$\Delta p' = \Delta p(1 \pm \epsilon)$ = measured pressure difference

ϵ = Experimental error in per cent of Δp

Case A

$$\frac{\Delta p_a}{p_1} >> 1 \qquad (\Delta p_a \approx p_a)$$

$$p_a'/p_1 = \frac{\Delta p_a(1 \pm \epsilon) + p_1}{p_1} = \frac{p_a \pm \epsilon \Delta p_a}{p_1}$$

$$1 \pm e = \frac{p_a'/p_1}{p_a/p_1} = 1 \pm \epsilon \frac{\Delta p_a}{p_a} \approx 1 \pm \epsilon$$

As $\Delta p/p_1$ tends to infinity, the over-all error tends to the experimental error.

Case B

$$\frac{|\Delta p_b|}{p_1} << 1 \qquad (p_b \approx p_1)$$

$$\frac{p_b'/p_1}{p_b/p_1} = 1 \pm \epsilon \frac{|\Delta p_b|}{p_b} = 1 \pm \epsilon\alpha = 1 \pm O(\eta^2)$$

where ϵ, α, and η are small quantities with respect to unity. Hence, as $|\Delta p|/p_1$ tends to zero, over-all error tends to a small quantity of the second order.

Case C

$$\frac{\Delta p_c}{p_1} = -1 + \alpha \qquad (0 < \alpha << 1)$$

$$\frac{p_c'/p_1}{p_c/p_1} = 1 \pm \epsilon \frac{\Delta p_c}{p_c} = 1 \mp (1-\alpha)\epsilon \frac{p_1}{p_c}$$

$$p_c'/p_c \approx 1 \mp \epsilon \frac{p_1}{p_c}$$

but $$\frac{p_1}{p_c} >> 1$$

As $\Delta p/p_1$ tends to (-1), the over-all error tends to infinity.

The validity of these conclusions is illustrated by the following numerical examples:

Suppose $\epsilon = \pm 10\%$.

Consider the initial conditions N_2 - Air with $p_4/p_1 = 10{,}000$ and $T_4/T_1 = 1.0$. For simplicity, assume the ideal theory is valid. Consider a test section Mach number $M_T = 7.0$. Then

$$p_T/p_o = 242 \times 10^{-6}$$
$$p_1/p_o = 1/61.4$$
$$p_1/p_T = 67.3$$
$$\Delta p' = (p_1 - p_T)(1 \pm .1)$$
$$\therefore \quad 59.7\, p_T \leq p_1 - p_T' \leq 73.0\, p_T$$
$$-.086 \leq p_T'/p_1 \leq .112$$

whereas

$$p_T/p_1 = .0149$$

Thus, in this case, with only a 10% experimental error, the calculated p_T/p_1 can be as high as 7.5 times its true value $(1 + \epsilon\, p_1/p_T)$ or one gets the absurd result of negative pressure ratios $(1 - \epsilon\, p_1/p_T)$.

Consider now another case with He - Air at $p_4/p_1 = 13500$, $T_4/T_1 = 1.0$. Let $M_T = 5$. Then

$$p_T/p_o = 190 \times 10^{-5}$$
$$p_1/p_o = 1/303$$
$$p_1/p_T = 1.74$$
$$.53 \leq p_T'/p_1 \leq .618$$

whereas

$$p_T/p_1 = .575$$

Hence now, corresponding to a 10% experimental error, the maximum over-all error is 8%. The improvement of the accuracy over the previous case is evident.

3. Nozzle Performance

The results of the foregoing analysis will now be tied into the general hypersonic shock tube problem. Given the initial conditions (i.e., the gas combination, pressure ratio, temperature ratio) the values of M_S, M_2, p_2/p_1 (hence p_o/p_1) can be determined by direct measurements within experimental error. Next, for a desired Mach number M_T, p_T/p_o and hence p_T/p_1 depend on p_o/p_1 (since γ is known for the given gas); but the analysis just carried out indicates that the over-all error depends on p_T/p_1. Hence, raising the absolute value of p_1 or of p_o is of little help as far as the error is concerned. The error analysis has indicated roughly the manner in which the over-all error varies as a

function of p_T/p_1. Given the initial conditions (or M_S and γ), reliable pressure studies in the nozzle can be carried out only up to a Mach number $M_T \leq M_{o_T}$, where M_{o_T} (the optimum Mach number) corresponds to $p_T/p_1 = 1.0$.

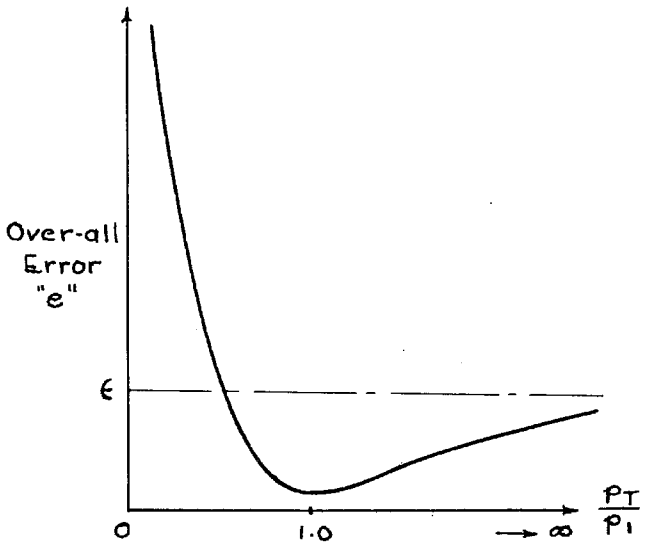

In Figs. 32 and 33, M_{o_T} is shown plotted against M_S for the cases $\gamma_1 = 7/5$ and $\gamma_1 = 5/3$ on the basis of ideal theory. The dependence on temperature of the specific heats of all gases, except the monatomic gases below their ionization temperatures, makes them undesirable for the purpose of determining the nozzle performance.

Hence, the following procedure may be suggested: A monatomic gas suitable for the production of strong shock waves in the uniform tube is to be used as the "standard gas" for the determination of nozzle performance. If, then, the results of the pressure studies along the nozzle with this gas are found to be in agreement with the corresponding one-dimensional, isentropic channel flow relations, the same conclusion might be assumed to hold for other gases. From previous arguments, the most practical gas combination which fulfills the desired requirements seems to be He - A, but even with this combination the accuracy limits are reached at around $M_T = 5$ for shock waves which can be produced within practical limits.

However, one need not necessarily depend on static free stream

pressures for nozzle survey. Although less sensitive than p_1/p_o to changes in Mach number, p_{T_o}'/p_o (where p_{T_o}' is the Rayleigh-Pitot total head) is amply sensitive for survey purposes. With this quantity, very high free stream Mach numbers can be surveyed within the accuracy criteria for pressure gages. p_{T_o}' can be measured by mounting the gage on a sphere or cylinder normal to the flow. Figure 35 shows the optimum Mach numbers, M_{o_T}', which correspond to $p_{T_o}'/p_1 = 1$, plotted against M_S for $\gamma_1 = 7/5$ and $\gamma_1 = 5/3$. The difference between M_{o_T} and M_{o_T}' for a given M_S is quite remarkable. For a monatomic gas, the Mach numbers ($M_T \geq 5$) can probably be most satisfactorily determined by total head survey. Figure 34 shows the variation of p_o/p_{T_o}' versus M_T for $\gamma_1 = 5/3$ and $\gamma_1 = 7/5$.

4. Problems Amenable to Quantitative Study with the Hypersonic Shock Tube

It is now assumed that the test section conditions are known fairly accurately by means of the methods discussed in the previous sections. It is further believed that densities and pressures are the two variables which are best suited to measurement in the test section. The use of the interferometer for density studies is limited to relatively-high pressures and pressure gradients in the expansion chamber. For pressure studies, the restrictions are less severe. The only criterion in quantitative pressure studies is that the pressure to be measured should not be much lower than the zero reference of the gage (p_1 in the shock tube). Hence, it is perfectly permissible to study pressures on an inclined surface even if the free stream test section pressure is much lower than p_1.

The bulk of the quantitative studies with a hypersonic shock tube will consist of pressure measurements. Of all the gages which can be used for such purposes, it is believed that the piezoelectric gage is the most suitable. While most other types of gages are bulky, piezoelectric gages as small as 1/16 inch in diameter and 1/32 inch high are commercially available; hence, such pickups can be installed on any part of a model for local measurements and, in particular, close to the leading edge. The mechanical details of the support mechanism are simpler than those of most other types, and the electronic circuit is not unconventional. With some care, piezoelectric gages can be calibrated to within 5% (Figs. IV and V). A 10% accuracy can be achieved without difficulty.

A highly interesting hypersonic flow problem, for the study of which the hypersonic shock tube and piezoelectric gages are particularly suitable, is concerned with viscous interaction at the leading edge. In continuously-operating hypersonic wind tunnels appreciable effects have been noted at Mach numbers as low as six. With the extremely high temperatures, low densities, low Reynolds numbers, and relatively high Mach numbers which can be produced with the shock tube, very pronounced effects and interactions may take place near the leading edge. Factors such as dissociation, ionization, variable specific heats, and bow wave curvatures caused by relaxation time effects may well lead to important contributions of which almost nothing is known so far. Even for $M_S = 7.5$ in air, luminescence has been observed on those parts of the model most nearly normal to the flow at the test section. Moreover, in the problems of this type the interest lies in the difference between

the pressures measured at the leading edge (i.e., of a wedge) and some distance downstream, where the interaction effects will have died out. If one of the pressures is taken for reference, the other deviates from it by a small amount. On the basis of the error studies carried out in Section III.B.2, it is concluded that such investigations can be undertaken with a satisfactory degree of accuracy.

IV. THE GALCIT HYPERSONIC SHOCK TUBE

With the aim of verifying and supplementing the studies briefly outlined in the previous sections, work was started on the design and construction of a hypersonic shock tube. The tube has been in operation for a year. In this new field of application of the shock tube, where very little experience and data were available, it was decided to adopt as simple and as cheap a design as possible, one which could be realized with the use of commercially-available products but without great sacrifices as to its desired properties:

(1) The tube must operate at high pressure ratios to produce strong shocks.

(2) Because of the limitations on the sensitivity of shadow and schlieren apparatus, the tube must operate at relatively-high expansion chamber pressures p_1 (hence p_4)

(3) Flexibility of design to permit:

  (a) Pressure and flow studies at various positions along the uniform chamber and the nozzle

  (b) Pressure and flow studies on models at the test section

  (c) Installation of different nozzle shapes and variation of throat openings to allow the study of problems associated with flow establishment, boundary layer removal, Mach number limitations, and steady flow durations with different test section flow properties.

A. Structural Features

The main external features of the tube are shown in Fig. I and Plates 1 to 4 . The over-all length of the tube was dictated completely

by the availability of space in the laboratory. After much consideration as to possible locations for the shock tube, available space in the laboratory being extremely limited, the tube was finally installed in a very narrow aisle between one wall of the building and a row of compressors which feed the GALCIT hypersonic wind tunnels. With the noise and the heat from the running compressors, the conditions under which the tests had to be carried out were far from comfortable and were distracting. The same unavoidable limitations in space also dictated the rather unorthodox arrangement of the instrumentation and optical systems. Plans are in progress to remove the tube to a more suitable location. The over-all length of the present tube is twenty-six feet. The main sections of the tube are the compression chamber, the uniform expansion section, and the divergent section. Each one of these three main sections is supported by welded tubular structures mounted on wheels in such a way that the shock tube, as a whole and in parts, is mobile.

1. Compression Chamber

In order for the compression chamber to withstand the high pressures, a circular section was almost imperative. The compression chamber is a six-foot long SAE-4135 alloy steel pipe of 3 inch inside diameter and 3/4 inch wall thickness. Pressures in excess of 2000 psi can safely be contained in this chamber. No machining was done on the inner surface of the pipe since (because of the non-uniform tube to be discussed in the next section) the maximum flow speed in this tube is below 220 ft./sec. ASME standard 2000 lb. flanges at the two ends join the pipe to the transition section at one end to a blind flange at the other. The blind flange has various openings and inserts for the pressure leads, gages,

and diaphragm rupture mechanisms. Plain O-ring seals were adequate to seal the coupled faces.

2. Transition Section

From the standpoint both of studying the flow in the uniform section and of mounting flush pressure gages without disturbing the flow, the uniform expansion chamber was made rectangular in cross section. To join the circular compression chamber to this rectangular tube, a transition section was used. For ease of accurate machining, the transition section was made out of two pieces, which form the upper and the lower halves of the nozzle. A smooth contour was then machined on each piece by the GALCIT electronic contour machine. Then the two pieces were soldered together, and the outside was machined to a pipe thread. This unit was then screwed into the tapered pipe-thread fitting in an ASME standard 2000 lb. flange. When a considerable torque is applied, the tapered fitting exerts a large radial force which helps relieve the load from the relatively-weak solder joint holding the two pieces of the transition section together. The transition nozzle changes from a 3 inch diameter circular section bolted to the compression chamber face to a 7/8" x 2-7/8" rectangular section at the uniform expansion chamber end, in a length of $3\frac{1}{2}$ inches. The two parts are made of plain carbon steel. The compression chamber to expansion chamber area-ratio is $A_C/A_E = 2.80$.

3. Diaphragm Section

The diaphragm is inserted between the expansion chamber and the transition section. The cross-sectional dimensions at that point (and

throughout the rest of the uniform expansion chamber) are 7/8 in. x 2-7/8 in. Only two alloy steel bolts join the transition section to the uniform chamber. A one-inch turnbuckle is used to move the compression chamber with respect to the uniform expansion tube. When the two bolts are loosened, the turnbuckle, which is easily operated by hand, rolls the compression tube away from the expansion chamber. The diaphragm, a two-inch wide ribbon of plastic or metallic foil, is replaced. The turnbuckle is used to bring the two sections together which are bolted again to seal the joint. The alignment of the two sections is automatically accomplished by guide-bars fastened to the transition section flange. No gaskets or other sealing methods are used since the diaphragm itself acts as an excellent gasket.

4. Diaphragm Materials

All the investigations with Nozzle No. 1 were done with cellophane and acetate plastic diaphragms. A .010 inch acetate plastic ribbon could stand a little over 100 psi. across the diaphragm. For higher pressures, thicker diaphragms or a series of thin diaphragms were used. The calibration runs for the piezoelectric gages were done at very low pressure ratios with cellophane diaphragms.

The acetate plastic diaphragms shattered into small, sand-like particles with occasional large pieces. The damage done by these small diaphragm pieces (pitting, chipping, denting metallic surfaces and nozzles; breaking the leading edges of the models; scratching the windows, etc.) was surprisingly serious. Because of this, the work with Nozzles No. 2 and 3 was done with metallic diaphragms. However, when used alone, the sharp edges of the uniform expansion and transition

sections tended to tear and weaken the diaphragm. Hence, the metallic foils were sandwiched between two pieces of .01" plastic ribbons which acted as gaskets and gave additional strength. A .005 inch copper foil used in this way could support 550 to 600 psi.

5. Diaphragm Rupture Mechanisms

Two methods of breaking the diaphragm were used. In the first method, a very small, streamlined pneumatic cylinder was mounted into the compression chamber, a few inches behind the transition section. A piston with two sharp prongs was pushed out of the cylinder when a small amount of high pressure air was admitted into it. After the diaphragm was broken, a spring pulled the piston back. The over-all diameter of the piston-cylinder assembly was 3/8".

The second method is manual and consists simply of a pointed 1/4" rod laid inside the tube and protruding out of one end. When this end is pushed into the tube, the other end punctures the stressed diaphragm. For thick plastic diaphragms and for metallic foils the pneumatic system was not strong enough to perform satisfactorily; hence, the manual method is being used.

6. Uniform Expansion Chamber

The uniform expansion chamber is 7/8" x 2-7/8" in cross section and eleven feet long. The simple assembly consists of two 1/2" x 5-1/2" cold rolled steel plates and two 7/8" x 1-1/4" cold rolled steel bars bolted together and sealed by O-rings. Dowel pins, five on each side along the length, keep the two machined end faces in accurate

alignment. None of the other faces were machined because of the bad tendency of cold rolled steel to warp when the internal stresses are relieved. Only the surfaces wetted by the flow were finished with emery-cloth. Two 3 inch diameter observation windows are located at 68" and 116" from the diaphragm section. These holes are used to install either windows for flow studies or various electronic trigger mechanisms and pressure pickup assemblies. The uniform expansion chamber is joined to the nozzle inlet by two alloy steel bolts. Tapped holes close to the diaphragm section are used to drive out the air and admit gases other than air into the expansion chamber.

7. Divergent Section

The divergent section consists of a steel frame 2-7/8" wide and 1/2" thick and two big steel plates forming the side walls. The frame diverges from 6" to 45" at a distance of 60" from the end of the uniform expansion chamber, with a total divergence angle of 45°. The height of the frame then remains at 45" for another 44", to the end of the nozzle. The two side walls have contours similar to the inner frame but with a few inches larger dimensions. The two side walls are made out of 1 inch thick hot rolled steel plates, rough-ground on the inside faces and stiffened by ribs welded on the outside surfaces. Normally, with the expansion chamber evacuated, each plate carries a total load of 50,000 pounds distributed uniformly.

At the test section, located 62" from the end of the uniform expansion chamber, is a 7" diameter window. The models are mounted directly on the windows in such a way that any desired angles of attack

can be set by rotating the windows in their seats. Commercial plate glass, checked for flaws by schlieren beams, was used for the windows.

The central frame (sandwiched between the side walls) is bolted rigidly to the uniform expansion tube, while the two side plates are supported on a separate tubular structure mounted on wheels. Hence, when this dolly is pulled away, the two side walls slide with respect to the central frame, and the inside of the divergent section becomes accessible for changing of the nozzle and other alterations.

The nozzle blocks are bolted onto the frame. Bolts all around the frame squeeze the two side plates tightly against the frame. Sealing is again accomplished by O-rings.

At the far downstream, vertical end of the frame are five 2-1/4 inch diameter holes. When the expansion chamber is evacuated, five light, aluminum valves are sucked into these holes, and O-rings seal the cracks. When the tube is exploded, these valves pop open and relieve the internal pressure as soon as it exceeds the ambient atmospheric pressure.

8. Nozzles

The nozzle blocks are bolted inside the diverging portions of the upper and lower walls of the central frame. Three nozzles have been used so far.

a. Nozzle No. 1 (Fig. IIa)

This is a simple, double wedge nozzle which takes the 7/8" x 2-7/8" flow at the end of the uniform tube and expands it to 4.0" x 2-7/8" at the test section. The total angle of divergence is 45°.

The nozzle blocks are made out of wood and are polished along the surfaces wetted by the flow. O-rings close to the flow surfaces seal the blocks from the steel side walls.

b. Nozzle No. 2 (Fig. IIb)

After a few months' operation, the wooden blocks were badly chipped and damaged. To increase the Mach number and to study the feasibility of bleeding the boundary layer at the inlet to the nozzle, Nozzle No. 2 was designed. The wedge angle of the two steel throat pieces was made small enough to produce attached shocks above $M_2 = 1.40$. The position of the leading edges was such as to admit the flow ahead of the first expansion wave from the end of the uniform expansion chamber. The height "d" of the nozzle was set at 3/16". Different nozzle expansion ratios were achieved simply by moving the nozzle blocks to vary the throat height.

c. Nozzle No. 3

This nozzle was identical to Nozzle No. 2, except that the throat opening was set at 1/2".

9. Pressure System

Only the He - Air and the N_2 - Air combinations have so far been used. The pressurized gases are available commercially in 2200 lb. bottles. A 3000 psi full scale gage indicates the line pressure, and a 1000 lb. full scale laboratory gage is used for the compression chamber.

The maximum compression chamber pressure was limited to 900 psi for economical reasons. The greatest part of the tests was done with 400 - 600 psi in the compression chamber. At 2000 psi, one bottle of pressurized gas is necessary for each shot, whereas more than fifteen runs can be made per bottle at 500 psi. For calibrating the piezoelectric gages at very low pressure ratios, mercury columns are used to measure the pressures in the two chambers.

10. Vacuum System

The power plant of a small supersonic tunnel in the laboratory was used as a pump discharging to the atmosphere to evacuate rapidly the expansion chamber. With the inlet dead-ended, the compressor can pump a vacuum of 3 mm. Hg. abs. It is possible to evacuate the expansion chamber to this pressure within a few minutes. The pressures in the expansion chamber were measured by mercury manometers or 20 mm. and 10 mm. full scale Wallace-Tiernan gages calibrated by Alphatron ionization gages.

B. Instrumentation

The apparatus used on the shock tube (Cf. Fig. I and Plate 5) is conventional and is commercially available. The great emphasis has been laid on pressure studies and photographic flow studies. The various pieces of equipment are briefly discussed below. The use of an interferometer is being planned for future work.

1. Trigger Group

The triggering of the equipment is accomplished entirely by the piezoelectric gages which, at the same time, are used for quantitative study of the ensuing flow. The pulses from the gages are fed to cathode followers with sufficiently large time constants and then to amplifiers on the instrument rack. Each amplifier has two circuits, one of which leads to thyratron tubes for triggering. The other branch is used for direct voltage amplification.

2. Shock Wave Propagation

The thyratron outputs triggered by two crystal gages spaced a known distance apart along the tube are fed to the "start" and "stop" terminals of an electronic counter. The interval of time registered on the counter indicates the time it takes the shock wave to travel between the two stations. The Potter counter in use measures 100,000 μsecs. full range in intervals of 0.625 μsec.

3. Piezoelectric Gages

Very high static temperatures are produced in the uniform expansion chamber for a very short duration. Hence, it was considered advisable to use quartz pickups in this section. Each of the two quartz pickups now in use consists of a stack of six crystals 1/4 inch wide by 1-1/4 inch long and 1/32 inch thick. The 1-1/4 inch side is put normal to the flow to reduce the response time and partially span the wall. The outputs of these gages were calibrated at 80 (mv./psi) $\pm$ 10%.

For measuring the pressures at the test section and around the models, a smaller pickup was used. This unit consisted of a 3/8" dia-

meter barium titanate crystal. The natural frequency of the crystal was found by measurement to be around 50 KC. The output was calibrated at 52 $\frac{mv.}{psi}$ (1 $\frac{mv.}{mmHg}$) ± 10%.

4. Pressure Recording

The output from a crystal (after impedance matching and amplification) was fed to a delay unit. After a predetermined delay interval, the pulse triggered the X sweep on a 512 Tektronix scope. The output from a second gage, placed downstream from the first gage, was fed directly to the Y sweep on the scope. The trace on the scope was photographed by a 1.5 f. lens Leica camera.

5. Delay Chasis

The electronic delay chassis used provided a maximum delay of 10,000 μsec., controllable to intervals of 1 μsec.

6. Flow Photography

The shadow and schlieren time histories of the flow were obtained by feeding a suitably-delayed trigger pulse to a spark unit. The spark assembly and its power supply were designed and built by Marvin E. Jessey of the Guggenheim Aeronautical Laboratory of the California Institute of Technology. The estimated duration of the spark is less than 1 μsec. A point spark was used for shadow photography, and a slit spark gap for schlieren photography. The intensity of the light was adequate for any fast film, such as Du Pont 428 or Kodak Ponatomic-X.

7. Optical System

The schlieren system used consisted essentially of a lens-mirror arrangement. The light from the spark was made parallel by means of a lens. The beam was passed through the test section and focused on a knife edge by means of a spherical mirror. Shadow photographs were obtained by removing the knife edge and letting the beam fall directly on photographic film. (Actually, three mirrors are used in the present set up in order to fit the system into the extremely-limited space.) The whole system was made out of parts which were already available in the laboratory.

V. EXPERIMENTAL INVESTIGATIONS

The main topics of investigation and the results of the work done to date with the GALCIT hypersonic shock tube discussed in Section IV are outlined in the following sections.

The experiments so far have been of an exploratory character and were undertaken in order to get as many data as possible on the possibilities of the shock tube described in the previous sections. On the basis of these experiments, it is now possible to undertake a well defined program of aerodynamic research.

In view of the many uncertainties and limitations involved in the properties of hypersonic flows which can be generated by the shock tube and the great importance of pressure studies for quantitative work (as analyzed in Sections II and III), the bulk of the investigations have been concentrated on flow studies and pressure measurements. The following are the main questions to which answers were sought:

(1) How closely can the theoretical maximum Mach numbers be realized at the test section?

(2) How soon after the passage of the first shock wave do the second shock wave and the zone of separation get swept past the test section?

(3) What is the lower limit of M_S for flow to be established in the nozzle?

(4) How long and how uniform is the steady flow?

(5) What order of experimental error is to be expected from pressure studies, and what are the over-all errors for different p_1/p_T?

(6) How serious are the deviations from ideal shock tube flow in the uniform tube at high initial pressures and pressure ratios?

(7) Is it possible to remove the boundary layer and establish hypersonic flow at the test section with the use of nozzles similar to Nozzle No. 2 and Nozzle No. 3?

Unless specifically noted otherwise, the experiments to be discussed were performed with $T_4/T_1 = 1.0$. In those cases where the results are shown plotted against p_4/p_1, it is to be understood that this ratio is the equivalent pressure ratio in a uniform tube. Specifically, if the actual chamber pressures (as indicated by the gages) are p_4' and p_1', then

$$p_4/p_1 = G(p_4'/p_1')$$

where G is the gain factor for $A_c/A_E = 2.80$ as shown in Fig. 15.

A. Calibration of the Apparatus

1. Piezoelectric Gages

The same shock tube in which quantitative pressure studies are subsequently made is also the best instrument for initially calibrating the pressure gages. The principle is as follows:

At very low pressure ratios the flow produced in a shock tube is in extremely good agreement with theory. Before calibrating the gages, this fact should be verified for the given shock tube by measuring the speed of propagation of the shock wave and comparing it with the initial pressure ratio to see if the theoretical relations are satisfied.

Once the strength M_S of the shock wave is thus determined very

accurately, the amplitude of the step

$$p_2 - p_1 = \left[(p_2/p_1) - 1\right] p_1$$

is accurately known, since both p_1 (from the manometer or other vacuum gage) and p_2/p_1 (from M_S) are known to a high degree of accuracy. The flow behind a weak shock in the shock tube is very uniform and gives a well defined step function in pressure. By making p_2/p_1 very low and using various values of p_1, the gages can be calibrated over a wide range of $(p_2 - p_1)$. These gages may then be used for the study of flows with very strong shocks (large p_2/p_1) so long as p_1 is sufficiently low to make $(p_2 - p_1)$ fall within the range of calibration.

In calibrating the gages used in this project, the expansion chamber was held at or near atmospheric pressure, with the compression chamber either at or slightly above atmospheric pressure. The temperatures were given a minute or more to equalize. Very thin cellophane diaphragms were used to keep the disturbance to the flow at a minimum. Upon rupturing the diaphragm, the speed of propagation of the shock wave could be determined from the time interval registered on the electronic counter.

In calculating M_S, the value of "a_1" must be calculated from an accurate reading of the local temperature. The effect of humidity on a_1 was found to be negligible.

These series of calibration runs have also afforded the opportunity to check the theory of non-uniform tubes. On Fig. 15 is shown the gain factor G as a function of M_S for $A_c/A_E = 2.80$. Then, on Fig. III is shown plotted the experimental values of M_S against p_4/p_1. The circled points are not corrected for G, whereas the plain points are corrected for G

corresponding to each p_4/p_1 by the values given on Fig. 15. The scatter of the corrected points from the theoretical curve is less than 1/2% up to $p_4/p_1 \cong 3.0$.

Hence, for all the calibration runs, p_4/p_1 was kept below 3.0. The results are given on Figs. IV and V, and typical traces of the calibration curves are to be found on Plate 6 . These calibration runs have been carried out quite frequently (every few weeks) to correct for long-time drift in the electronic circuit, but no noticeable shift in the gage outputs has been observed. The maximum scatter on these figures is below ±5%. It is believed that the experimental error in pressure measurements can be kept below 10% without great difficulty. The linearity of the output within the calibration range is seen to be very satisfactory.

The gage-outputs are fed to suitable cathode followers for impedance matching. The circuit time constant must be much larger than the expected duration of uniform flows in order to allow faithful reproduction of the pressure pulse with negligible exponential decay. The amplified voltage is then measured either from the scope trace or by means of electronic peak-measuring instruments which have recently become commercially available.

If the scope is used, the photographed trace is enlarged by as much as ten times, and its amplitude and time scale determined by comparing it to a corresponding calibration trace which consists of square waves of known frequency and amplitude.

2. Oscilloscope

The calibration dials of the oscilloscope were frequently calibrated by feeding square or harmonic waves of known amplitude and frequency from a reliable external source, such as the Hewlett-Packard oscillators and square-wave generators.

3. Delay Chassis

Although the delay chassis used in the experiments showed high reproducibility over short periods of time (i.e., a few hours), the absolute values of the time delay drifted by large amounts over a period of days, or from one test period to another. A very simple method of calibrating the delay before and after every test period is to wire the counter across the delay chassis terminals; upon feeding a pulse to the chassis, the counter registers the accurate delay period. If the counter is not being used for measuring the shock wave propagation speed, then this method can be used to obtain the correct delay period for every shot.

4. Amplifiers

The frequency response, noise, and drift characteristics of the amplifiers can be studied by ordinary methods in electrical engineering practice. The amplifiers used in the project showed a flat response up to frequencies in excess of 100 KC. It was found, however, that the noise introduced by A. C. power supplies made it difficult to work at high sensitivities. For such work, it becomes necessary to supply power from a D. C. source.

B. Pressure and Flow Studies

1. Shock Wave Propagation

Figure VI shows the experimental points for the Mach number of propagation, M_S, of the shock waves in the uniform chamber for N_2 - Air, as compared with the theoretical curve for different initial pressure ratios.

Although no difficulty was experienced at low pressure ratios, at high pressure ratios, with relatively high p_4, the time readings suddenly became very erratic. The source of this behavior was discovered to be the disturbances propagated along the metallic walls of the tube triggering the instruments permaturely. A small weight dropped on the tube from a height of a few inches produced signals of considerable amplitude at the pickups. Efforts to stiffen the tube and cut down the sensitivity of the pickup circuit have corrected this difficulty to some extent, but occasionally the instruments do get triggered prematurely for a series of runs, and some of the scatter shown in Fig. VI may have been caused by this fact. Unless the pickups are carefully shock-mounted, it is believed that for high pressure work a trigger mechanism completely independent of the tube, such as the light-screen method discussed in Ref. 5, is very desirable.

Although the subject of shock wave attenuation still remains a controversial topic (Refs. 9, 14, and 24), it is believed that Fig. VI gives a fairly good indication of the speed of propagation of the shock waves generated in this tube. It appears that the conditions at the

shock front do not deviate a great deal from theory up to fairly high pressure ratios and that the shock speeds appear to approach the theoretical curve at high pressure ratios. This behavior is in agreement with the results of the pressure studies analyzed in the next section, but this may be accounted for as being due to the faster formation of the shock wave at high pressure ratios.

2. Pressure Studies in the Uniform Tube

These series of tests were carried out to study the uniformity, magnitude, and duration of the pressures in Regions 2 and 3, as a function of time, at a station a few inches upstream of the inlet to the diverging section. Both the quartz and the barium-titanate pickups were used to obtain pressure data from a large number of runs. The driver gas was either nitrogen or helium with air in the expansion chamber in all cases.

Before discussing the results in detail, some general remarks should be made. In Plates 7 and 8 are shown some typical pressure traces from the quartz and the barium-titanate crystals. A study of these traces shown the great importance of having satisfactory damping with a carefully-matched circuit. If the crystals are under-damped, the response is fast, but there is a large overshoot and transient vibrations. For large pressure ratios and long durations of uniform flows, these effects are not objectionable (Plate 7a); but for low pressure jumps and short durations, the overshoot amplitude and the transient duration may be of the same magnitude as the amplitude and the duration of the step pulse (Plate 7c,d). This makes it very difficult to measure and study the pressure traces accurately. Some damping eliminates

this difficulty (Plate 7i), but care must be taken that the pickup is not over-damped, since, unless the flow duration is sufficiently long, a fictitious pressure rise is indicated on the scope behind the shock front,* and a great deal of response sensitivity is sacrificed.

Plates 8a and 8b illustrate the great importance of the time constant of the follower-circuit. Particularly for large pressure jumps, due to the exponential decay, a small amount of electronic leakage may lead to a large drop in amplitude during a given period.

a. Studies with N_2 - Air

The study of a large number of traces obtained from runs with widely-varying initial conditions leads to the following conclusions:

At low pressure ratios the flow behind the shock wave is in excellent agreement with theory in all respects (i.e., the duration of flow, arrival of the rarefaction wave, magnitude of the jump, uniformity of flow, etc.).

For strong shock waves, the first noticeable characteristics in the pressure traces are as follows (Cf. Plate 9): The pressure behind the shock wave exhibits a gradual rise** which tends to level off. There follows a small but distinct dip in pressure preceding an abrupt change in slope caused by rising pressure. The underdamped crystals afford a very good means of qualitatively detecting the turbulence level in the various flow regions.

---

* Theoretically, the pressures behind strong shocks in gases with variable specific heats do rise by a slight amount, but at high temperatures the relaxation time is usually much smaller than the duration of uniform flow.

** This is not due to damping in the crystal, since it is observed even when the crystal is slightly under-damped.

Following a slight tendency to level off, the first change in pressure gives way to a second abrupt change and a rapid turbulent rise. This rather unexpected behavior is actually in good agreement with conclusions reached in Ref. 6, on the basis of flow Mach number studies. In this report, a pressure dip just ahead of the contact surface is predicted as being caused by the formation of weak rarefaction waves due to shock interactions during the initial formation of the plane shock wave. Again, on the gasis of the studies reported in Ref. 6, a rise in pressure is expected behind the contact surface. It is also expected that this region should approach the contact surface front with increasing pressure ratio. It is observed that this rise is due to the appearance of a "region of transient shock waves" behind the contact surface, the causes of which are not clearly understood.

Hence, it is strongly believed that the rear of the small pressure dip indicates the front of the contact zone. The pressure rises through the contact zone, then tends to level off. The second abrupt discontinuity in slope is caused by the arrival of the rarefaction wave, since the pressure exhibits a monotonic, rapid rise.

The gradual rise in pressure behind the shock front and ahead of the contact surface becomes more pronounced with increasing shock wave strength. This behavior may be attributed to two main causes:

(1) The initial shock wave has not had sufficient time to form; hence, it is followed by a region of weaker compression waves and transverse waves (Refs. 6 and 24).

(2) The growth of boundary layer along the walls of the tube tends to reduce the effective section of the chamber. Hence, the situation is similar to that of supersonic flow into a

slightly converging channel, with the accompanying compression waves which form along the walls propagating into the flow. The qualitative shape of the pressure rise compared with the usually assumed geometry of the displacement thickness behind the shock supports this point of view.

If the gradual rise is due to the insufficient time of formation of the shock wave, then the maximum pressure in the flow ahead of the contact surface must be lower than that predicted by the ideal theory. The results of the runs with both N_2 - Air and He - Air contradict this view. In Figs. VII and VIII, the lower end of each run indicates the pressure ratio immediately behind the shock, whereas the upper end corresponds to an average pressure in the flow ahead of the contact surface. At high pressure ratios, the deviation of the upper end from the theoretical curve is believed to be beyond experimental error. Thus, one is tempted to believe that this rise is due mainly to a boundary layer growth or a similar disturbance in the flow.

b. Studies with He - Air

The tests with helium were undertaken mainly to investigate the region $4 \leq M_S \leq 7.5$. The main difference between the traces obtained in this series of tests and the ones discussed in the previous section is that the beginning of the rarefaction wave is indistinguishable. Following the relatively-smooth flow in Region 2 and a slight dip, the pressure starts rising abruptly and monotonically.

From Fig. VIII it is observed that the pressure behind the shock front tends to increase beyond the theoretical values at high pressure ratios. This tendency was observed for N_2 - Air in Fig. VII and is in

agreement with the shock wave propagation studies given in Fig.VI. Although a conclusive explanation cannot be presented, it is felt that a much larger tube may greatly reduce the discrepancies noted. In addition to the possible boundary layer growth effect, the pressure rise in Regions 2 and 3 may, in some way, also be related to mixing at the contact zone. With a gas as diffusive as helium at a few hundred pounds of pressure in one chamber and air at a few millimeters of mercury in the other, with a relatively-thick diaphragm in between, a great deal of mass transport should take place following the rupture of the diaphragm, and the purely wave phenomenon assumed in the ideal theory should be seriously violated.

In concluding this section, it must be emphasized that although the results to which attention has been drawn are believed to ve balid beyond experimental error, it is doubtful that a satisfactory explanation can ever be given. Fig.IX shows roughly the measured duration between the shock wave and the front of the mixing zone following the pressure dip.

3. Luminescence Behind the Shock Wave

With helium-air operation around $p_4/p_1 = 6000$, a noticeable luminescence appears at the uniform section. At higher pressure ratios this luminescence becomes more striking and bluish-white in color. Moreover, at the test section there appears a faint blue background and stronger whitish luminescence around those sections of the model at high angles of attack with respect to the flow.

On the basis of existing theories, the stagnation temperatures at which luminescence has been observed are too low for ionization in air. Three explanations may be suggested:

(1) Burning of diaphragm particles

(2) Combustion of the impurities in air and/or dirt and dust along the walls of the tube

(3) A phenomenon which the existing theories fail to account for

The first possibility is eliminated by the fact that no detectable change in the intensity of the glow takes place whether the diaphragm is plastic (which shatters to small pieces), or copper or aluminum foil (which fold out without breaking). Instead of the third, one would rather believe the second alternative, even though it seems improbable that dirt and dust should remain on the walls after a great many shots with metallic diaphragms.

It has not so far been possible to devote the attention and time which this phenomenon deserves, but future investigations to disclose the nature of the causes producing the luminescence observed in the flow are being planned. Other investigators in this field have, reportedly, been puzzled by similar observations (Refs. 10 and 22).

4. Flow Studies at the Test Section: Nozzle No. 1

The structural features and the dimensions of this nozzle have been discussed in Section IV.A.8 and illustrated in Fig. IIa. The cross section of this simple double wedge nozzle is 7/8" x 2-7/8" at the inlet and diverges out to 4.0" x 2-7/8" at the test section, with a total divergence angle of 45°. The reasons for choosing these particular geometry and dimensions are summarized below:

(1) From Figs. 7 and 8, it can be seen that the maximum test section Mach number is between 6.5 and 7.5 for N_2 - Air or He - Air operation at high pressure ratios. Hence, it was decided to try first

a nozzle which would be expected to produce a Mach number of six, to find out if a Mach number so close to the maximum value could be obtained with this tube. It will be seen from Fig. 32 that this was an unfortunate choice from the point of view of quantitative pressure studies, particularly with N_2 - Air. For He - Air, the situation is somewhat improved, but not a great deal. Nevertheless, the pressure traces could still be used to determine the time it took for the zone of separation to get swept past the test section and the duration and uniformity of the subsequent steady flow.

(2) If a Busemann type nozzle were chosen, with the same inlet dimensions and the same expansion ratio, either the distance to the test section would have to be very great, or the maximum divergence angle, already of a rather unusual magnitude, would be extremely steep.

(3) Since the height of the nozzle at the test section is 40 inches, and since only one or two inches of the central portion was occupied by the model and used for measurements, it was hoped that the divergence of the streamlines at the test section would be negligibly small.

(4) A simple double-wedge nozzle is much easier to machine and replace in case of damage than a parallel-flow nozzle of the Busemann type.

Hence, for the purpose of these exploratory investigations it was decided to use a double-wedge nozzle to get rapid, even if not very accurate, data. The flow studies were made around two-dimensional wedges, at various angles of attack, which spanned the tunnel with a clearance of less than .003 inches before the tube was evacuated. It is

believed that with the expansion chamber under vacuum, the side walls actually pressed against the ends of the model. The reasons for using two dimensional models were the following:

(1) The mounting problem was very greatly simplified by mounting the model rigidly on the test section window, (Plate 3b), and the angle of attack of the model could be changed by rotating the window.

(2) The schlieren and shadow photographs are much better defined for two-dimensional flows at low densities than for three-dimensional flows.

The flow Mach numbers were measured from the wave angles and the angles of detachment. In order to check for the possible effects of boundary layer growth on the shock wave angles, measurements were taken over a wide range of angles of attack and different pressures, while the pressure ratio was kept unchanged (i.e., different Reynolds numbers). All the models had from .002 to .005 inch diameter bluntness at the leading edge in order to prevent chipping.

At hypersonic Mach numbers, a small error in the angle of attack or the measured shock wave angles lead to large errors in the measured Mach number. To reduce the errors due to the human element, each photograph was measured by more than one individual, and more than once in cases which showed large scatter. In some of the clear photographs with well-established flows, the total scatter between three or four measurements was not more than five minutes of a degree. Near the start and the break-down of the flow, however, the scatter was more than a degree. The lower limit on experimental error was set at plus or minus fifteen minutes of a degree. The angle of attack could not be controlled

closer than ten or fifteen minutes. The maximum scatter was used for all cases above fifteen minutes.

a. Studies with N_2 - Air

A typical flow history is shown on Plates 10 to 13. The passage of a very weak shock wave (Plate 10) is followed by a region of subsonic flow. A very simple and convenient means of detecting this flow is to sprinkle some fine powder on the model. A cloud rising over the model indicates the start of flow at the test section even when the shock wave is not caught on the photographs. This flow is followed by the appearance of small shock waves at the leading edge, which gradually grow and form a well-defined flow pattern. Meanwhile, the boundary layer grows, as can be detected from the downstream shift of the shock wave starting at the bottom corner (Plates 11,12,13). Following a noticeable darkening of the waves, the flow becomes very turbulent, and the shock waves take an irregular pattern.

The times at which these events, as well as similar disturbances observed in the pressure traces, take place make it strongly probable that the darkening of the shock waves is a rough indication of the arrival of the cool contact zone. Some time after the observed irregularities in the shock wave pattern, small diaphragm particles, and then larger ones, appear in the flow. In some of the photographs, the shock wave seems to have more than one branch. This is due mainly to the chipping of the leading edge which usually took place after about a dozen shots. The sidewall boundary layer interaction with the shock wave may be the cause of the grayish band around the shock wave, which was observed in some shots (Plates 12,13).

It was not possible to establish steady hypersonic flow in the nozzle for $p_4/p_1 < 2500$. It is doubtful that the flow got well established at $p_4/p_1 = 2500$. This may account for the consistent failure to reach Mach number six, as shown in Fig. XI . Unfortunately, the experimental uncertainty in the measured values of M_T is large enough to obscure the possible detection of effects such as reproducibility, boundary-layer growth, Mach number uniformity for each run, etc. Nevertheless, Fig. XII shows that the theoretical Mach number is closely attained at sufficiently high pressure ratios.

b. Studies with He - Air

The results of the runs with He - Air are shown in Figs XIII and XIV, and a flow history is presented in Plates 14 to 16. The very short duration of steady flow in the uniform tube with He - Air at high pressure ratios makes it quite impossible to derive definite conclusions from these figures. Although one is strongly tempted to say that Figs. XIII and XIV indicate that the important deviations due to variable specific heats, as analized in Section II.D, are verified, it may well be argued that due to the very short duration of the flow, it is by no means clear whether or not steady flow was established at the test section. Here again, one is faced with the great need for a much longer tube in order to be able to differentiate, with certainty, the various flow regions.

The pressure studies discussed in the next section will contribute considerably towards a better understanding of the general behavior shown in these figures.

5. Pressure Studies at the Test Section

A qualitative study of the pressure traces obtained at the test section may help towards a better understanding of the contents of the previous section. Plates 20 and 21 show a number of pressure traces for N_2 - Air and He - Air, presented in order of increasing pressure ratio p_4/p_1. The first sharp jump from the reference trigger line indicates the first shock wave. The highly-noisy trace which follows the first shock is due mainly to the transient vibrations of the pickup and does not indicate pressure fluctuations alone. The second shock wave is not well defined. Instead of a sharp discontinuity at the second shock wave, there is an abrupt change in slope, followed by a turbulent decrease in pressure. This region corresponds to what has previously been called the "zone of separation". The pressure eventually goes below the trigger pressure level, corresponding to p_1, and uniform flow is established at the test section.

With N_2 - Air, at low pressure ratios (Cf. Plates 20a to 20d) the duration between the shocks is relatively long, and below a pressure ratio of around 2000, uniform flow is never established at the test section. As the pressure ratio is increased, the duration between the shocks gets smaller, the zone of separation is swept by the test section faster, and an increasing duration of uniform flow is obtained. At high pressure ratios, the smooth flow is terminated by a turbulent zone. This breakdown of the smooth flow indicates either the arrival of the contact zone or some disturbances, which are reflected from the end of the tube, feeding from behind. The fact that the pressure does not keep increasing monotonically but falls back after each sharp rise

seems to favor the first alternative. Fig. XV shows the various regions of test section flow with N_2 - Air, as measured from a large number of traces.

As expected, the traces with He - Air operation are relatively irregular. Although the zone of separation is swept by just as fast, the duration of smooth flow is not only much shorter, but the pressure reaches a minimum and rises up again (Plates 21 a to d). At lower pressure ratios, the uniform flow breaks down almost as soon as the zone of separation is swept past the test section. These general features of the pressure traces are in agreement with the variation of Mach numbers shown in Figs. XIII and XIV.

Although an accurate measurement of the strength of the second shock wave is impossible from these traces, the pressure ratio across the first shock wave can be determined. Figures XVI and XVII show the variation of M_{S_1} as a function of p_4/p_1 for N_2 - Air and He - Air. For the sake of interest, on the same figures are shown the values for M_{S_1} in a Busemann nozzle corresponding to $p_4/p_1 = \infty$ and $M_T = 6.0$.

The absolute values of the test section Mach numbers measured from the pressure traces were found to be very erratic. For the strengths of the shock waves produced in these experiments, these results were expected to have large intrinsic errors (Cf. Section III.B.2) at the test section Mach number of six. In order to improve the over-all error, it was decided to measure the pressures on a 35° wedge surface. Since the flow for He - Air operation has already been found to be unsatisfactory, the runs were made with N_2 - Air only.

The expected theoretical pressures themselves cannot be stated

accurately due to the uncertainty in the measured test section Mach number. Hence, in Fig.XVIII, the theoretical results are represented by a band rather than a line. The lower limit of the band represents the values of p_T which would be calculated by assuming ideal theory, with $\gamma = 1.4$, to be valid throughout. The upper limit indicates the conditions with variable specific heats, using the lower limits of the experimental Mach numbers. Thus, the band indicates a fairly-conservative envelope for the expected pressures.

The spread shown in Fig.XVIII for the measured pressure ratios is caused by the noise level indicated in the pressure traces (Plate 22). Undoubtedly, the vibrations of the model when hit by the shock, and the unsteady establishment of the hypersonic flow are mainly responsible for this noise. Although a stiffer mounting with a symmetrical wedge may help a great deal towards reducing the noise, it is believed that a much longer duration of steady flow is necessary to allow the transients at the pickup to settle down.

6. Studies with Nozzles No. 2 and No. 3

The geometric details of these nozzles have been given in Fig IIb. One of the main reasons for this set of experiments was to find out the following:

(1) If uniform hypersonic flows at the test section could be obtained with this type of nozzle which, besides affording a very simple means of changing the expansion ratio, removes a very large portion of the boundary layer at the inlet to the nozzle

(2) If it is possible to obtain flows with Mach numbers in

excess of the maximum values shown in Figs. 7 and 8; and if so, how much in excess.

The wooden nozzle blocks were very badly chipped and damaged by the end of the experiments with Nozzle No. 1, so it was decided to use aluminum blocks (for lightness) with steel tips at the inlet. Experience with the chipping and deformation of the leading edges of the models at the test section also made it evident that metallic diaphragms would have to be used if the tips of the new nozzles were to be saved from getting damaged after a few shots.

The throat of Nozzle No. 2 was set at 3/16". The series of tests for N_2 - Air indicated subsonic but no supersonic flow. For He - Air operation, detached shock waves appeared ahead of the model for a short duration of time (Plates 23, 24).

The throat opening was then increased to 1/2". Corresponding to this area ratio $A_T/A_E = 80$, the section Mach number is expected to be around 6.8 - 7.0, and hence, just about the expected maximum Mach number for N_2 - Air operation.

For He - Air operation, detached shock waves for a short duration were again all that appeared. For N_2 - Air, however, there was a relatively-long period of subsonic flow, followed by the appearance of oblique waves at the leading edge. The waves were much fainter than those which appeared with Nozzle No. 1, because of the lower densities. The first measurable Mach number was around five, but increased rapidly until, for a duration of 100 to 200 microseconds, it reached a value between 6.5 and 8.0. Then the Mach number dropped very rapidly, and the smooth flow broke down. The whole duration of the observable supersonic

flow was less than 500 μ sec. The situations described are illustrated in Plates 25, 26.

It is believed that the reason for the failure of flow establishment with He - Air is the extremely-short duration of the flow, which made it difficult to get a uniform flow even with Nozzle No. 1.

VI. SUMMARY AND CONCLUSIONS

Following the tests with Nozzle No. 3 reported in the previous section, it was decided that further experimentation with the present tube would be of little consequence due to the extreme shortness of the flow duration for values of M_S above five or six. A great need was felt to undertake important improvements in the tube structure, electronic instrumentation, and the pressure gages. Work is now in progress to enlarge the cross sectional area of the uniform expansion chamber by a factor of three and lengthen the tube by an equal factor. Two addditional test section windows and a number of pressure gage stations will be machined on the two sidewalls to allow a much more complete survey of the flow through the nozzle.

On the basis of the investigations carried out so far, the following conclusions may be stated:

It is possible to produce hypersonic flows with very high stagnation temperatures with a shock tube. Such flows can be produced by accumulating a desired length of uniform supersonic flow behind a strong shock wave, and feeding it to a diverging, or a converging-diverging nozzle. As the first shock propagates down the nozzle, it is continuously decayed, and tends to an acoustic wave. A second shock wave "splits" from the first at the nozzle inlet, and propagates upstream with respect to the flow (but, initially, downstream with respect to the tube) with increasing strength. The strength of this shock wave is such as to bring to agreement the velocity and pressure of the flow immediately behind the first shock with that of the isentropic channel flow ahead of the second shock. Eventually the strength of the second shock

becomes such as to make it stationary with respect to the tube. This condition sets the maximum attainable test section Mach number which, for a given gas, is a function of M_S. Steady flow at the test section is established following the passage of the two shock waves and a zone of separation by the test section.

At the relatively high pressure ratios required for hypersonic shock tube work the actual flow exhibits serious deviations from the ideal shock tube flow model. Hence it becomes necessary to determine the flow conditions at the test section by direct measurements either at the test section, or at another station along the tube where flow conditions are more favorable to measurements. At high Mach numbers, the quantities determined at this station may be related to the test section conditions by static or total head surveys of the flow region between the two stations.

From the points of view of availability and suitability of instrumentation, and sensitivity to changes in the flow conditions, pressure is by far the most convenient variable to work with. To measure pressures within experimental accuracy, the quantity to be measured must be at least as large as the initial pressure sensed by the gage. Wherever conditions warrant its use, interferometry offers a second possibility for quantitative studies. The restrictions on the possible types of instrumentation which can be used with the shock tube impose, in turn, definite limitations on the nature of the problems which can be investigated on a quantitative basis using a shock tube.

REFERENCES

1. Courant, R. and Friedrichs, K. O.: "Supersonic Flow and Shock Waves", Interscience Publishers, (1948).

2. Lucasiewics, J.: "Shock Tube Theory and Applications", NRC Report No. MT 10, (Jan. 1950).

3. Lucasiewics, J.: "Flow in a Shock Tube of Non-Uniform Cross Section", NRC Report MT-11, (Jan. 1950).

4. Patterson, G. N.: "Theory of the Shock Tube", NOLM 9903, (1948).

5. Geiger, F. W. and Mautz, C. W.: "The Shock Tube as an Instrument for the Investigation of Transonic and Supersonic Flow Patterns", Engineering Research Institute, University of Michigan, (1949).

6. Lobb, R. K.: "A Study of Supersonic Flows in a Shock Tube", UTIA Report No. 8, (1950).

7. Lobb, R. K.: "On the Length of a Shock Tube", UTIA Report No. 4, (1950).

8. Duff, R. E.: "The Use of Real Gases in a Shock Tube", Engineering Research Institute, University of Michigan 51-3, (1951).

9. Hollyer, R. N.: "A Study of Attenuation in the Shock Tube", Engineering Research Institute, University of Michigan M720-4, (1953).

10. Resler, E. L.: "High Temperature Gases Produced by Shock-Waves", Ph.D. Thesis, Cornell University, (1951).

11. Parks, E. K.: "Supersonic Flow in a Shock-Tube of Divergent Cross Section", UTIA Report No. 18, (1952).

12. Hertzberg, A.: "Shock Tubes for Hypersonic-Flow", Cornell Aeronautical Laboratory, Inc., Report No. AF-702-A-1, (1951).

13. Hertzberg, A. and Kantrowitz, J.: "Studies with an Aerodynamically Instrumented Shock Tube", Journal of Applied Physics, Vol. 21, p. 874, (1950).

14. Lundquist, G. A.: "The N.O.L. 8 x 8 Inch Shock Tube; Instrumentation and Operation", NAVORD Report No. 2449, (1952).

15. Donaldson, C. du P. and Sullivan, R. D.: "The Effect of Wall Friction on Strength of Shock Waves in Tubes and Hydraulic Jumps in Channels", NACA TN 1942, (1949).

16. Emrich, R. J.: "Velocity Loss Measurements on Shocks in a Shock Tube", Princeton University Department of Physics, NR 061-020, (1948).

17. Bleakney, W.; White, D. R.; and Griffith, W. C.: "Measurements of Diffraction of Shock Waves and Resultant Loading of Structures", Journal of Applied Mechanics, Vol. 17, p. 493, (1950).

18. Laponsky, A. B.: "Observation of Shock Formation and Growth", Institute of Research, Lehigh University, Technical Report No. 1, (1951).

19. Hoover, H. L.: "Measurement by Times Spark Shadowgraphs of Shock Velocities in a Shock Tube", Institute of Research, Lehigh University, Technical Report No. 3, (1953).

20. Ferri, A.; Libby, P. A.; and Zakkay, V.: "A Theoretical Analysis of a New Type of Heater for an Intermittent Hypersonic Wind Tunnel", Polytechnic Institute of Brooklyn, Department of Aeronautical Engineering and Applied Mechanics, PIBAL Report No. 201, (1952).

21. Bethe, H. A. and Teller, E.: "Deviations from Thermal Equilibrium in Shock Waves", Aberdeen Proving Grounds, BRL Report No. X-117, (1945).

22. Fowler, R. G.: "Shock Waves in Low Pressure Spark Discharges", Physics Review, Vol. 88, p. 137, (1952).

23. Dosanjh, D. S.; Kovasznay, L. S. G.; Clarken, P. C.: "Study of Transient Hot wire Response in a Shock Tube", Johns Hopkins University, Department of Aeronautics, Report CM 725, (1952).

24. Glass, I. I.; Martin, W.; and Patterson, G. N.: "A Theoretical and Experimental Study of the Shock Tube", UTIA Report No. 2, (1953).

25. Carrington, T. and Davidson, N.: "Shock Waves in Chemical Kinetics: The Rate of Dissociation of N_2O_4", Journal of Physical Chemistry, Vol. 57, p. 418, (1953).

26. Woolley, H. W.: "The Effect of Dissociation on the Thermodynamic Properties of Pure Diatomic Gases", National Bureau of Standards Report 1884, (1953).

27. Duff, R. E. and Hollyer, R. N.: "A Feasibility Study for a Large Shock Tube for Blast Effect Determinations", Engineering Research Institute, University of Michigan, Report No. 51, (1951).

28. London, L.: "Feasibility of a Large Shock Tube", Armour Research Foundation Report, (1951).

29. Hollyer, R. N.; Hunting, A. C.; Laporte, O.; and Turner, E. B.: "Luminosity Generated by Shock-Waves", Nature, 171, 395, (1953).

30. Rinehart, J. S.; Allen, W. A.; White, W. C.: "Phenomena Associated with the Flight of Ultra-Speed Pellets", NOTS TM No. 338, (1951).

31. Marlow, D. G.; Nisewanger, C. R.; and Cady, W. M.: "A Method for the Instantaneous Measurement of Velocity and Temperature in High Speed Air Flow", Journal of Applied Physics, Vol. 20, No. 8, pp. 771-776, (1949).

32. Reed, W. T.: "Theory, Calibration, and Use of Diaphragm Blast Meters", NDRC A-392 or OSRD 6463.

33. Whitnam, G. B.: "Propagation of Spherical Blast", Proc. of Royal Society, A, Vol. 203, (1950).

34. Meyer, R. E.: "On Waves of Finite Amplitude in Ducts", Quarterly Journal of Mechanics and Applied Mathematics, Vol. V, Pt. 3, (1952).

35. Doering, W. and Burkhardt, G.: "Contributions to the Theory of Detonation", AMC - TR No. F-TS-1227-1A, (1949).

36. Guderley, G.: "Unsteady Gas Flows in Thin Tubes of Variable Cross Section", ZWB-FB 1744, (1942).

37. Hess, R. V.: "Study of Unsteady Flow Disturbances of Large and Small Amplitudes Moving Through Supersonic or Subsonic Steady Flows", NACA TN 1878, (1949).

38. Perry, R. W. and Kantrowitz, A.: "The Production and Stability of Strong Shock Waves", Journal of Applied Physics, Vol. 22, p. 878, (1951).

39. Lighthill, M. J.: "The Diffraction of Blast", Proc. of the Royal Society, A-198, (1949), and A-200, (1950).

40. Keenan, J. H. and Kaye, J.: "Gas Tables", John Wiley and Sons, (1948).

41. Bureau of Ordnance Publication: "Handbook of Supersonic Aerodynamics", NAVORD Report No. 1488, Vol. 5, (1953).

42. Shreffler, R. G. and Christian, R. H.: "Boundary Disturbances in High-Explosive Shock Tubes", Journal of Applied Physics, Vol. 25, p. 324, (1954).

43. Bergdolt, V. E. and Shear, D. D.: "Shadowgraph Spark Sources for the 12 Inch Pressurized Range", BRL Memorandum Report No. 742, (1953).

44. Vrebalovich, T.: "Glow Anemometry", California Institute of Technology, Ph.D. Thesis, (1954).

45. Nagamatsu, H. T.: "Theoretical Investigation of Detached Shock Waves", California Institute of Technology, Ph.D. Thesis, (1949).

46. Mack, J. E.: "Density Measurement in Shock Tube Flow with Chrono-Interferometer", Lehigh University, R. R. 4, (1954).

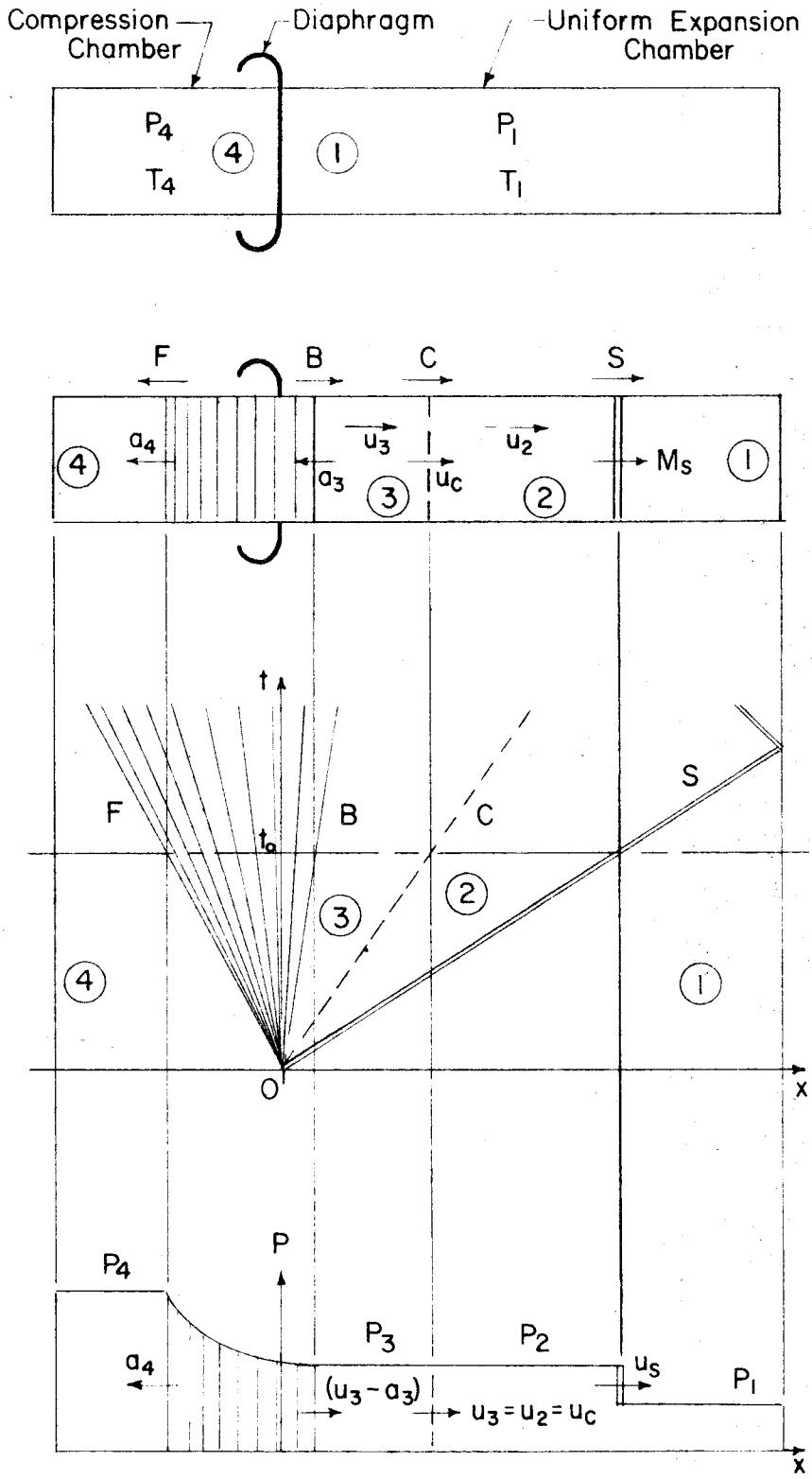

FIG. 1 — IDEAL FLOW MODEL IN UNIFORM SHOCK TUBE

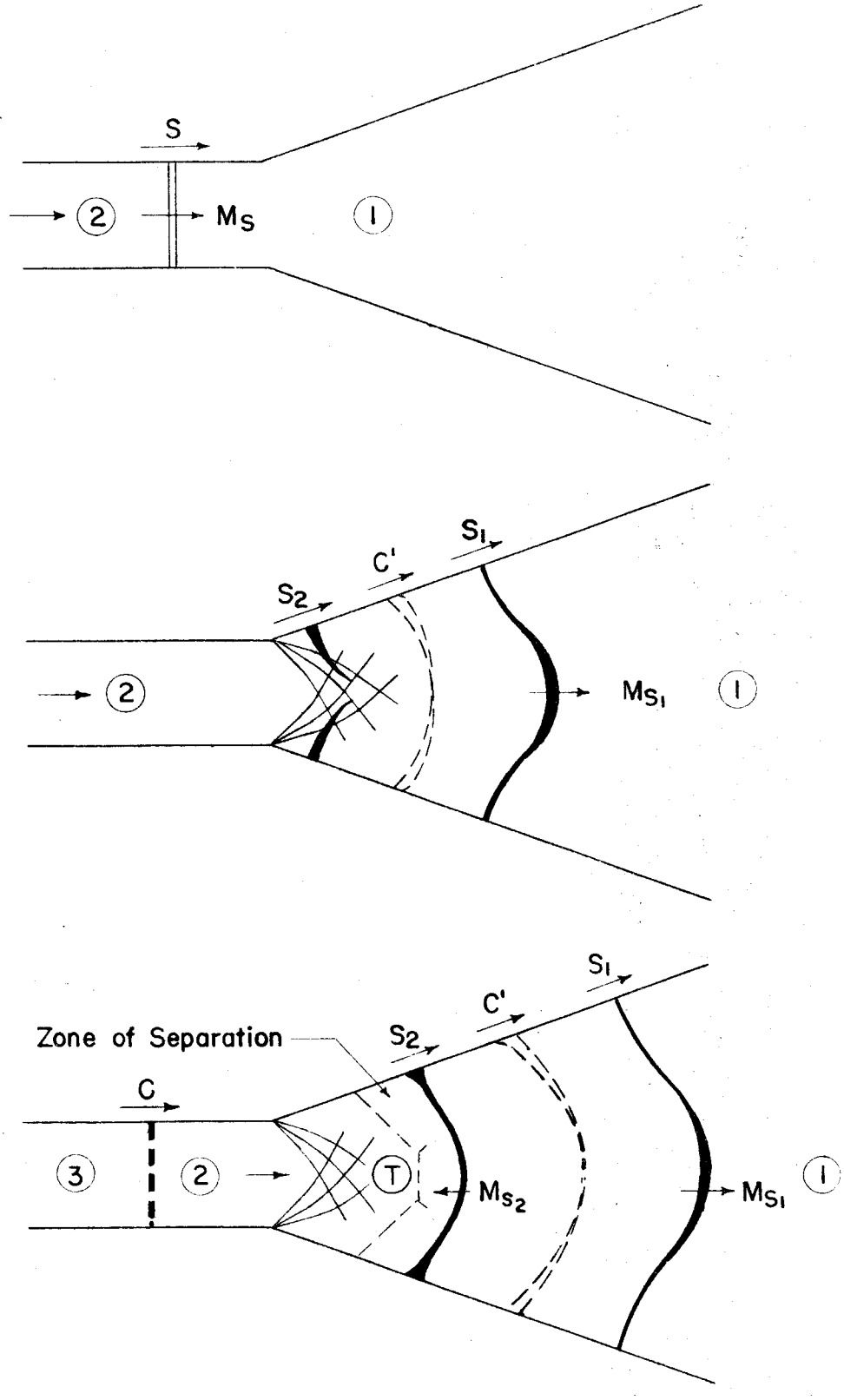

FIG. 2 — FLOW ESTABLISHMENT IN A D-NOZZLE

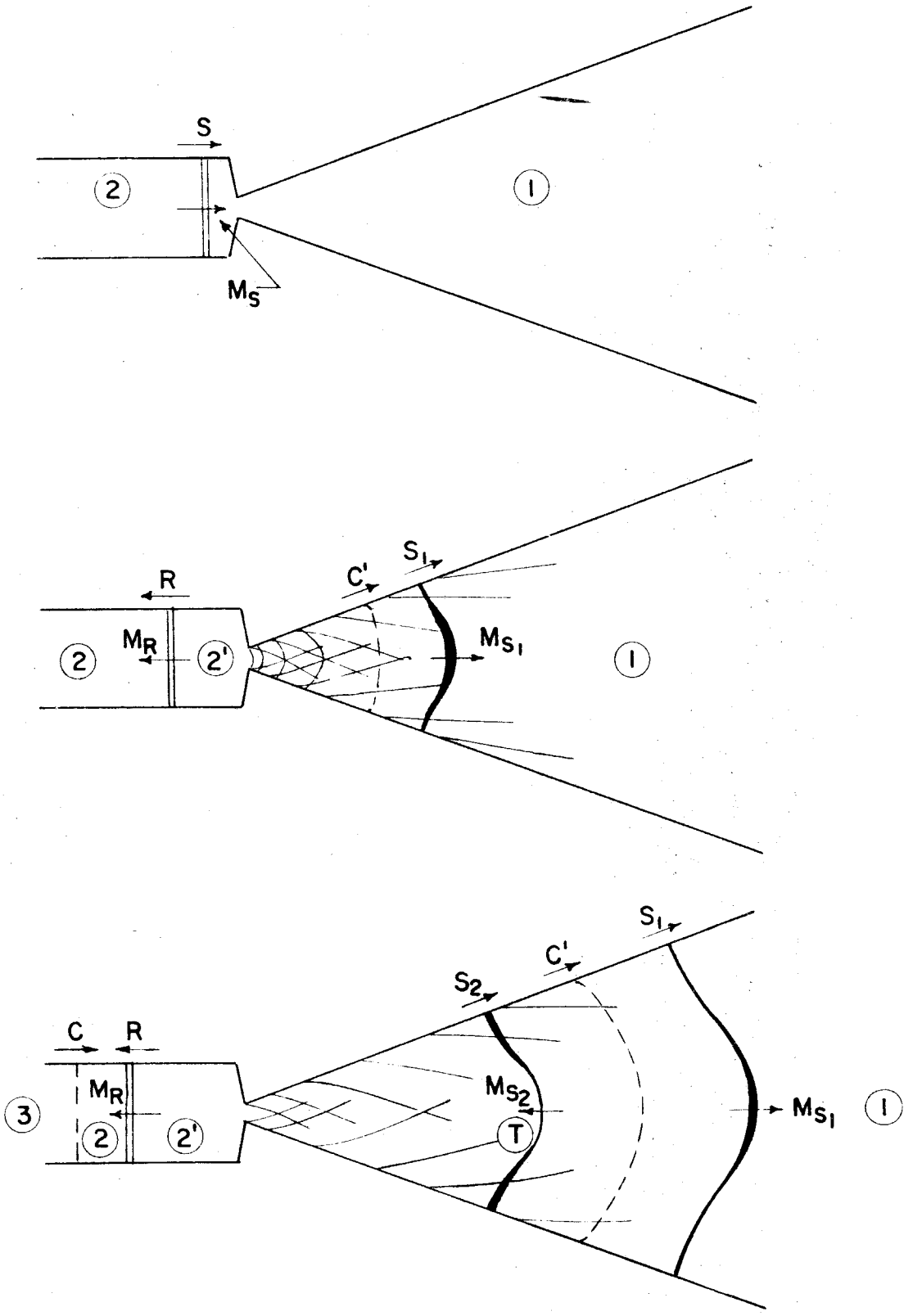

FIG. 3 — FLOW ESTABLISHMENT IN A CD-NOZZLE

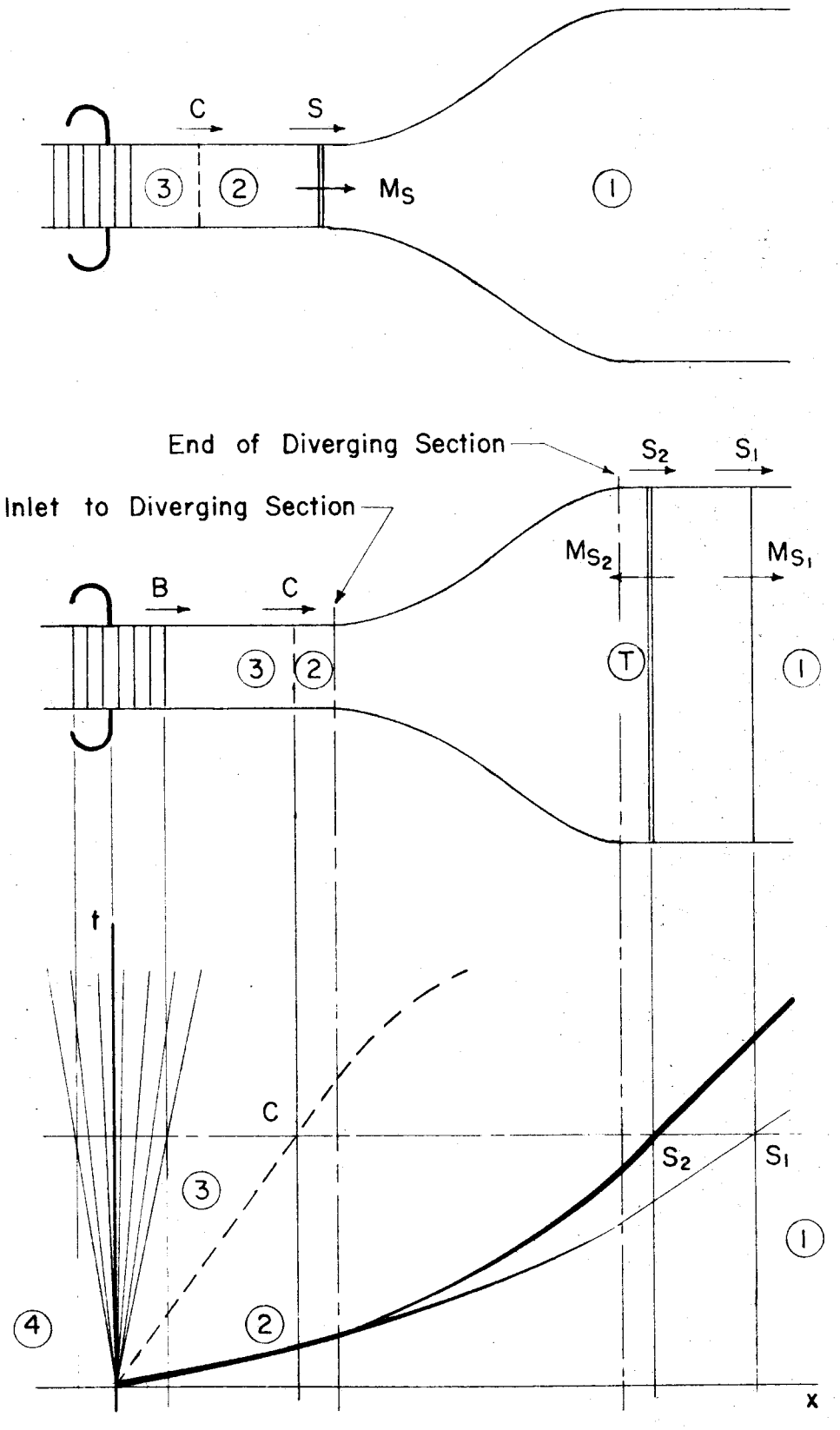

FIG. 4 — FLOW ESTABLISHMENT IN A BUSEMANN-NOZZLE

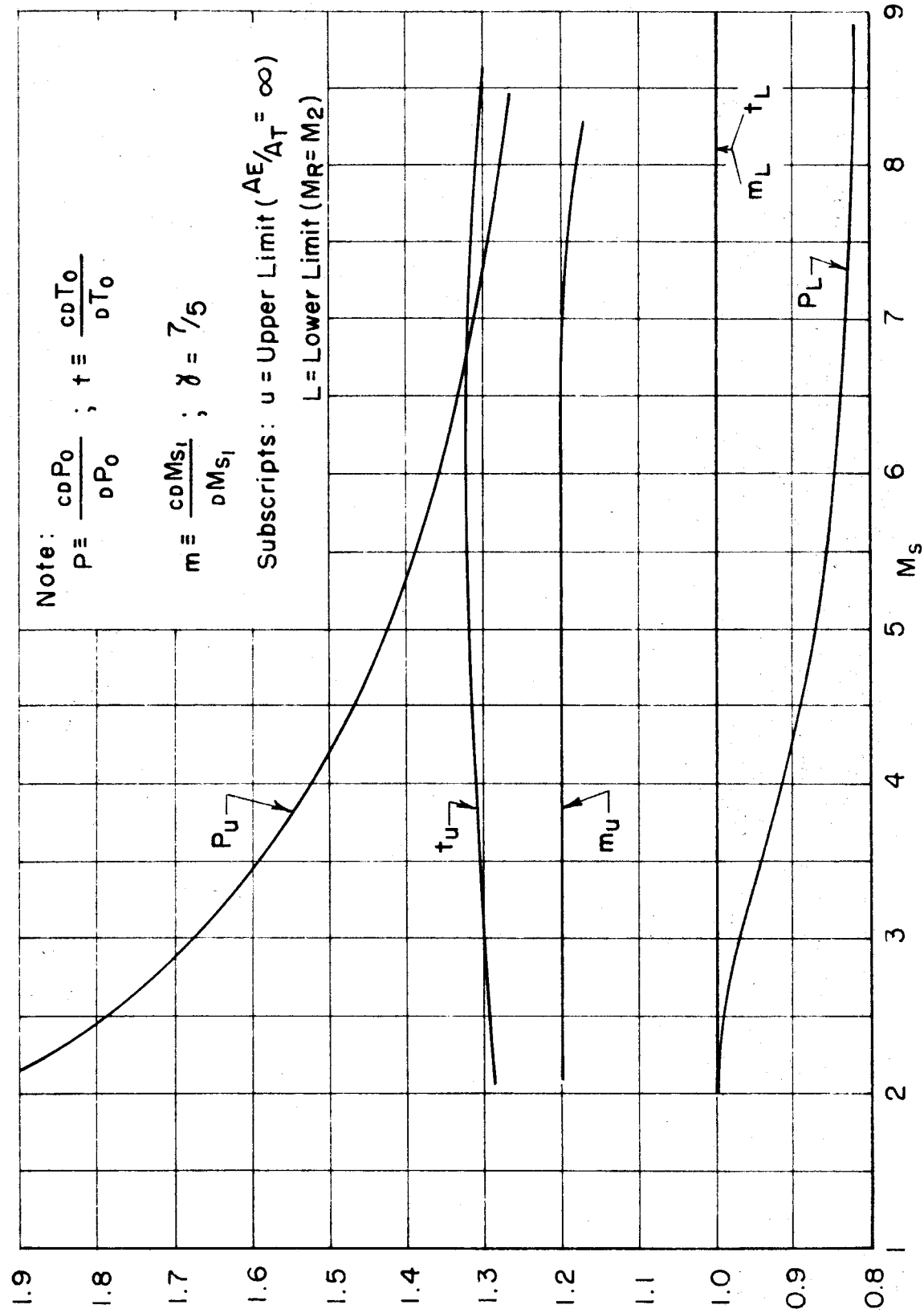
Note:
$P \equiv \frac{cDP_0}{DP_0}$; $t \equiv \frac{cDT_0}{DT_0}$
$m \equiv \frac{cDM_{S_1}}{DM_{S_1}}$; $\gamma = 7/5$
Subscripts: u = Upper Limit ($A_E/A_T^* = \infty$)
L = Lower Limit ($M_R = M_2$)
P_u
t_u
m_u
m_L t_L
P_L
M_S
1.9
1.8
1.7
1.6
1.5
1.4
1.3
1.2
1.1
1.0
0.9
0.8
1
2
3
4
5
6
7
8
9

FIG. 5

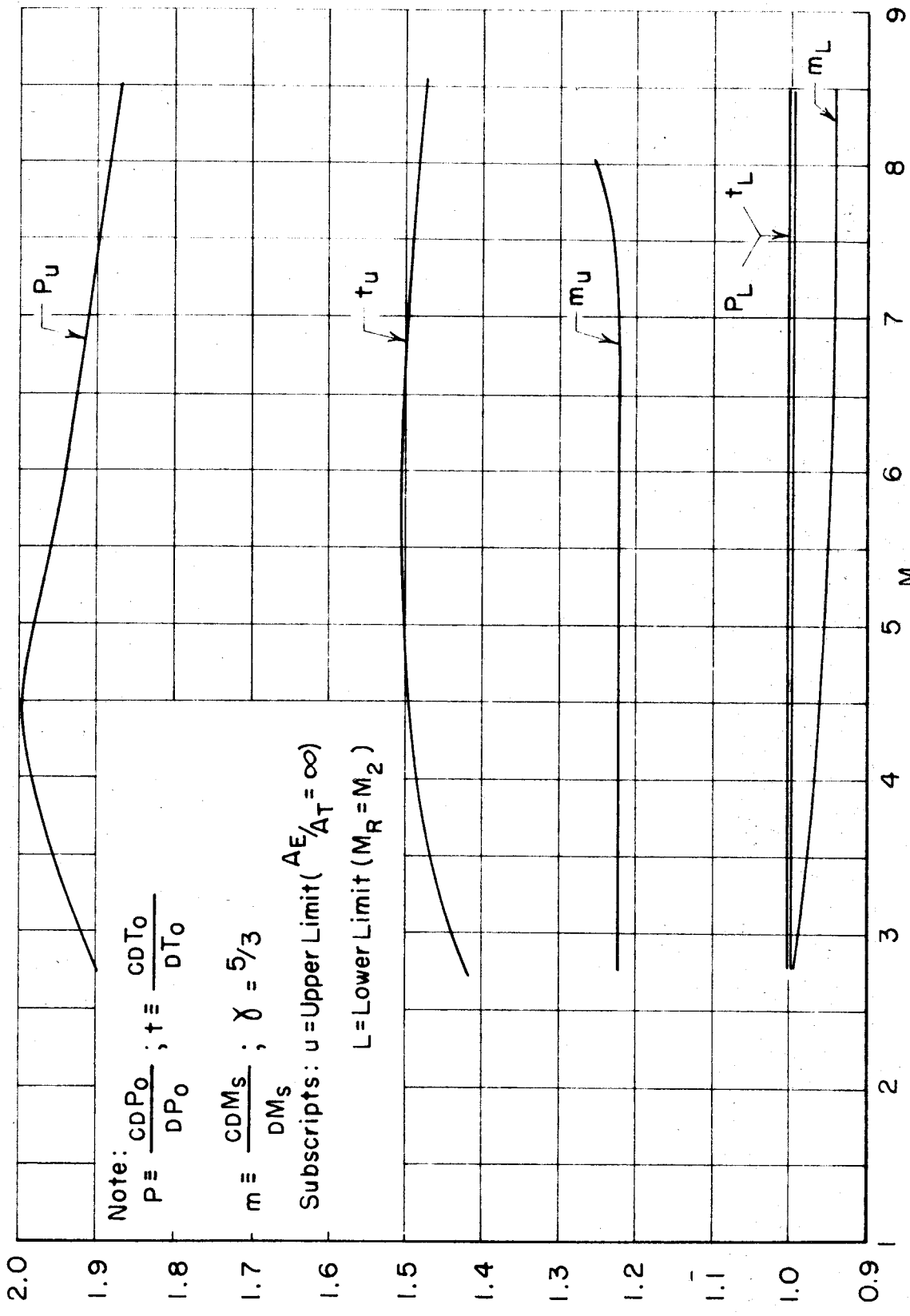
Note: $P \equiv \frac{cDP_o}{DP_o}$; $t \equiv \frac{cDT_o}{DT_o}$
$m \equiv \frac{cDM_s}{DM_s}$; $\gamma = 5/3$
Subscripts: u = Upper Limit ($A_E/A_T = \infty$)
L = Lower Limit ($M_R = M_2$)
P_u
t_u
m_u
P_L
t_L
m_L
M_s
2.0
1.9
1.8
1.7
1.6
1.5
1.4
1.3
1.2
1.1
1.0
0.9
1
2
3
4
5
6
7
8
9

FIG. 6

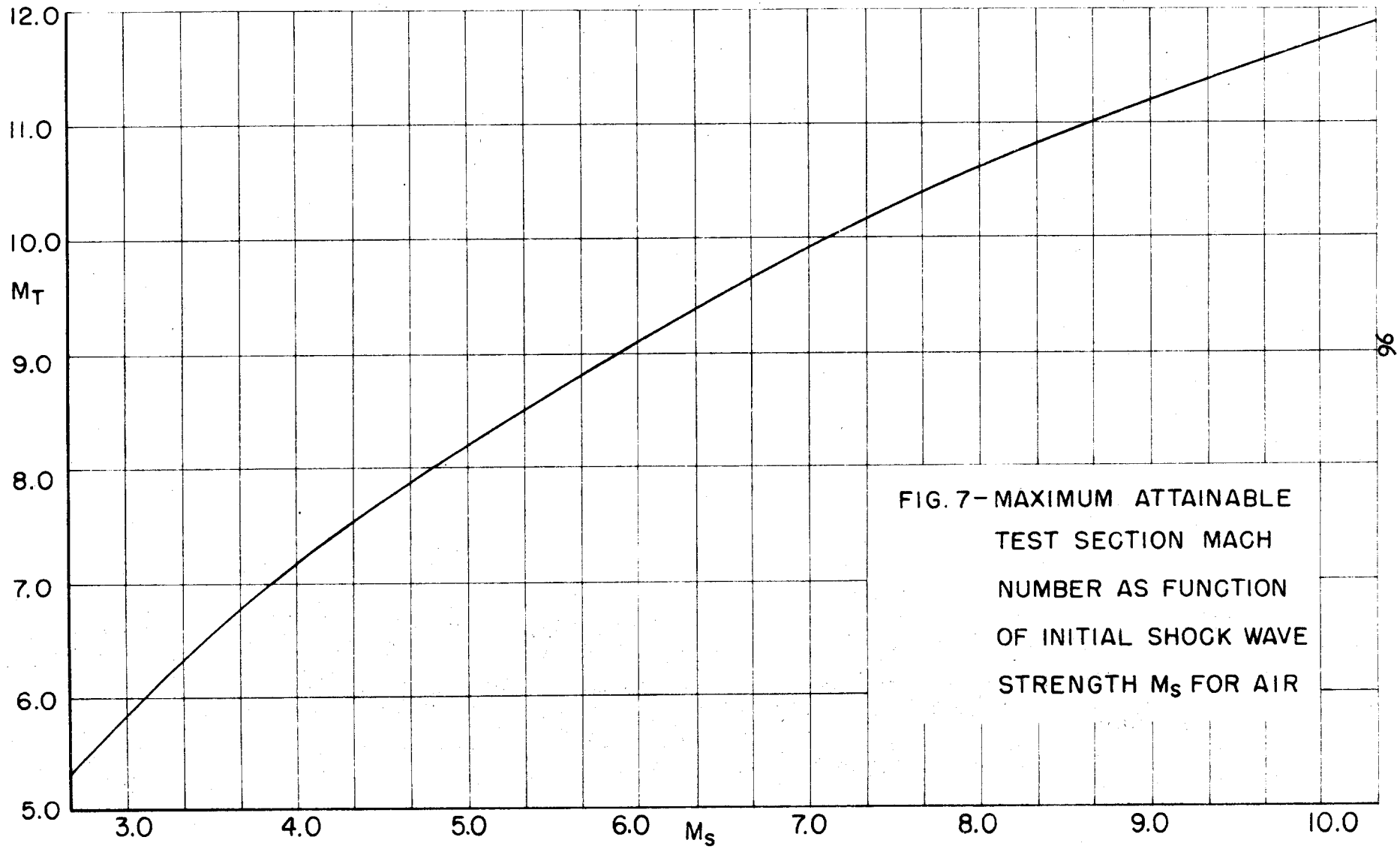

FIG. 7 – MAXIMUM ATTAINABLE TEST SECTION MACH NUMBER AS FUNCTION OF INITIAL SHOCK WAVE STRENGTH M_s FOR AIR

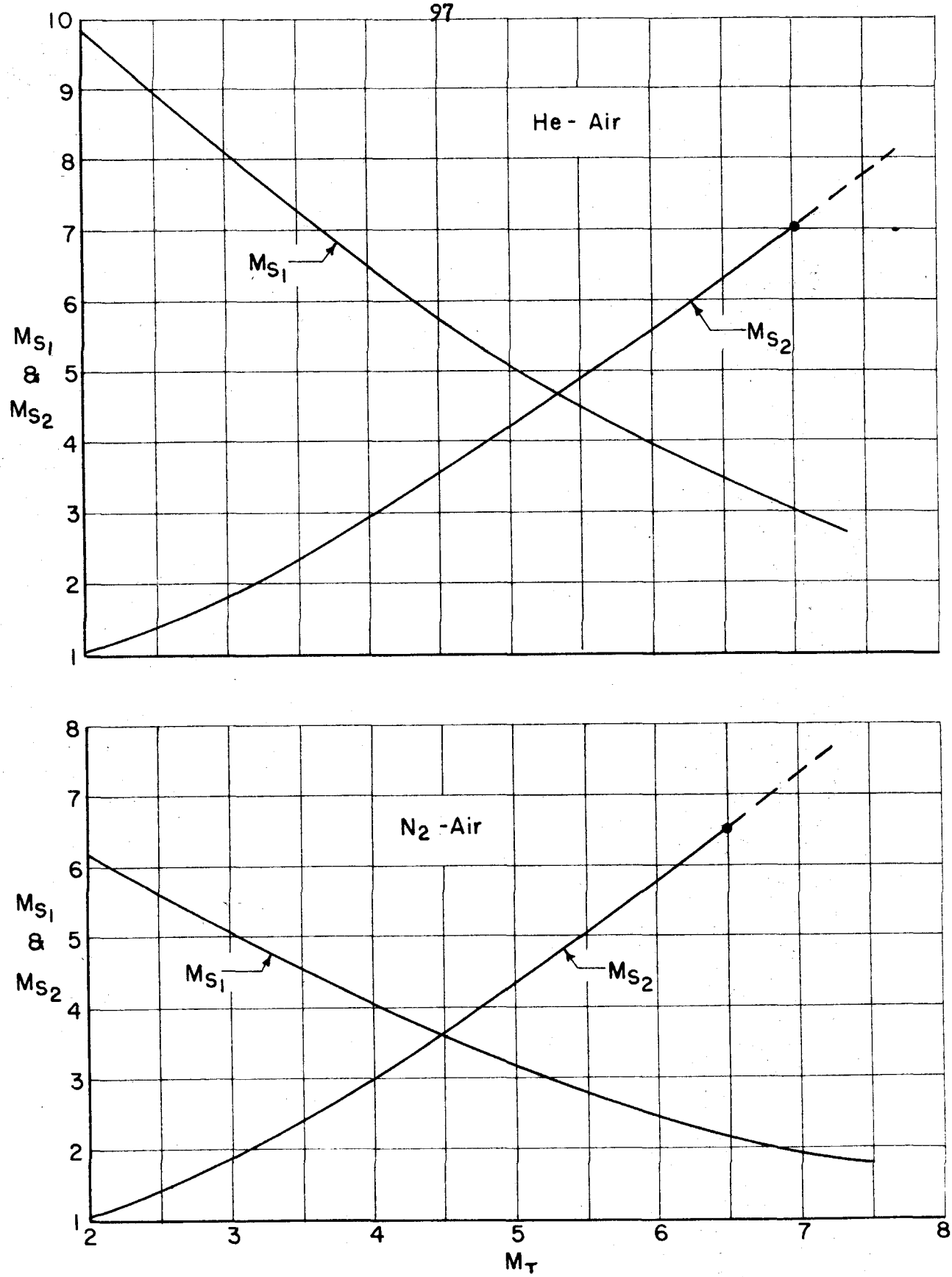

FIG. 8 — STRENGTHS M_{S_1} AND M_{S_2} OF THE TWO SHOCK WAVES IN A BUSEMANN NOZZLE AS A FUNCTION OF TEST SECTION MACH NUMBER M_T – $P_4/P_1 = \infty$, $T_4/T_1 = 1$

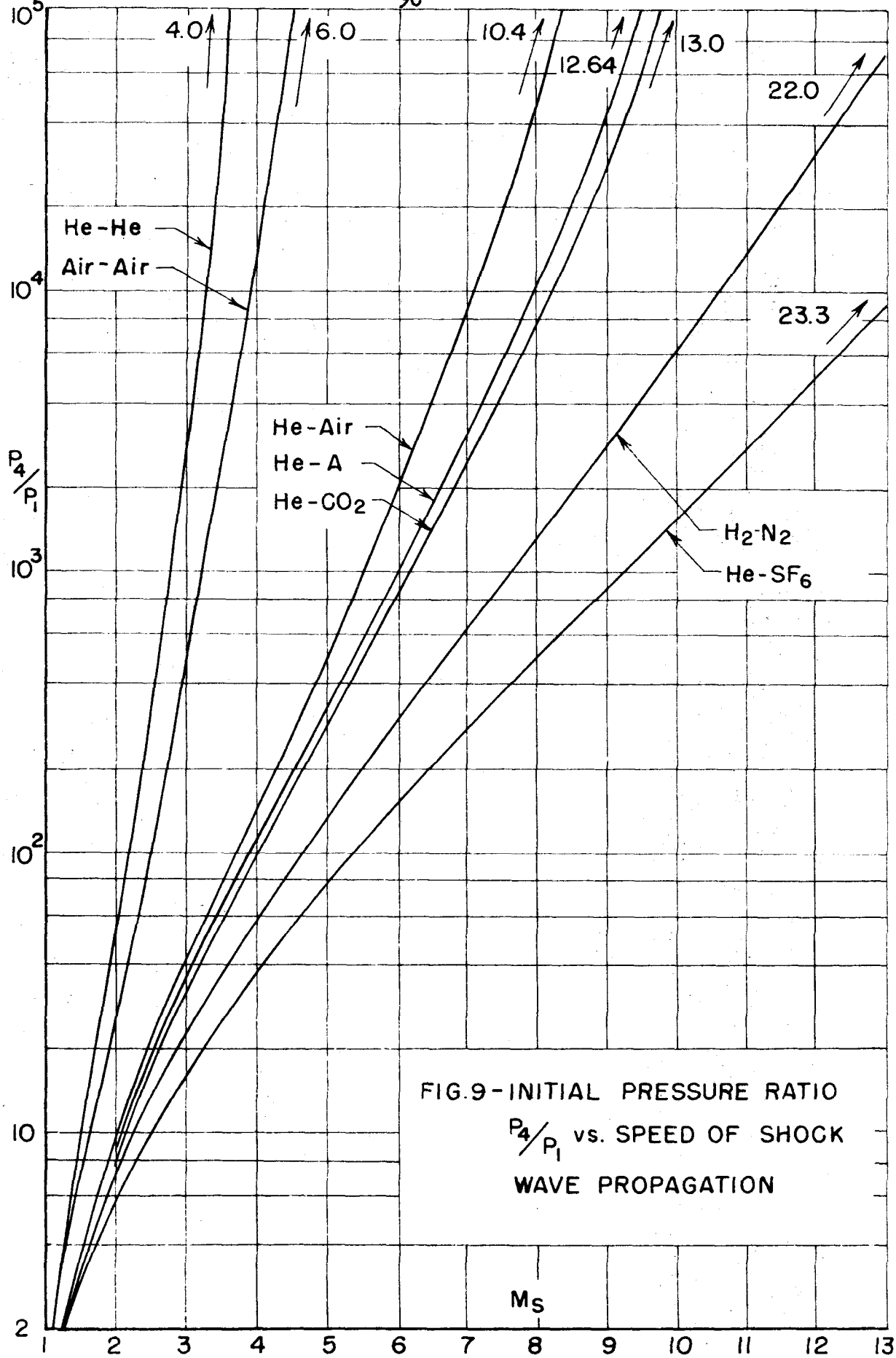

FIG. 9 - INITIAL PRESSURE RATIO P_4/P_1 vs. SPEED OF SHOCK WAVE PROPAGATION

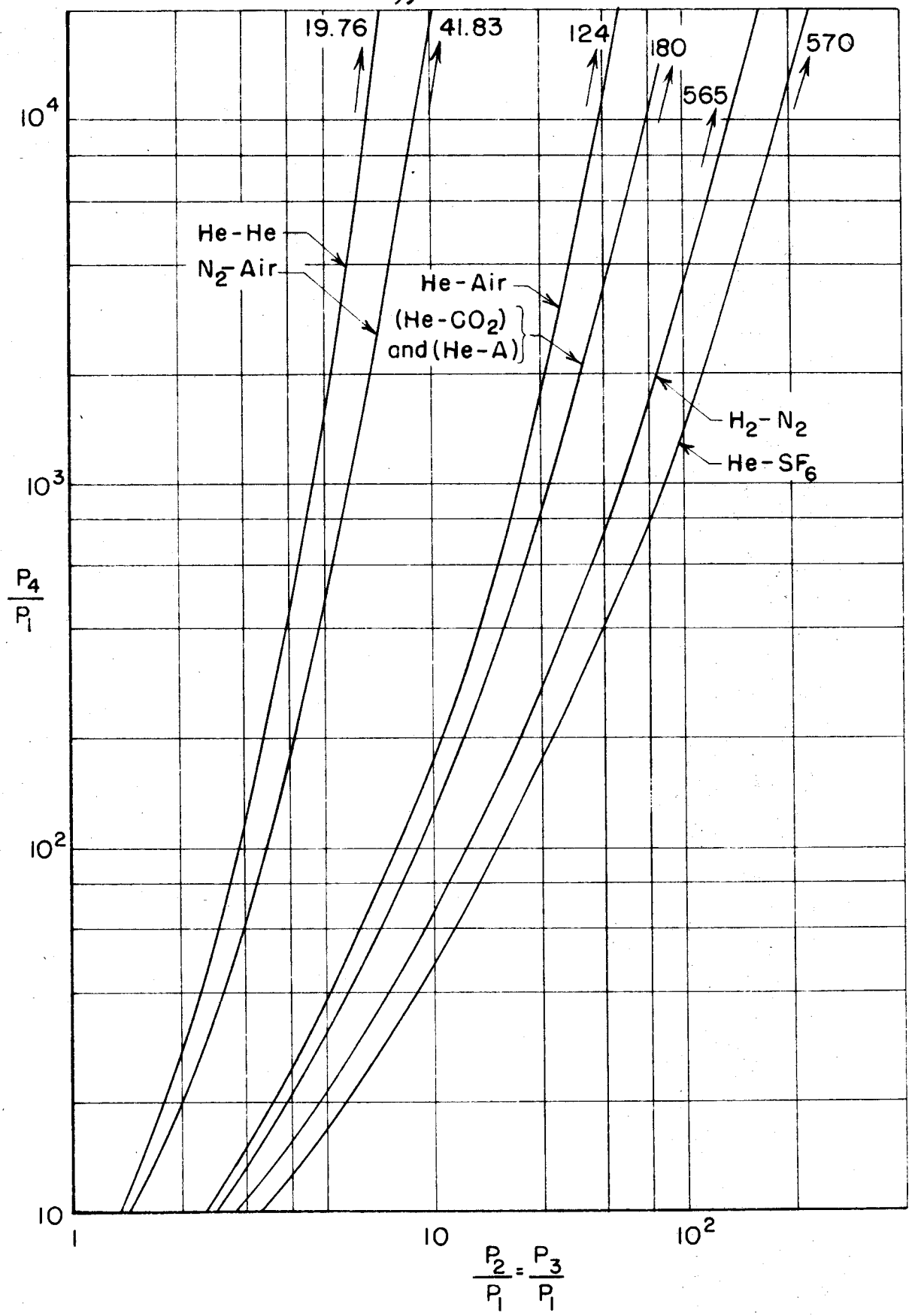
19.76
41.83
124
180
565
570
He-He
N2-Air
He-Air
(He-CO2) and (He-A)
H2-N2
He-SF6
10^4
10^3
10^2
10
1
10
10^2
P4/P1
P2/P1 = P3/P1

FIG. 10

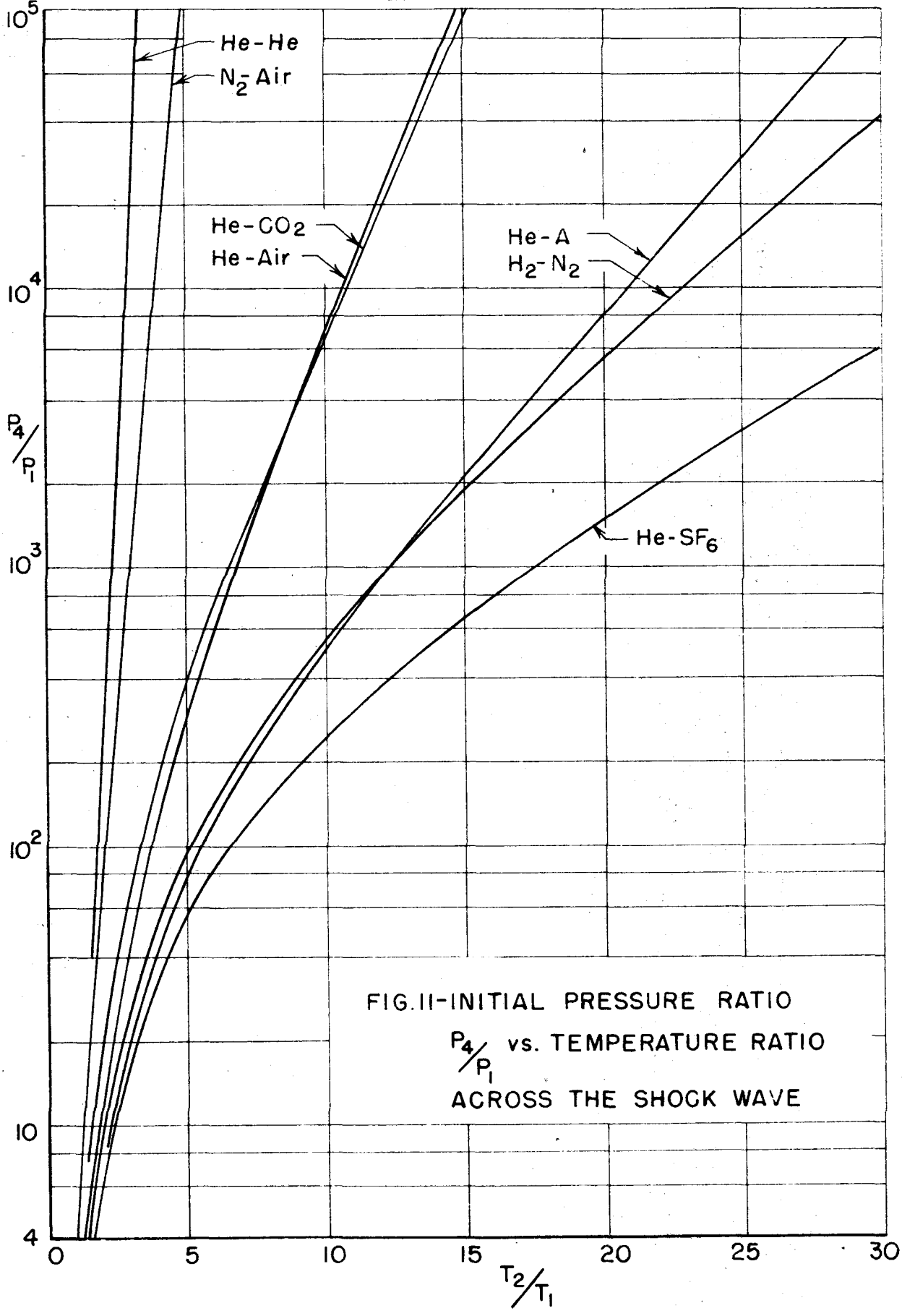

FIG. II-INITIAL PRESSURE RATIO P_4/P_1 vs. TEMPERATURE RATIO ACROSS THE SHOCK WAVE

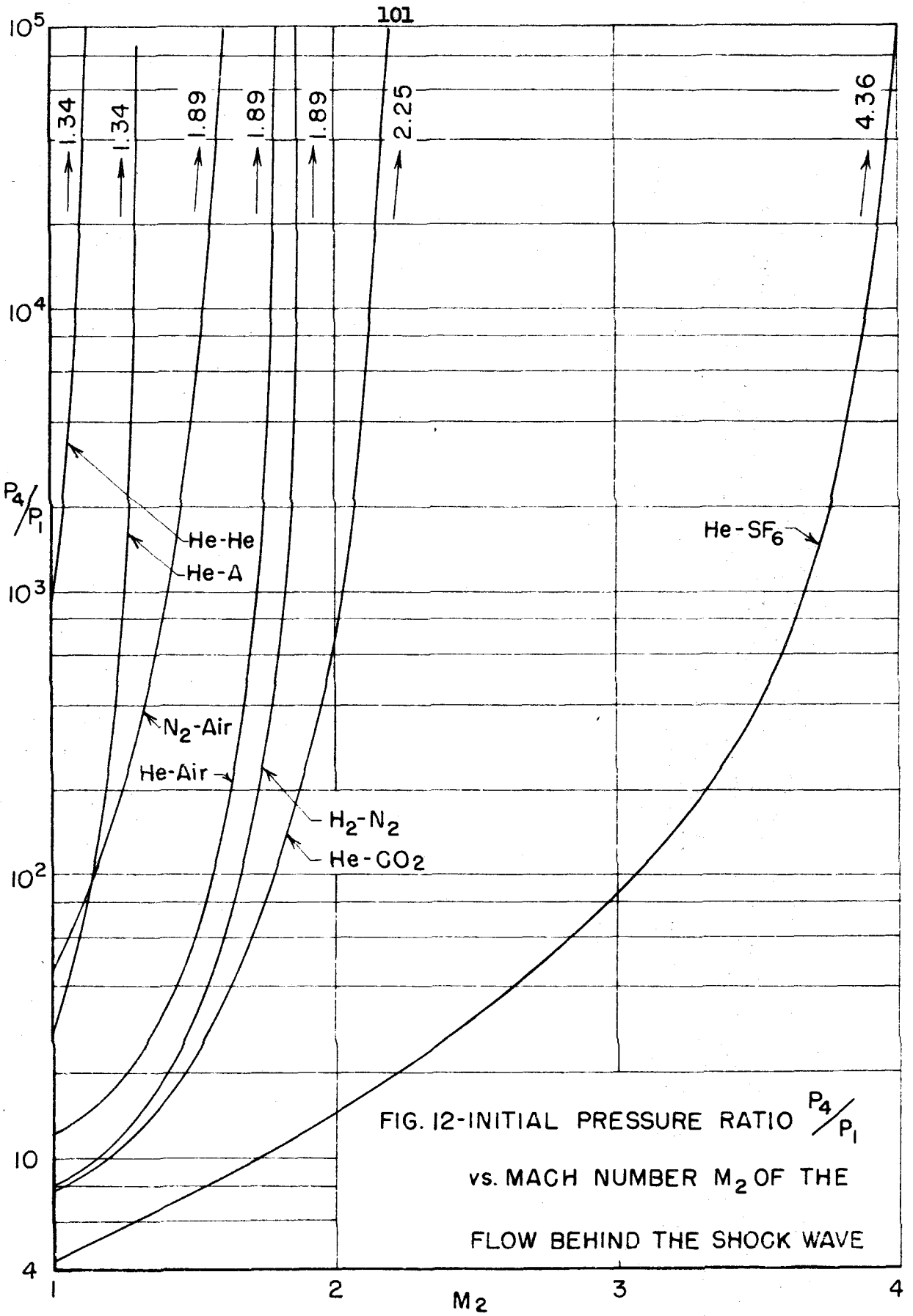

FIG. 12-INITIAL PRESSURE RATIO P_4/P_1 vs. MACH NUMBER M_2 OF THE FLOW BEHIND THE SHOCK WAVE

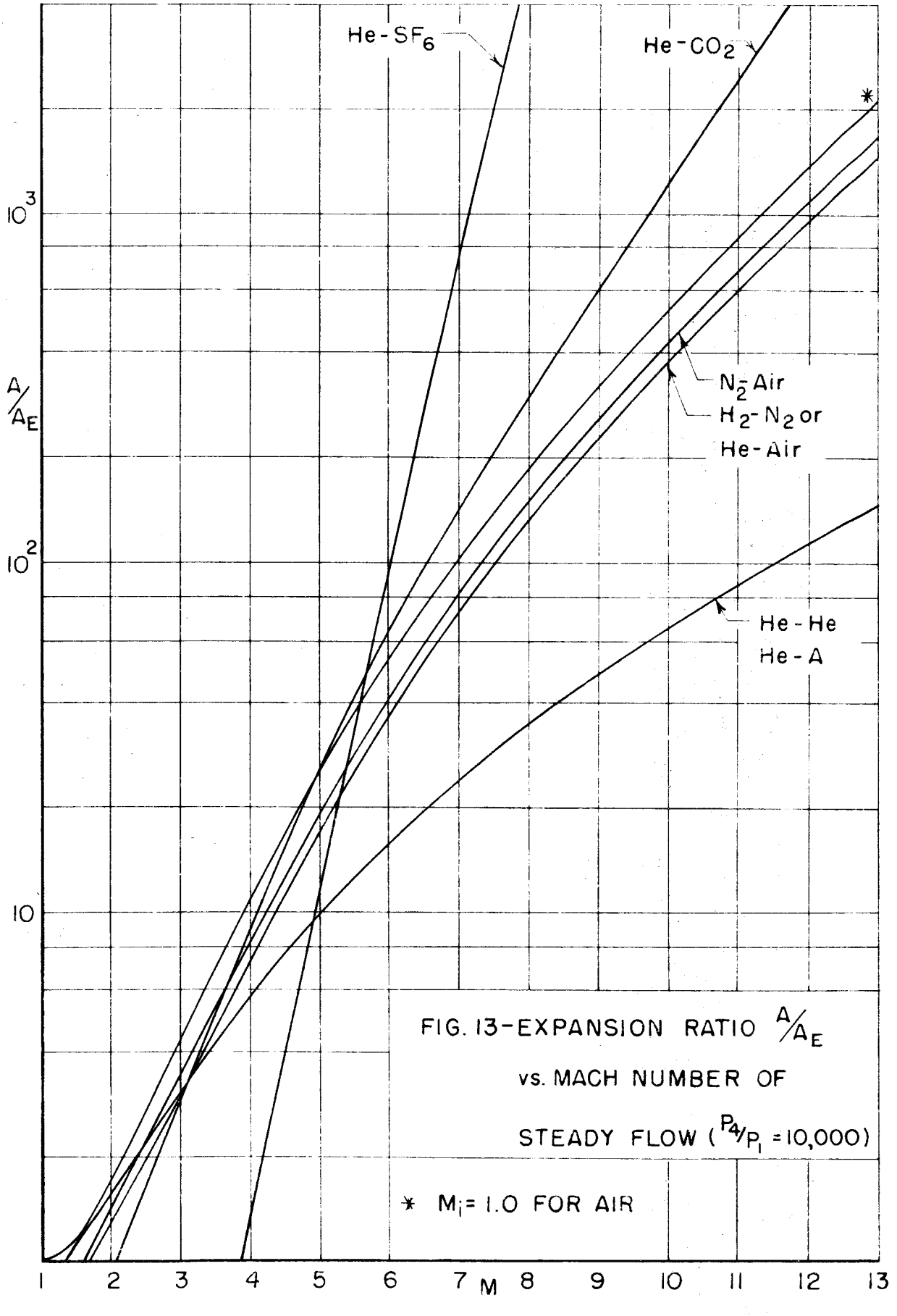

FIG. 13-EXPANSION RATIO A/A_E vs. MACH NUMBER OF STEADY FLOW ($P_4/P_1 = 10{,}000$)

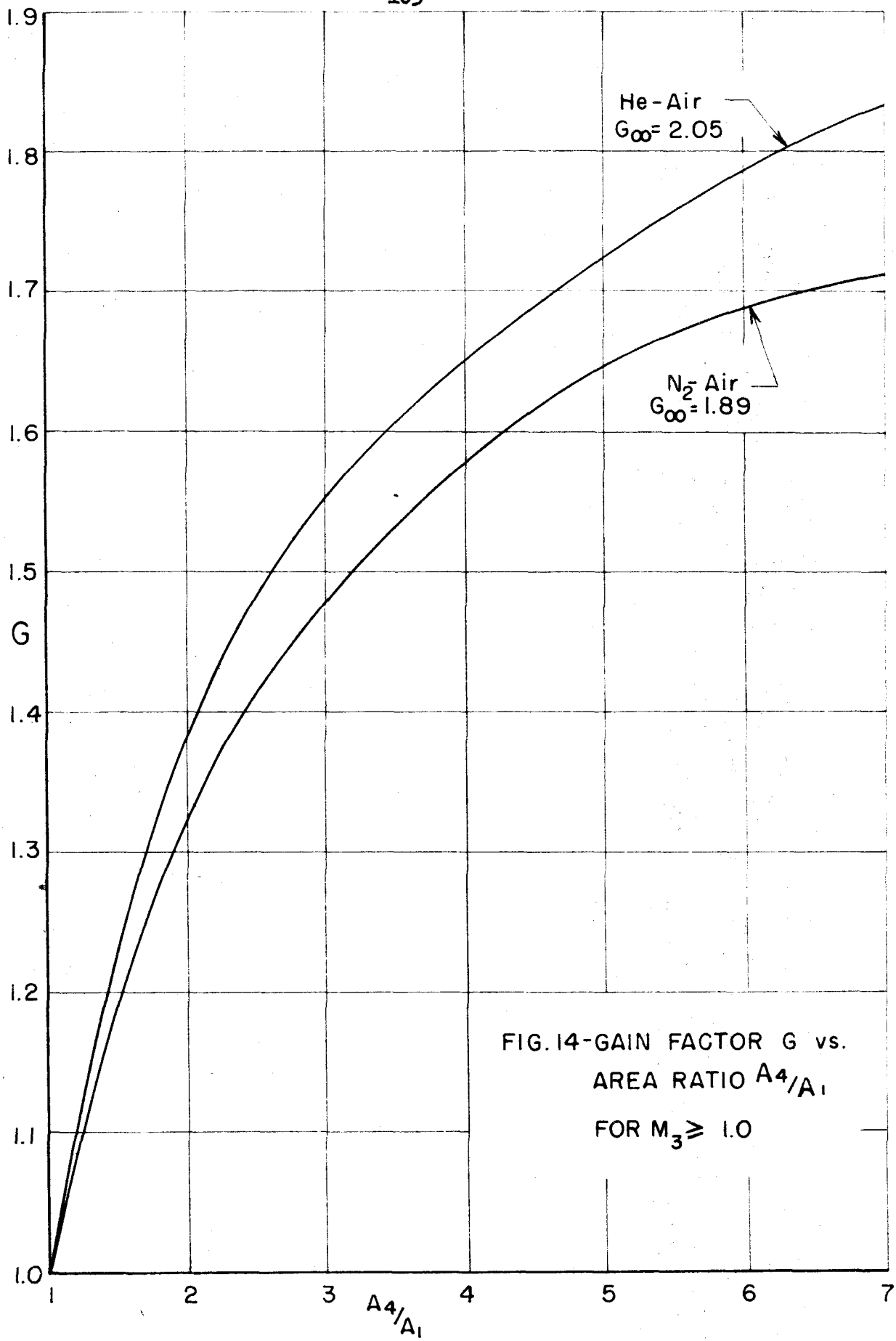

FIG. 14-GAIN FACTOR G vs. AREA RATIO A_4/A_1 FOR $M_3 \geq 1.0$

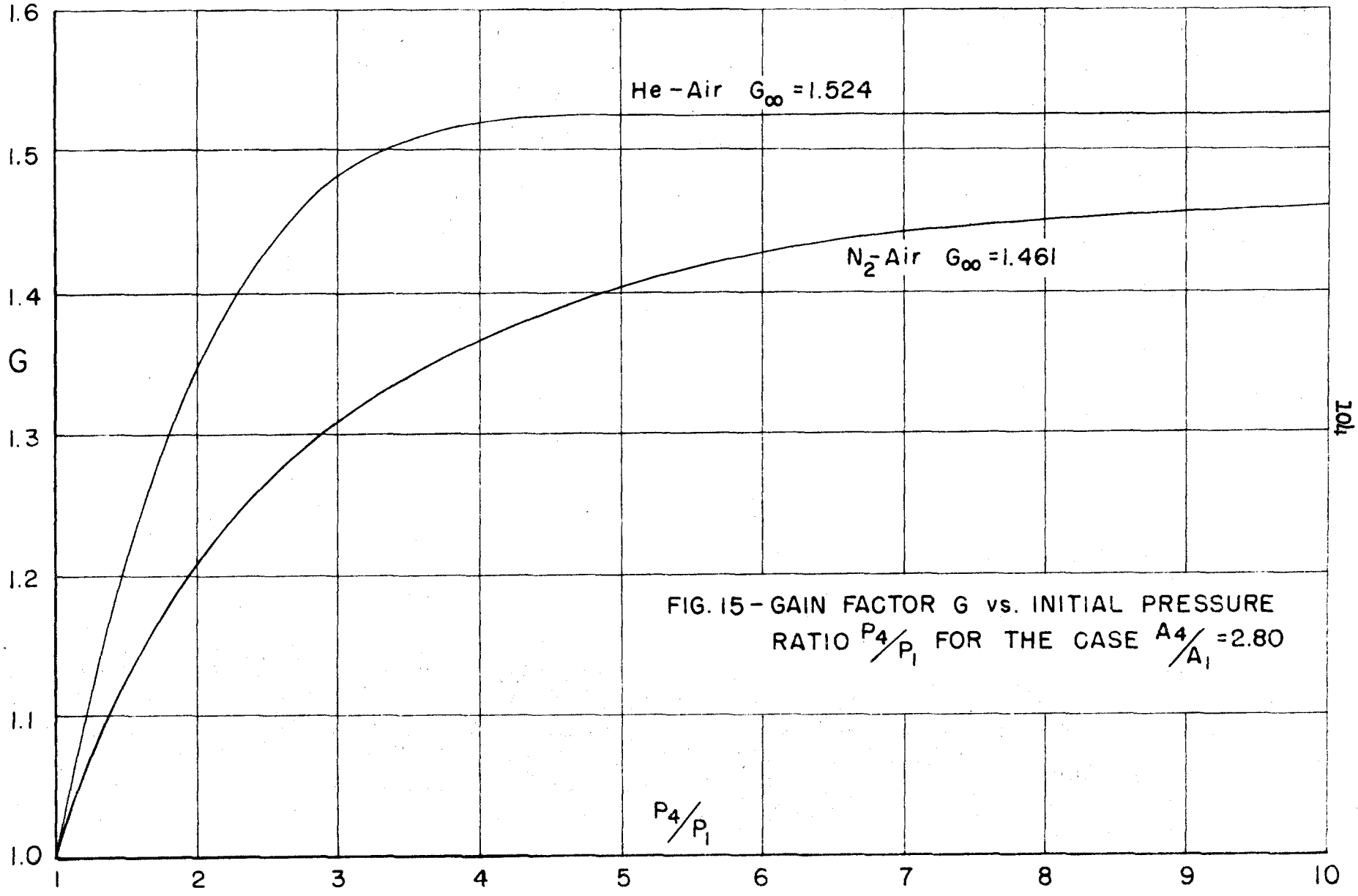

FIG. 15 - GAIN FACTOR G vs. INITIAL PRESSURE RATIO P_4/P_1 FOR THE CASE $A_4/A_1 = 2.80$

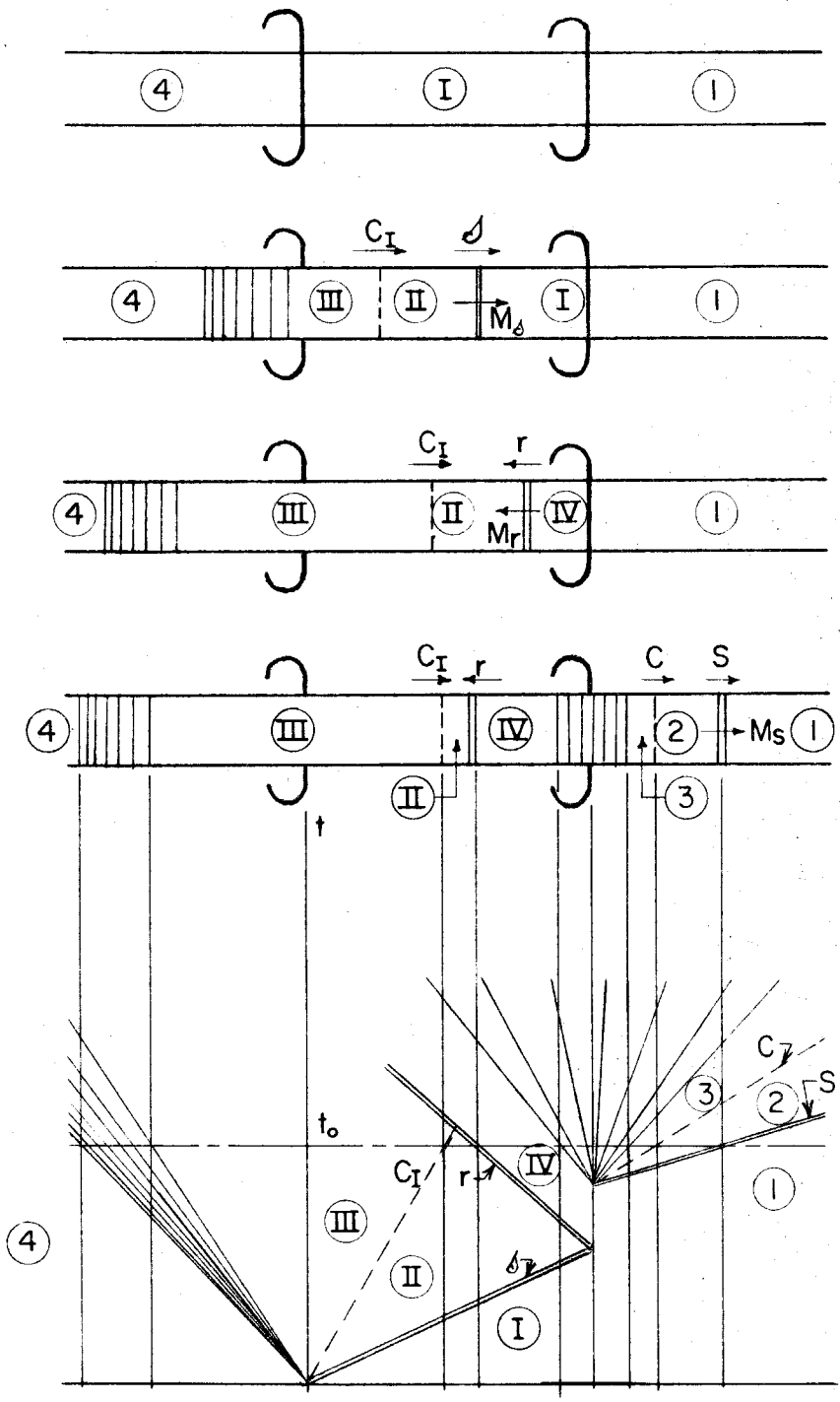

FIG. 16 — TIME HISTORY OF DELAYED DOUBLE DIAPHRAGM FLOW

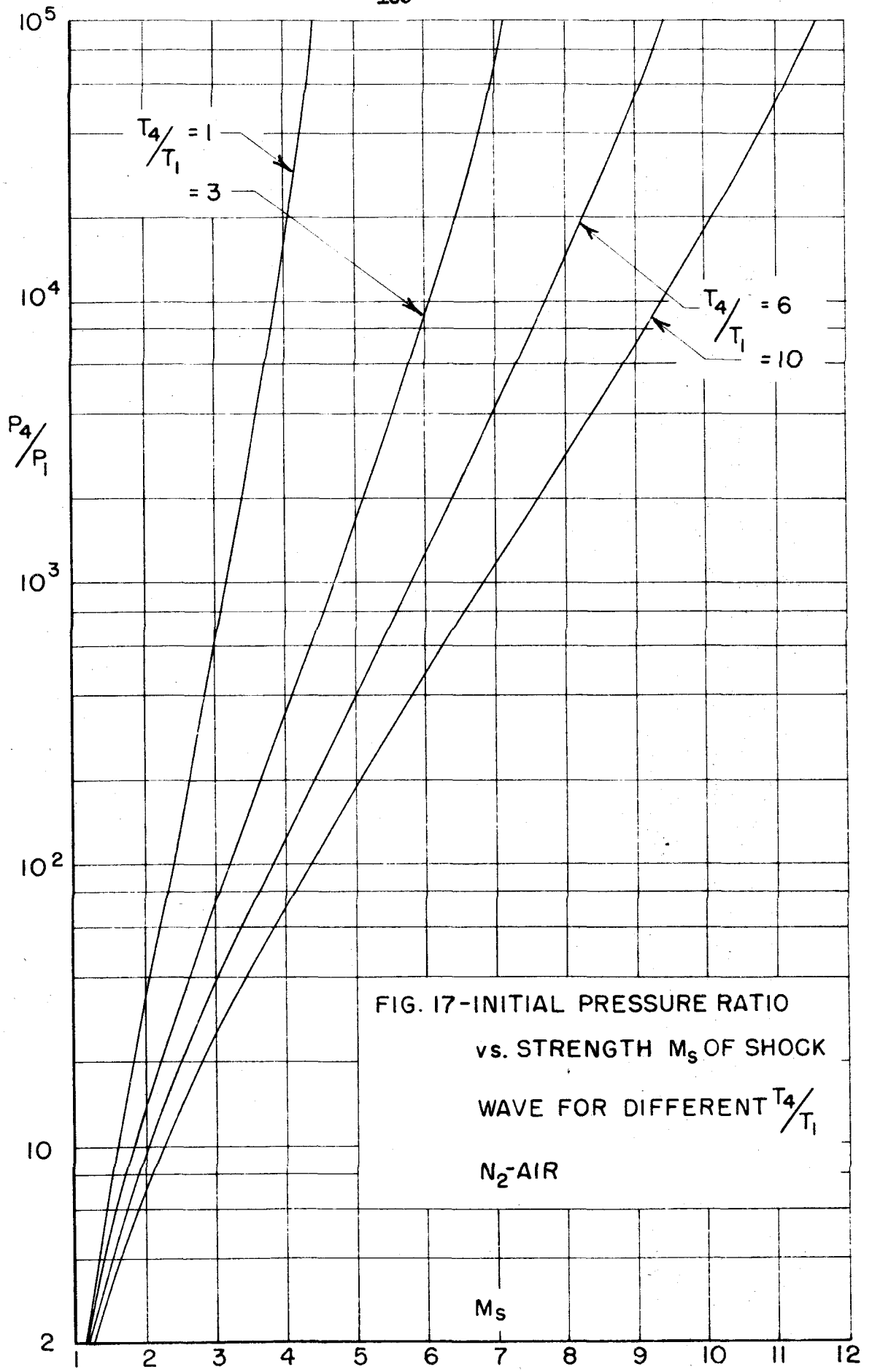

FIG. 17-INITIAL PRESSURE RATIO vs. STRENGTH M_s OF SHOCK WAVE FOR DIFFERENT T_4/T_1 N_2-AIR

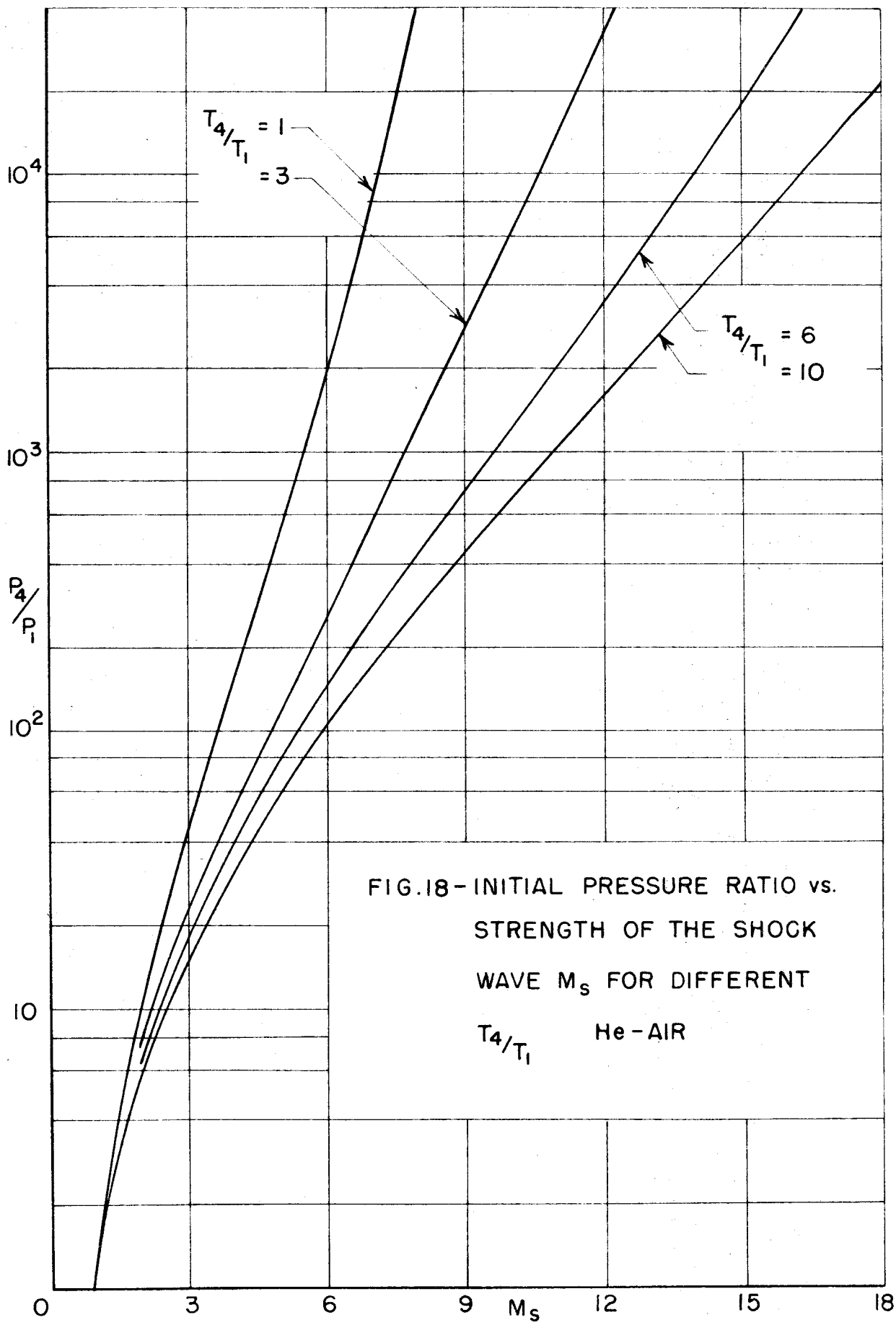

FIG. 18 - INITIAL PRESSURE RATIO vs. STRENGTH OF THE SHOCK WAVE M_s FOR DIFFERENT T_4/T_1 He - AIR

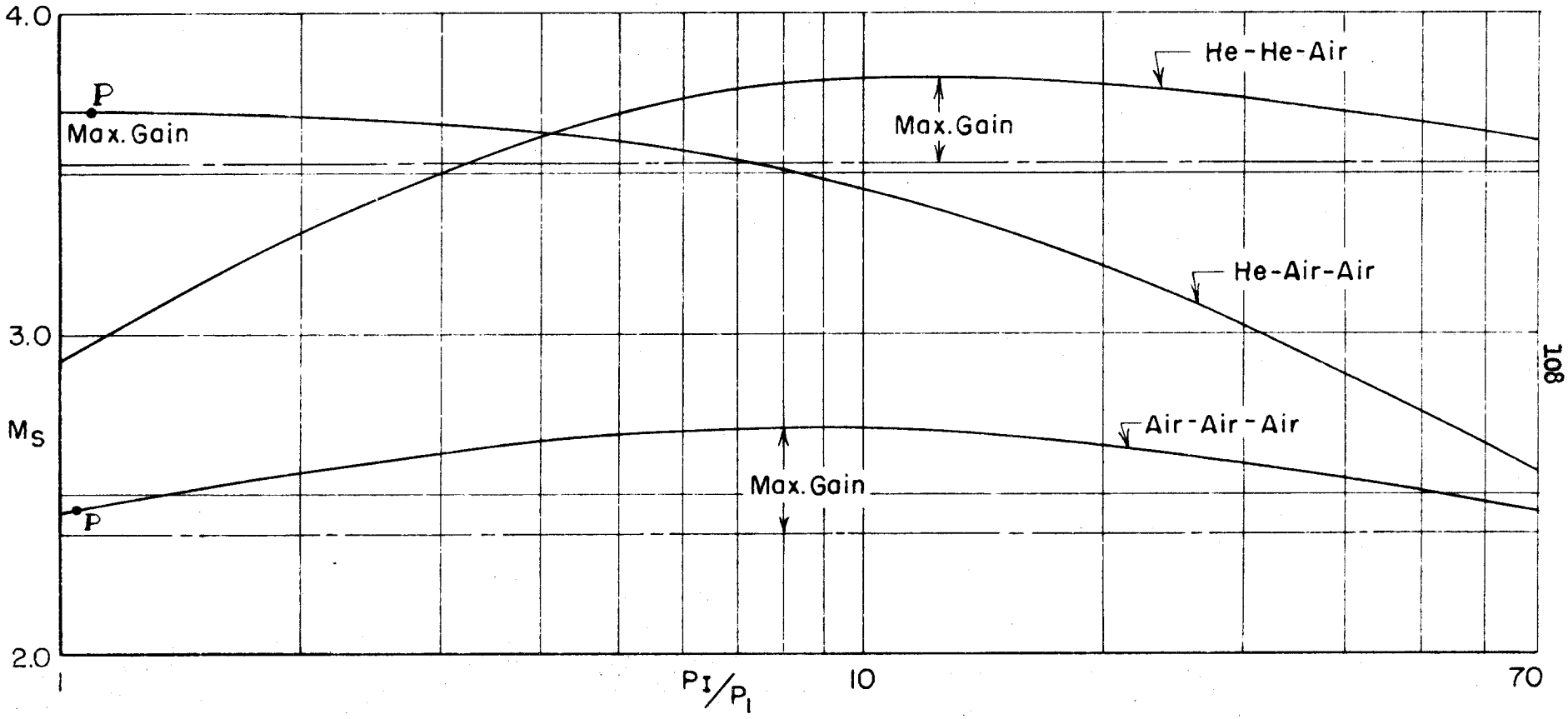

FIG.19-DOUBLE DIAPHRAGM METHOD STRENGTH M_S OF THE RESULTANT SHOCK vs. P_I/P_1 FOR $P_4/P_1 = 100$

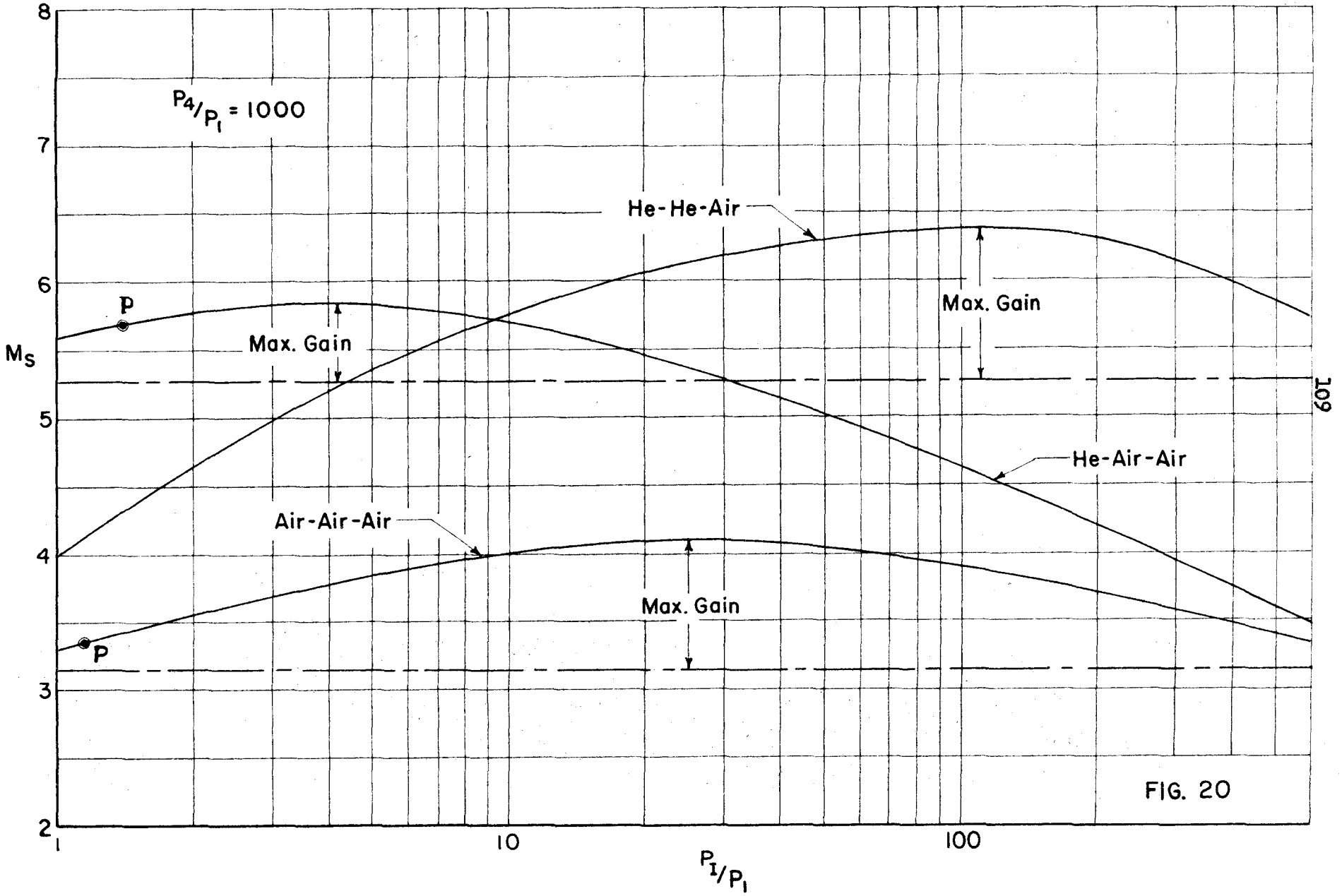
8
7
6
5
4
3
2
P_{4}/P_{1} = 1000
He-He-Air
P
Max. Gain
Max. Gain
M_S
He-Air-Air
Air-Air-Air
Max. Gain
P
1
10
100
P_I/P_1
109

FIG. 20

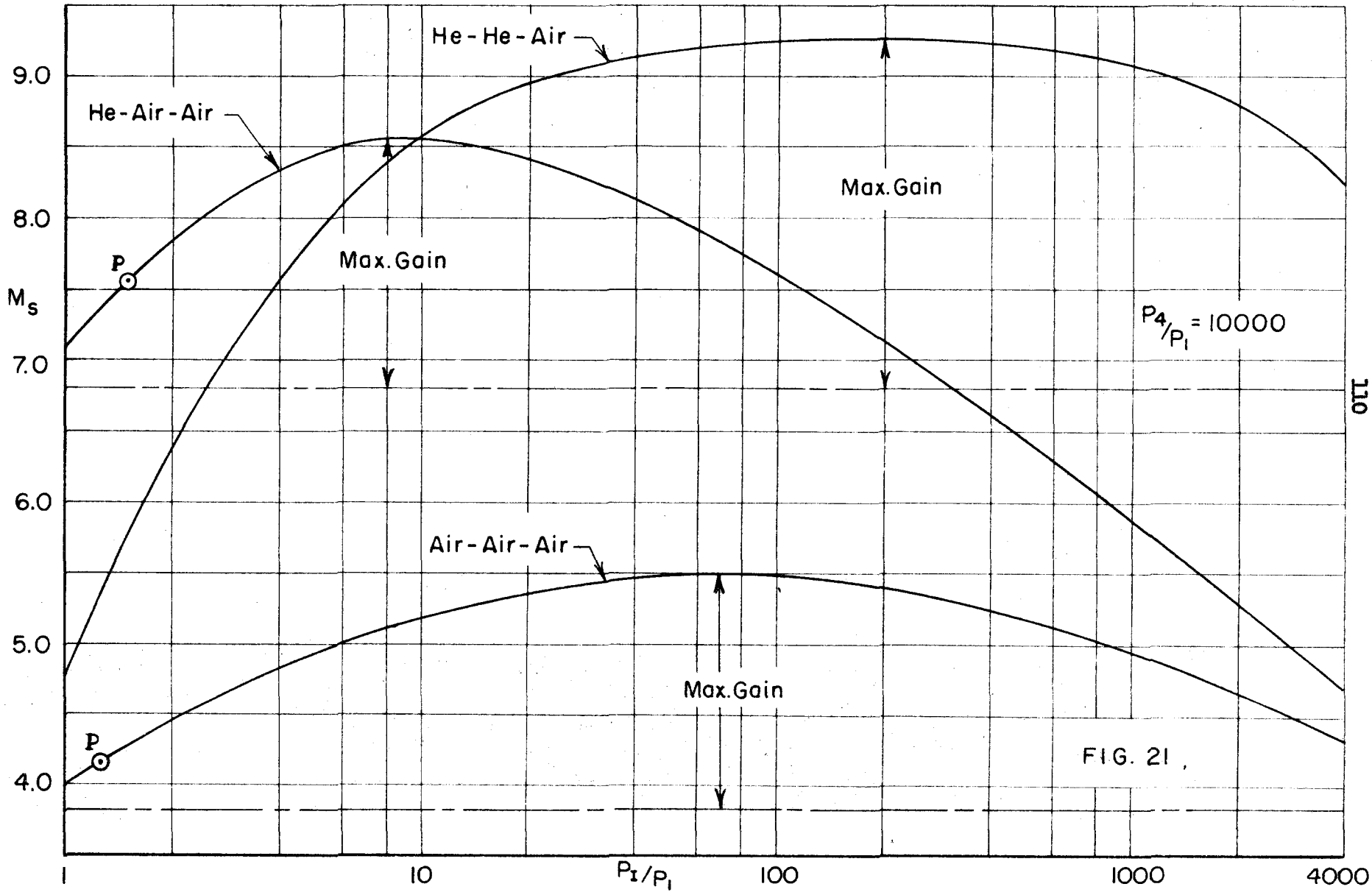
He - He - Air
He - Air - Air
Air - Air - Air
Max. Gain
Max. Gain
Max. Gain
P
P
M_s
$P_4/P_1 = 10000$
9.0
8.0
7.0
6.0
5.0
4.0
1
10
100
1000
4000
P_I/P_1
110

FIG. 21.

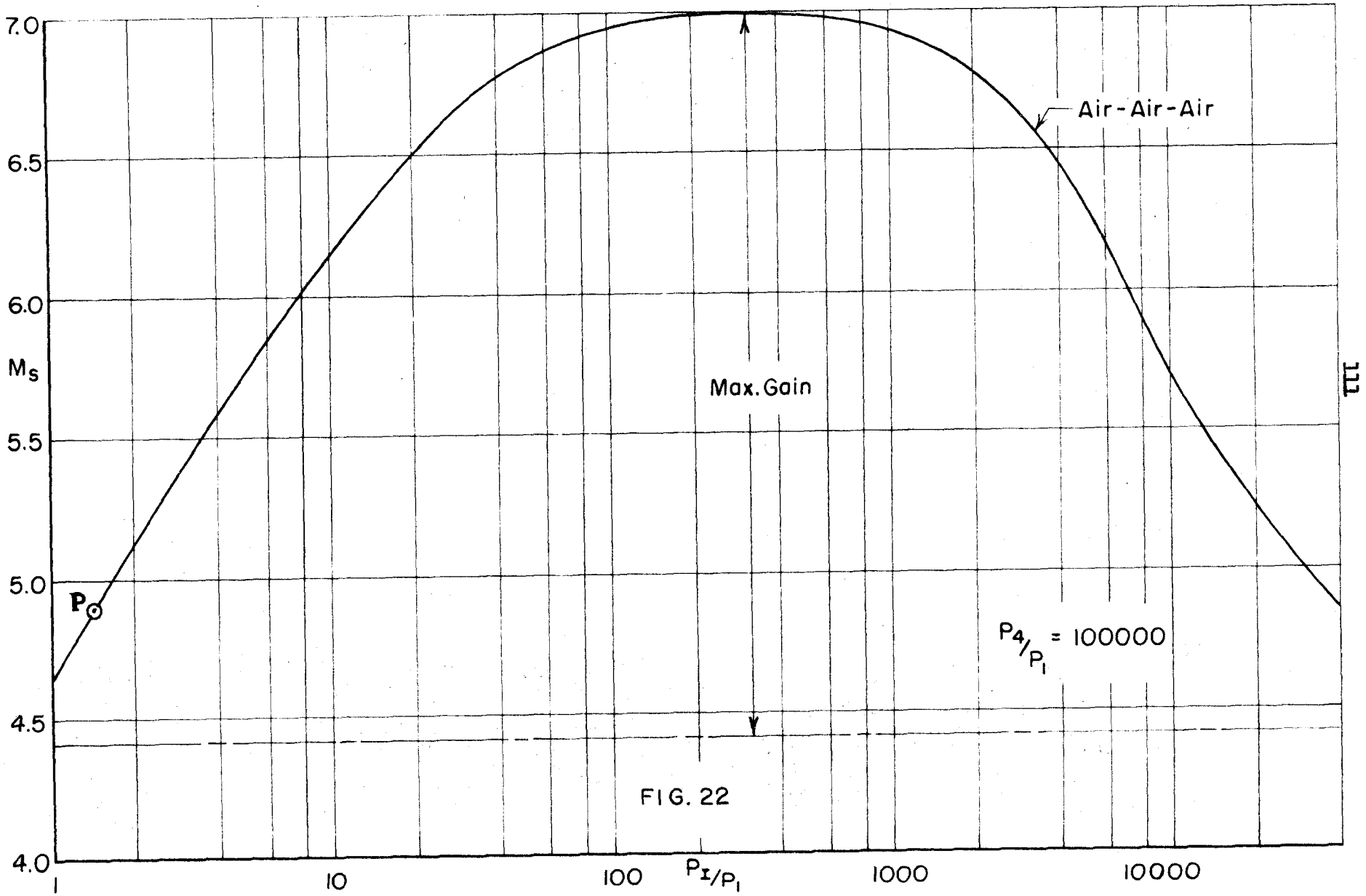
7.0
6.5
6.0
Ms
5.5
5.0
4.5
4.0
1
10
100
1000
10000
PI/P1
Air-Air-Air
Max. Gain
P0
P4/P1 = 100000
111

FIG. 22

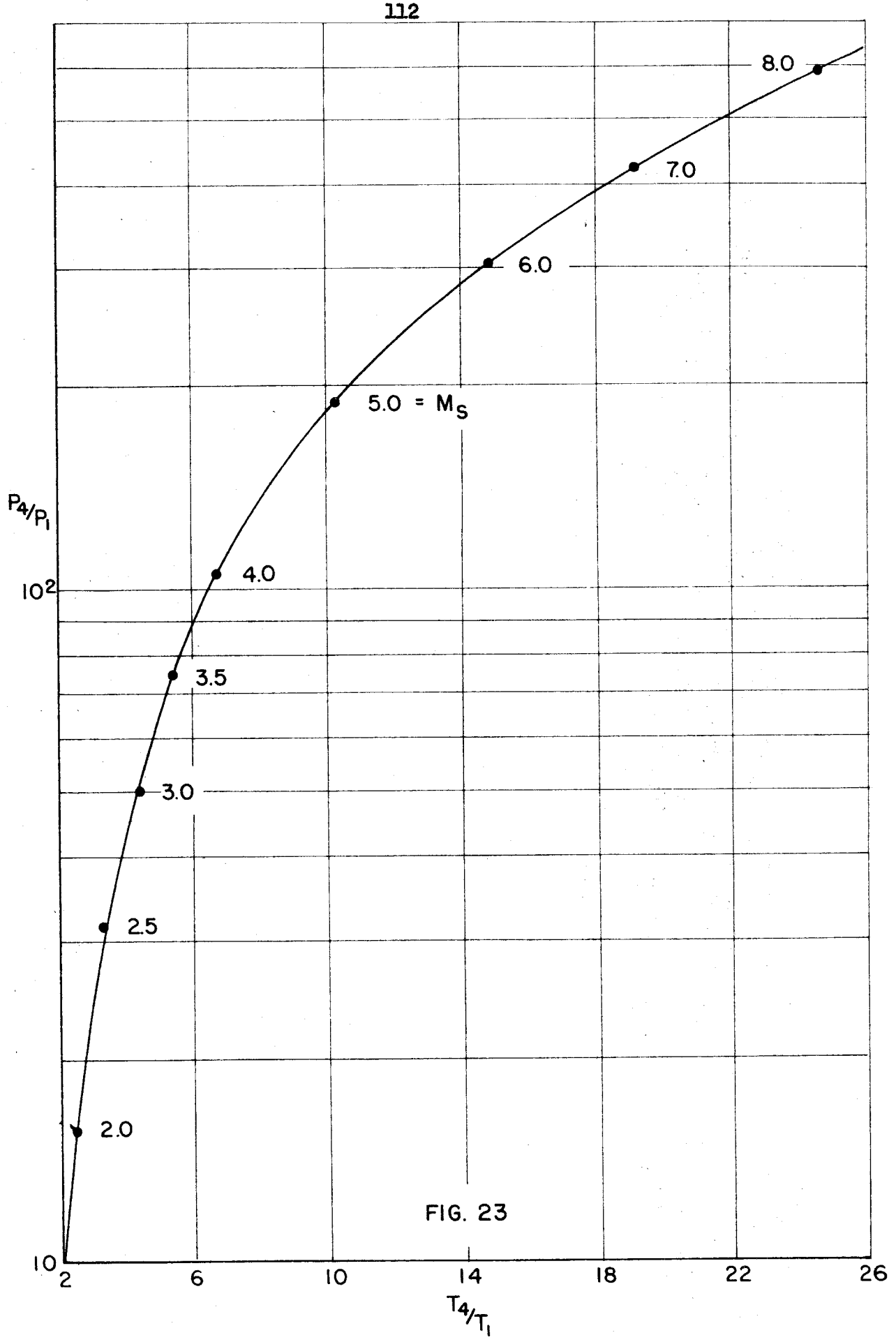

FIG. 23

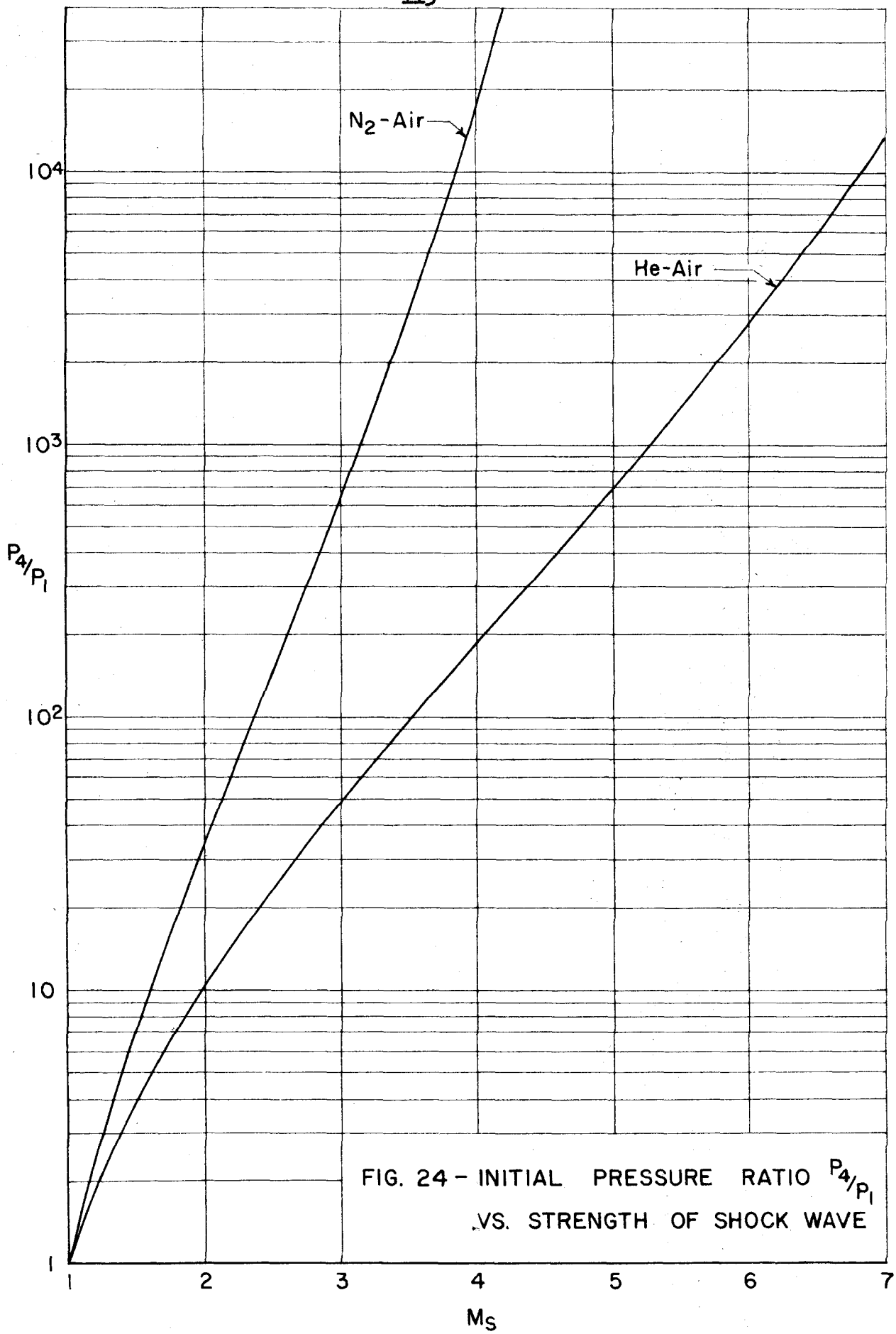

FIG. 24 - INITIAL PRESSURE RATIO P_4/P_1 VS. STRENGTH OF SHOCK WAVE

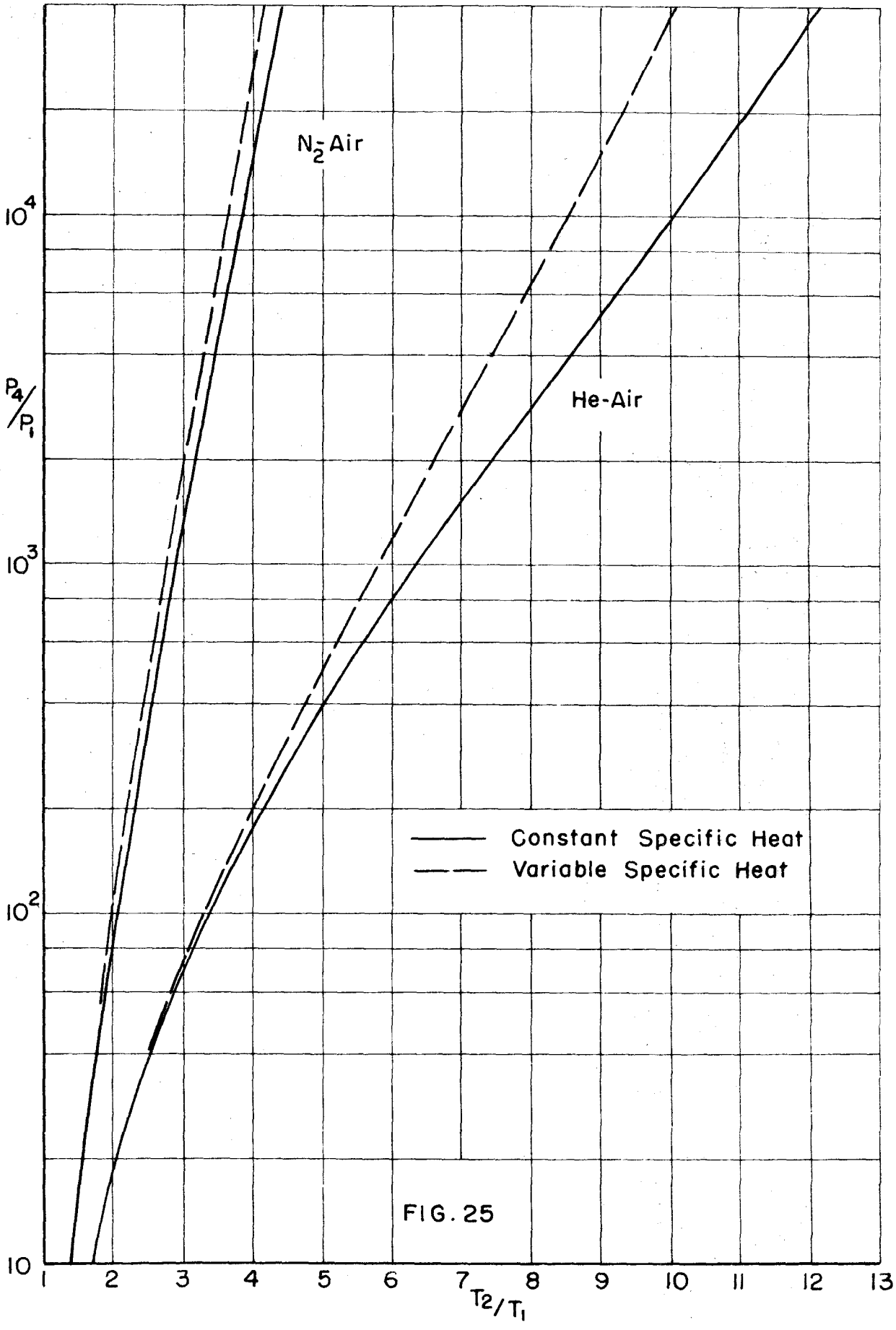
N_2-Air
He-Air
10^4
10^3
10^2
10
P_4/P_1
Constant Specific Heat
Variable Specific Heat
1
2
3
4
5
6
7
8
9
10
11
12
13
T_2/T_1

FIG. 25

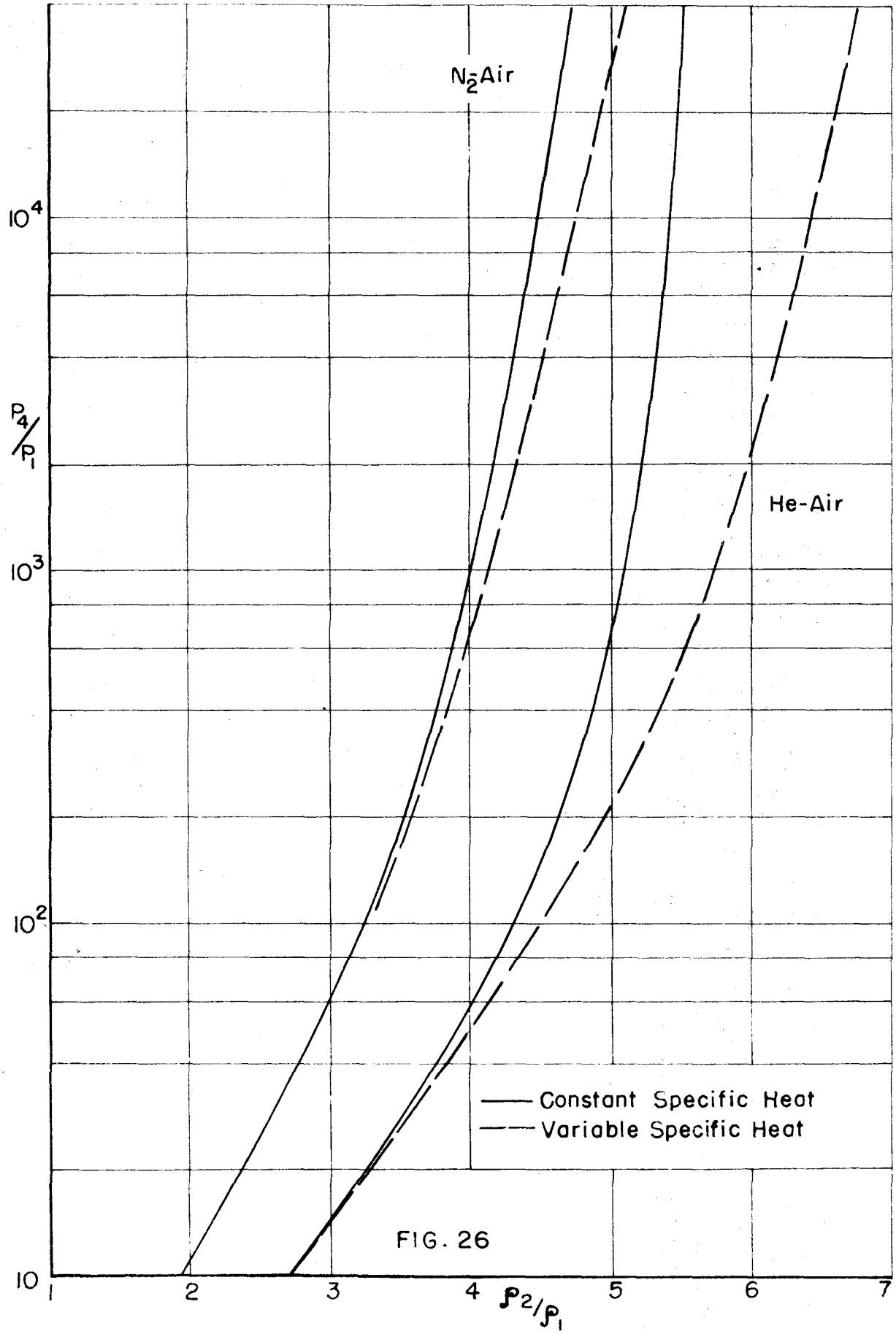
N_2-Air
He-Air
10^4
10^3
10^2
10
P_4/P_1
1
2
3
4
5
6
7
ρ_2/ρ_1
Constant Specific Heat
Variable Specific Heat

FIG. 26

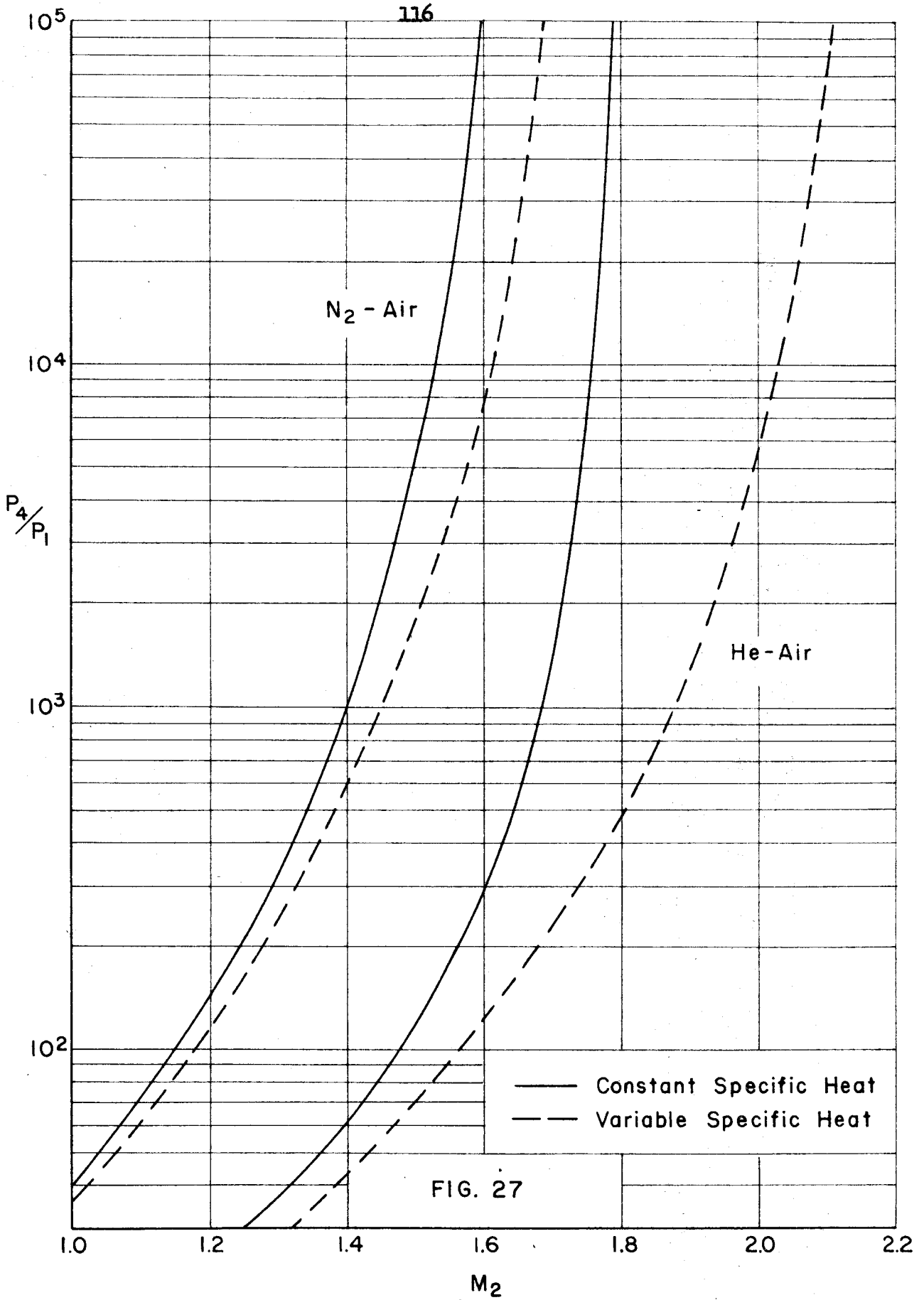
10^5
10^4
10^3
10^2
P_4/P_1
N_2 - Air
He - Air
Constant Specific Heat
Variable Specific Heat
1.0
1.2
1.4
1.6
1.8
2.0
2.2
M_2

FIG. 27

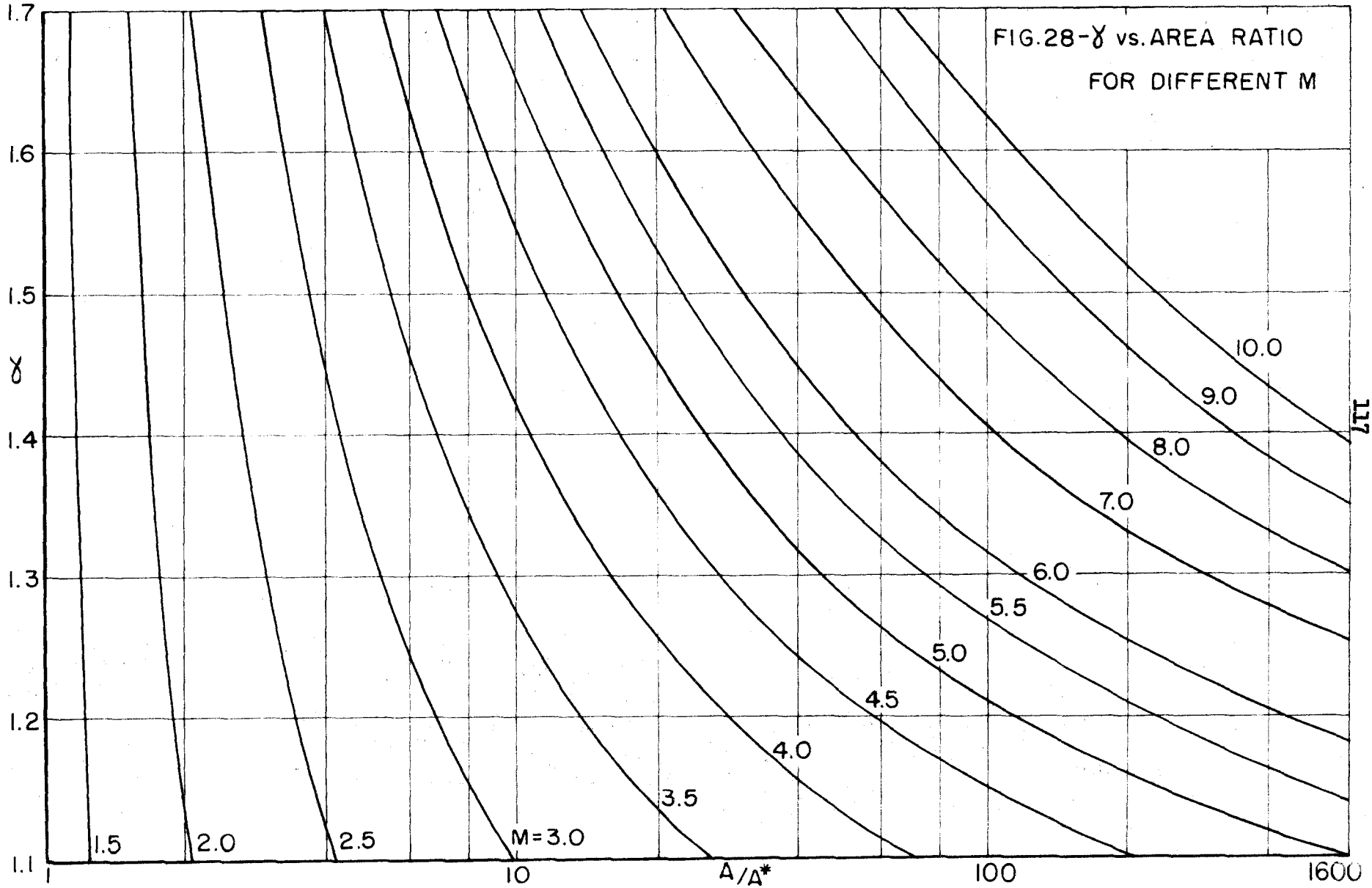
FIG.28-γ vs. AREA RATIO
FOR DIFFERENT M
γ
A/A*
1.7
1.6
1.5
1.4
1.3
1.2
1.1
1
10
100
1600
1.5
2.0
2.5
M=3.0
3.5
4.0
4.5
5.0
5.5
6.0
7.0
8.0
9.0
10.0

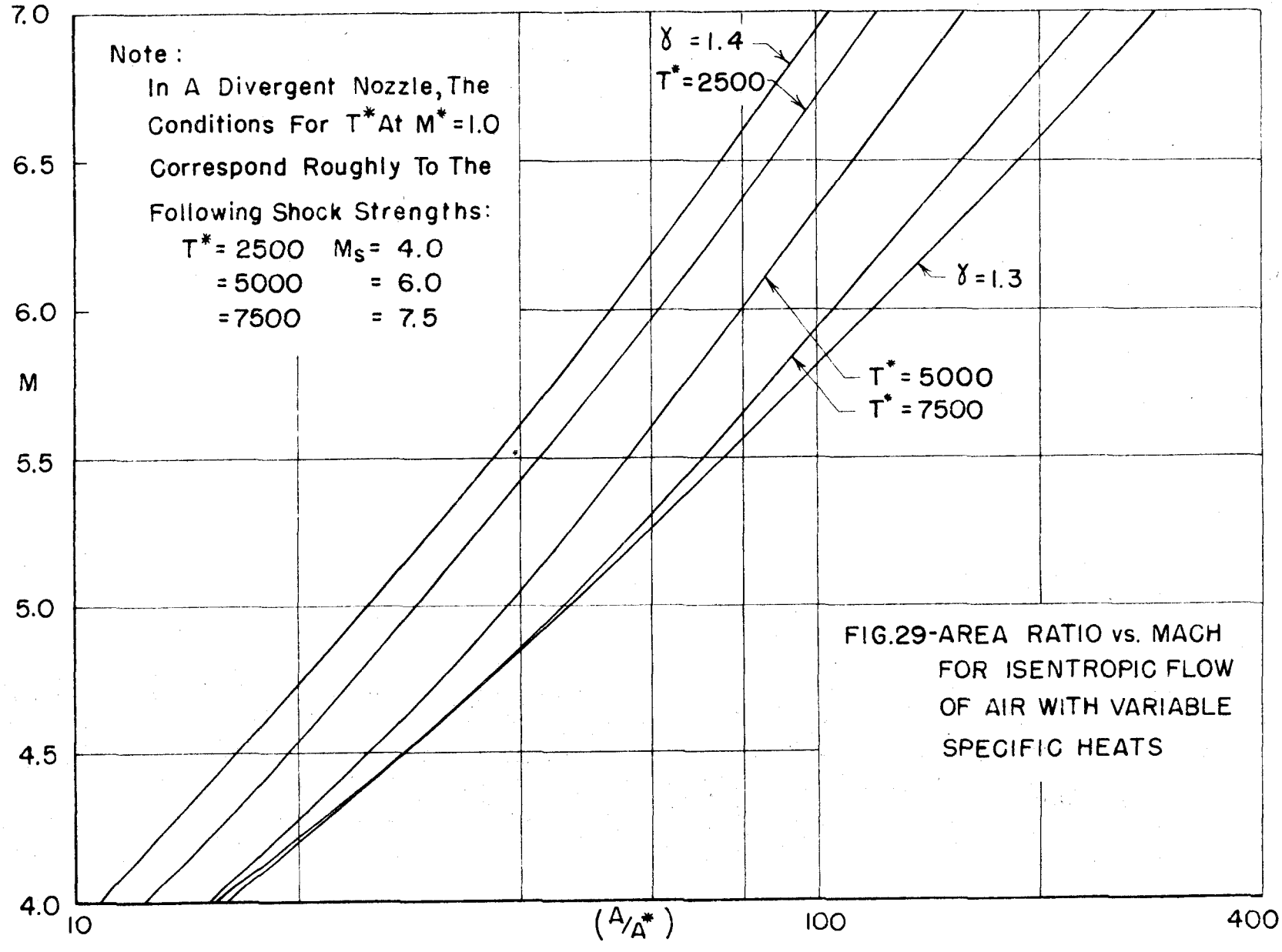

FIG.29-AREA RATIO vs. MACH FOR ISENTROPIC FLOW OF AIR WITH VARIABLE SPECIFIC HEATS

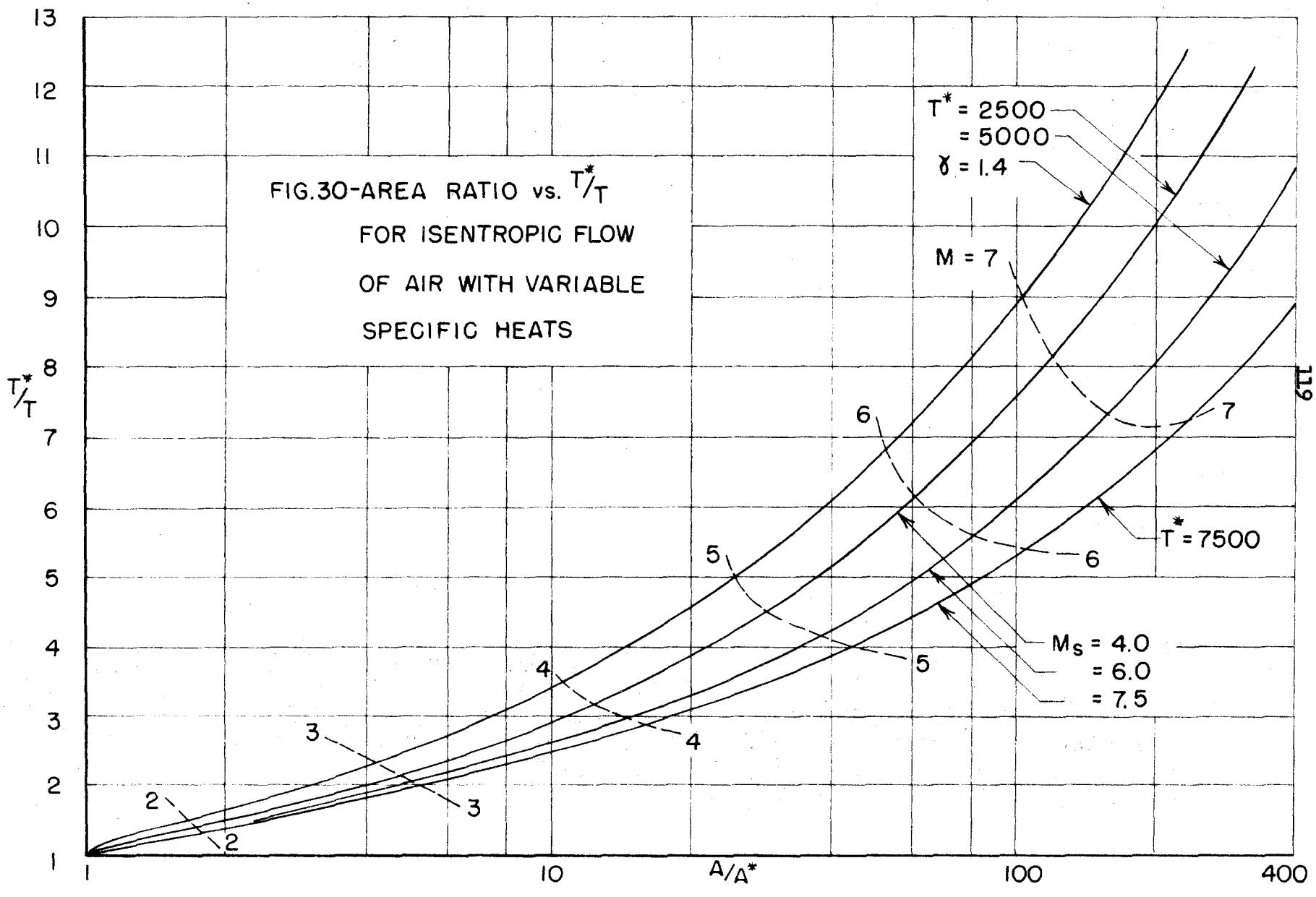
FIG.30-AREA RATIO vs. T*/T
FOR ISENTROPIC FLOW
OF AIR WITH VARIABLE
SPECIFIC HEATS
T*/T
A/A*
1
10
100
400
13
12
11
10
9
8
7
6
5
4
3
2
1
T* = 2500
= 5000
γ = 1.4
M = 7
T* = 7500
Ms = 4.0
= 6.0
= 7.5
2
3
4
5
6
7

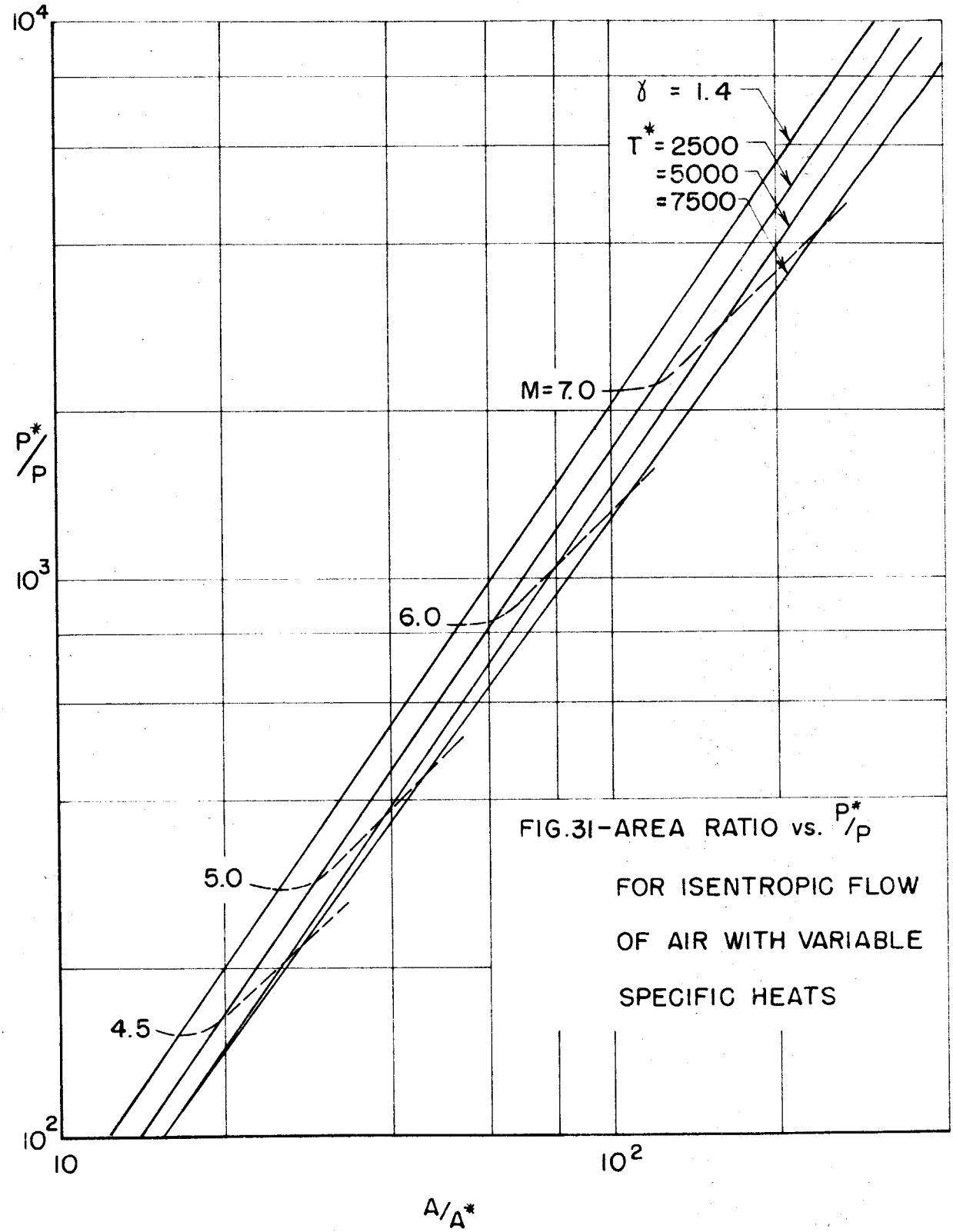

FIG.31–AREA RATIO vs. P^*/P FOR ISENTROPIC FLOW OF AIR WITH VARIABLE SPECIFIC HEATS

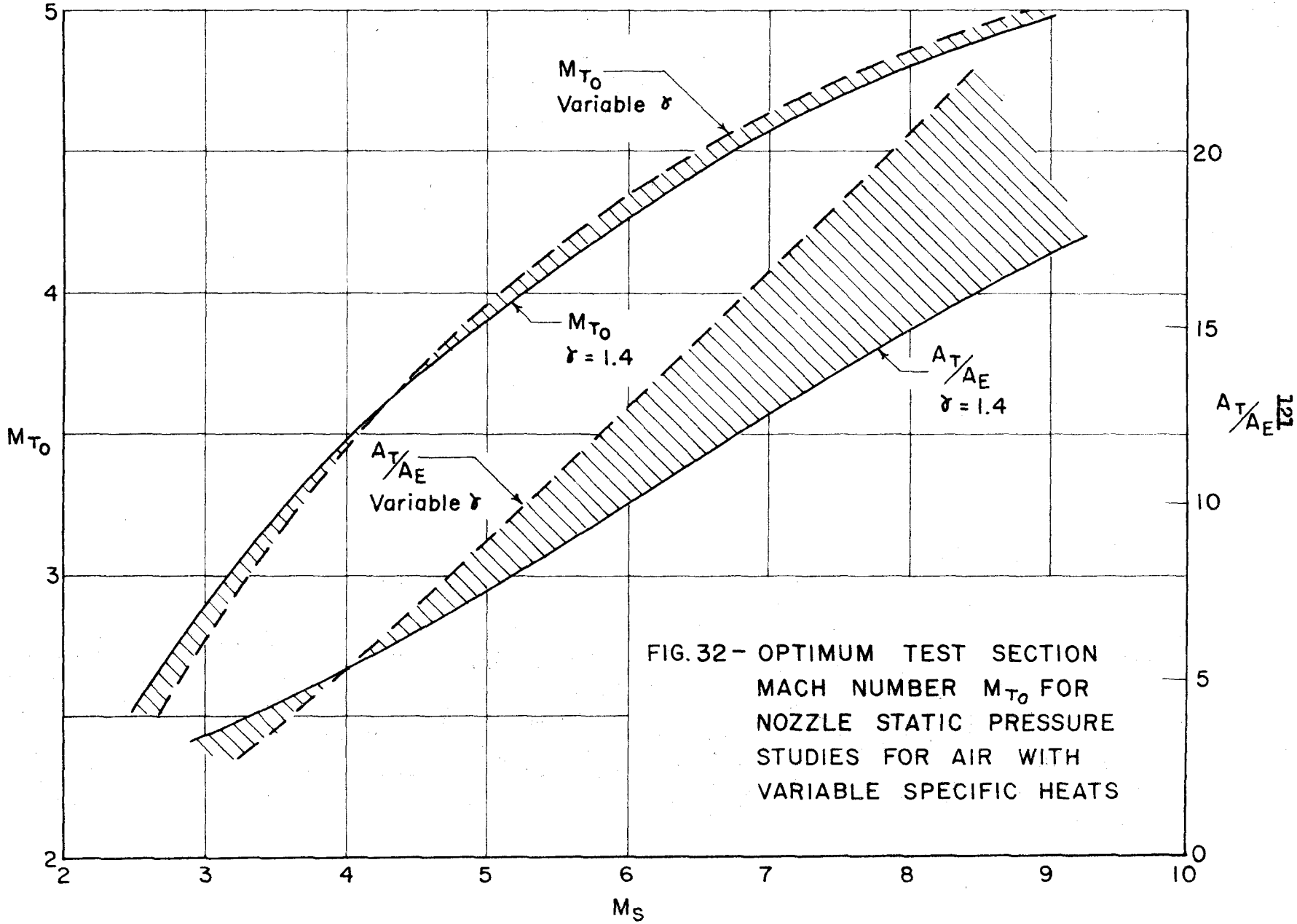

FIG. 32 – OPTIMUM TEST SECTION MACH NUMBER M_{T_o} FOR NOZZLE STATIC PRESSURE STUDIES FOR AIR WITH VARIABLE SPECIFIC HEATS

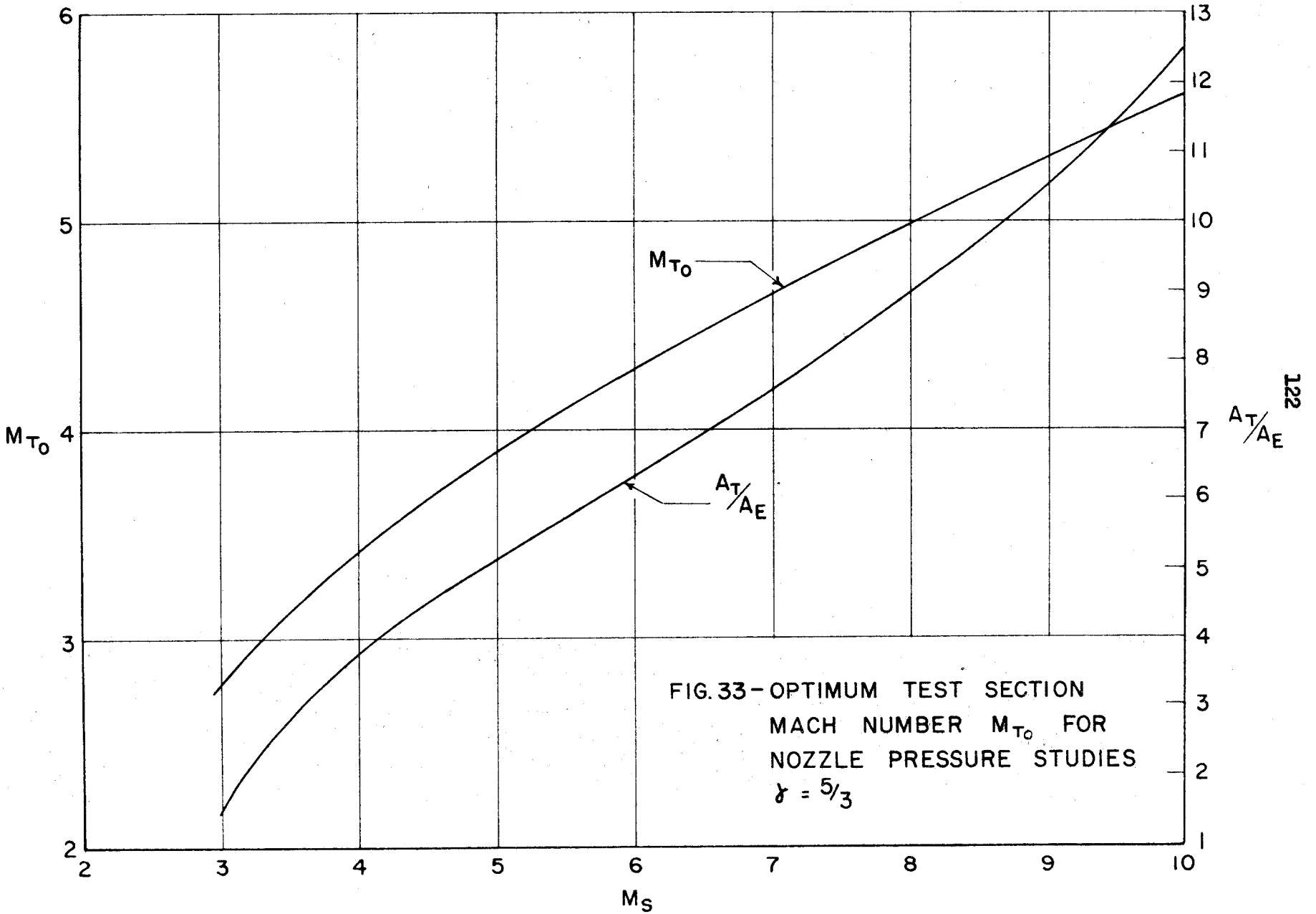

FIG. 33 – OPTIMUM TEST SECTION MACH NUMBER M_{T_0} FOR NOZZLE PRESSURE STUDIES $\gamma = 5/3$

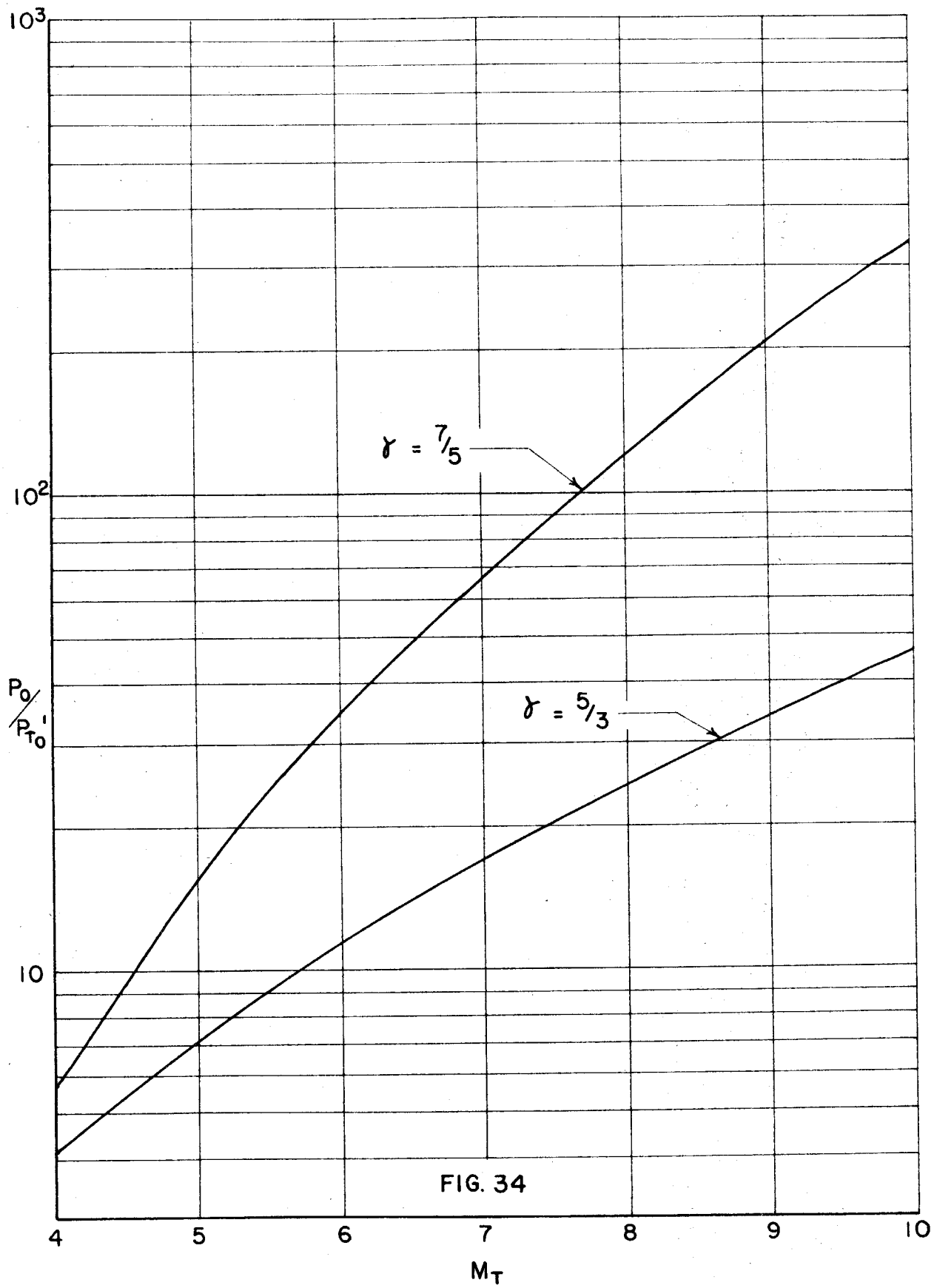

FIG. 34

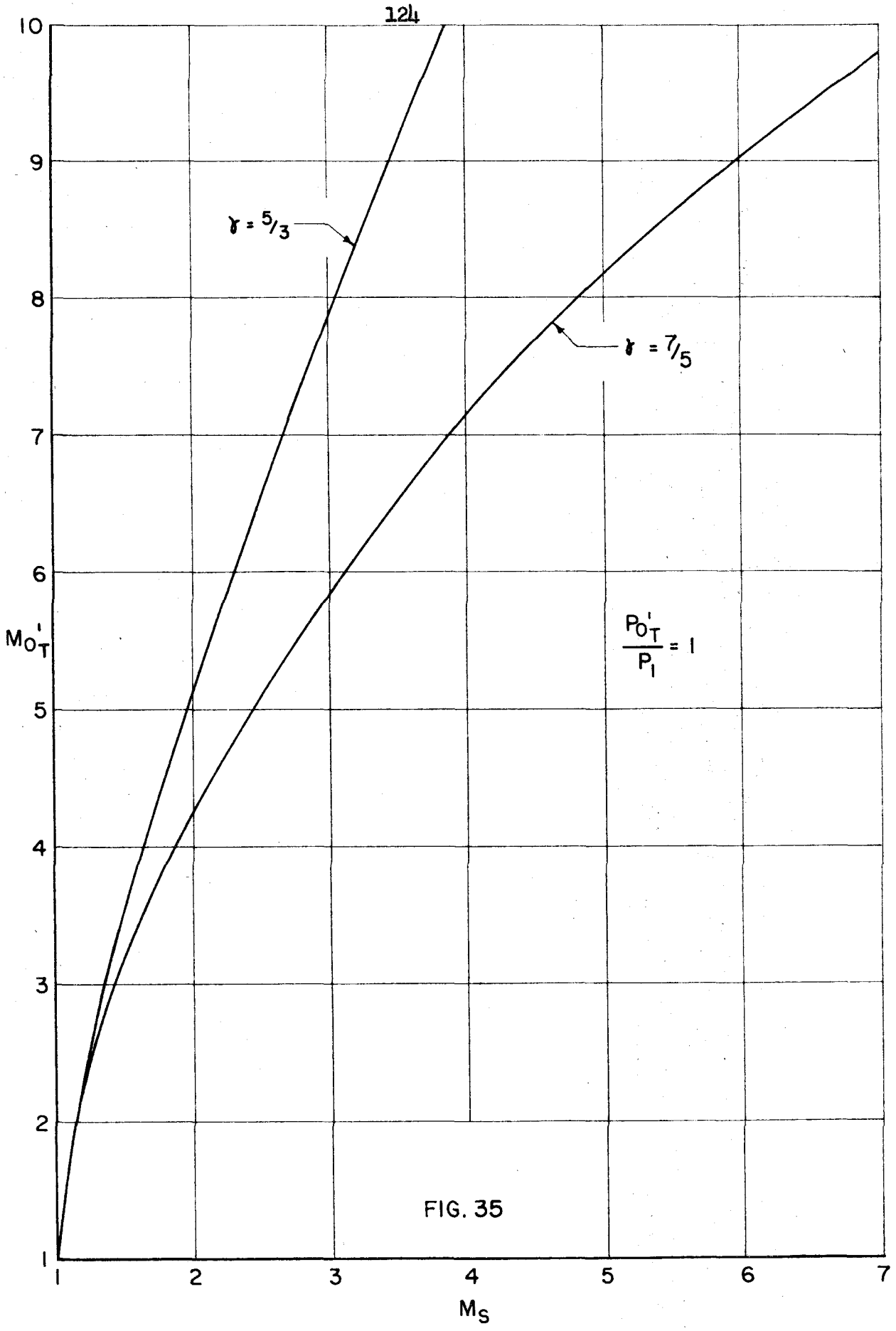

FIG. 35

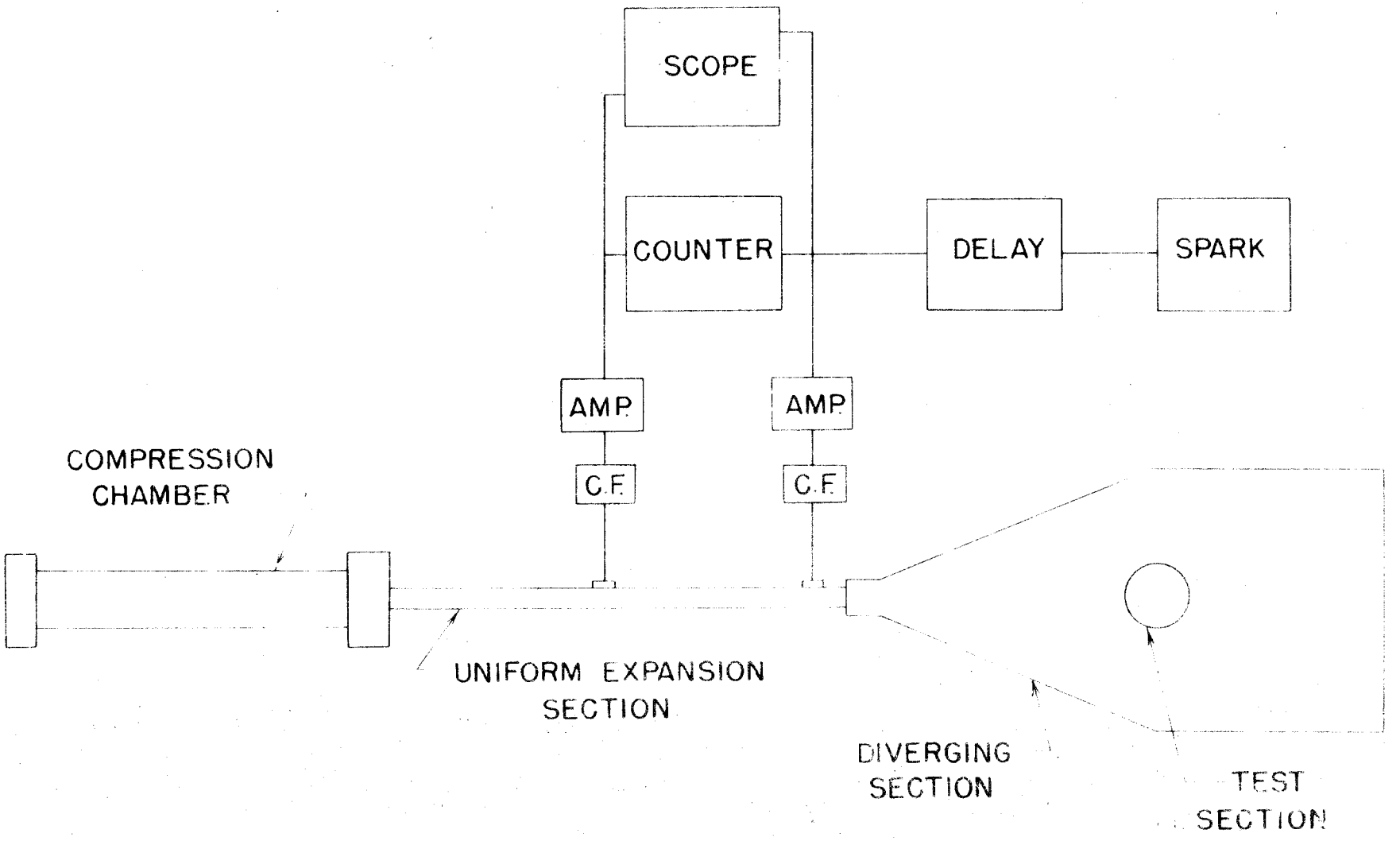

FIG. I

HYPERSONIC SHOCK TUBE

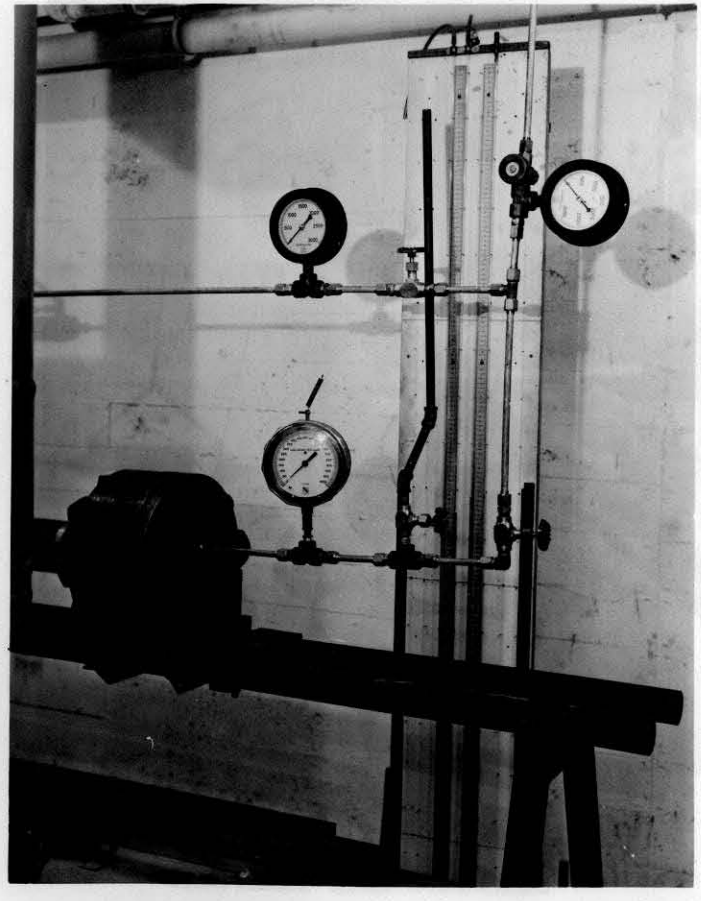

a) HIGH PRESSURE SYSTEM SHOWING THE END FLANGE OF THE COMPRESSION CHAMBER

PLATE 1

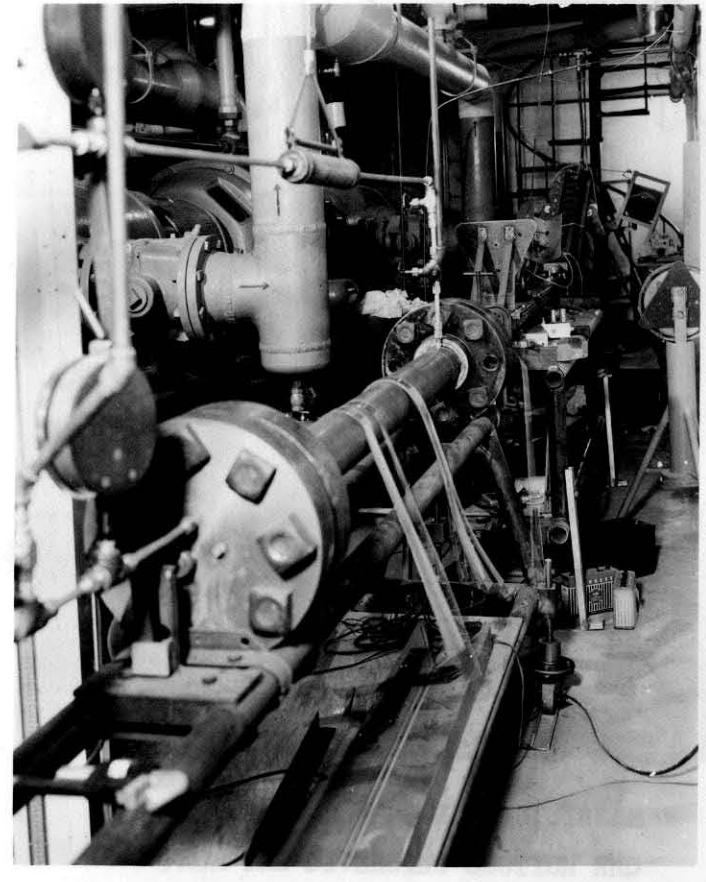

b) OVER-ALL VIEW LOOKING DOWNSTREAM FROM THE COMPRESSION CHAMBER END

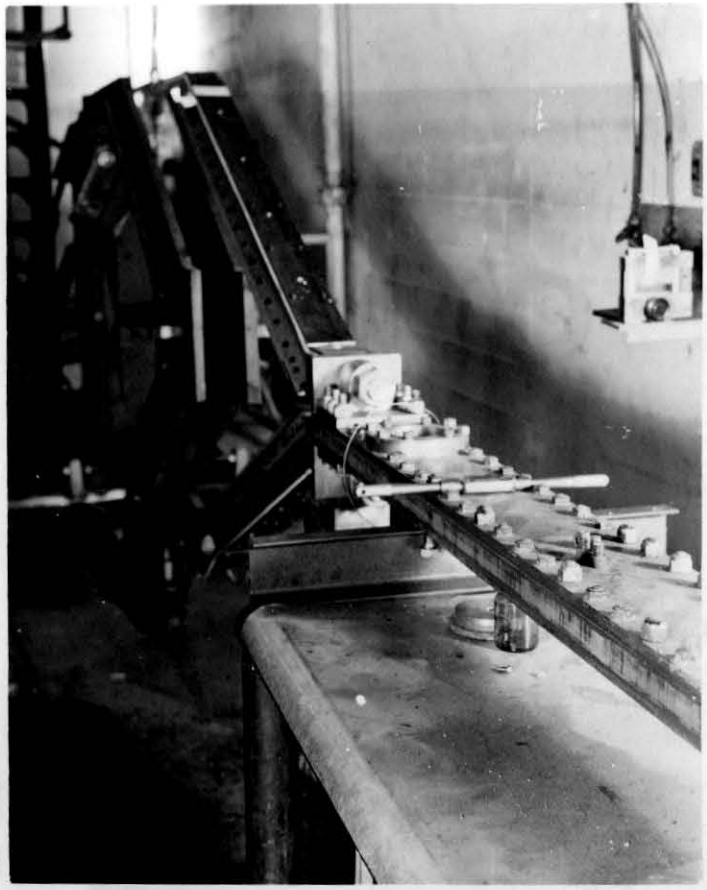

a) THE DIVERGING SECTION WITH PARTIALLY OPEN SIDEWALLS

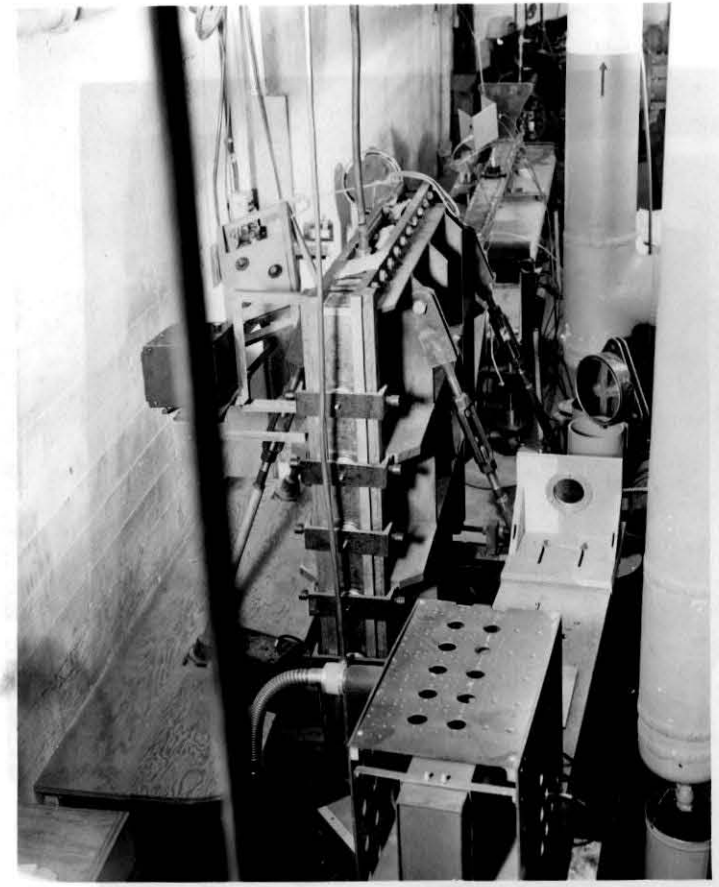

b) OVER-ALL VIEW LOOKING UPSTREAM FROM THE DIVERGING SECTION END

PLATE 2

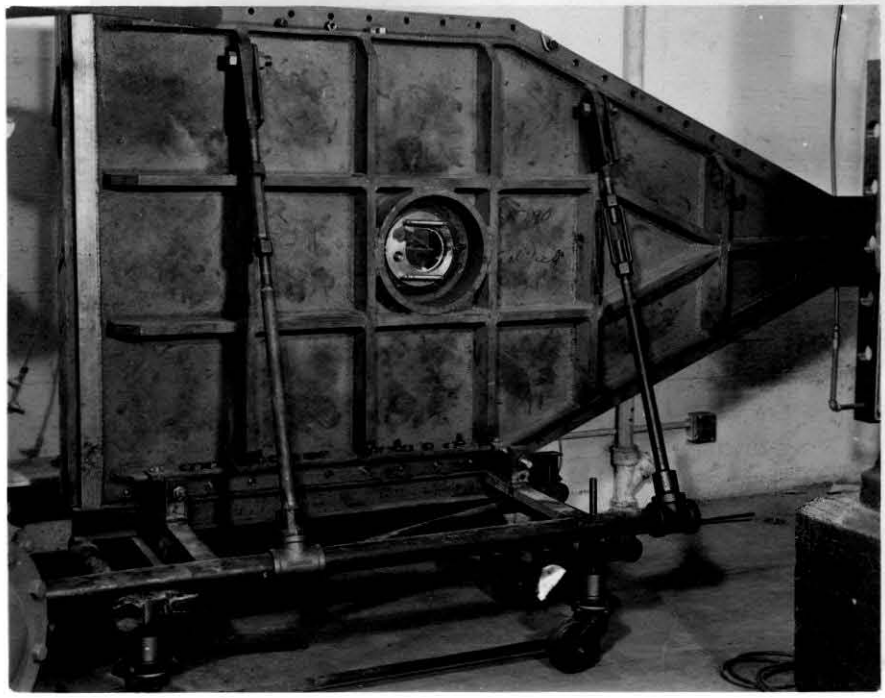

PLATE 3a - THE DIVERGING SECTION SIDEWALLS

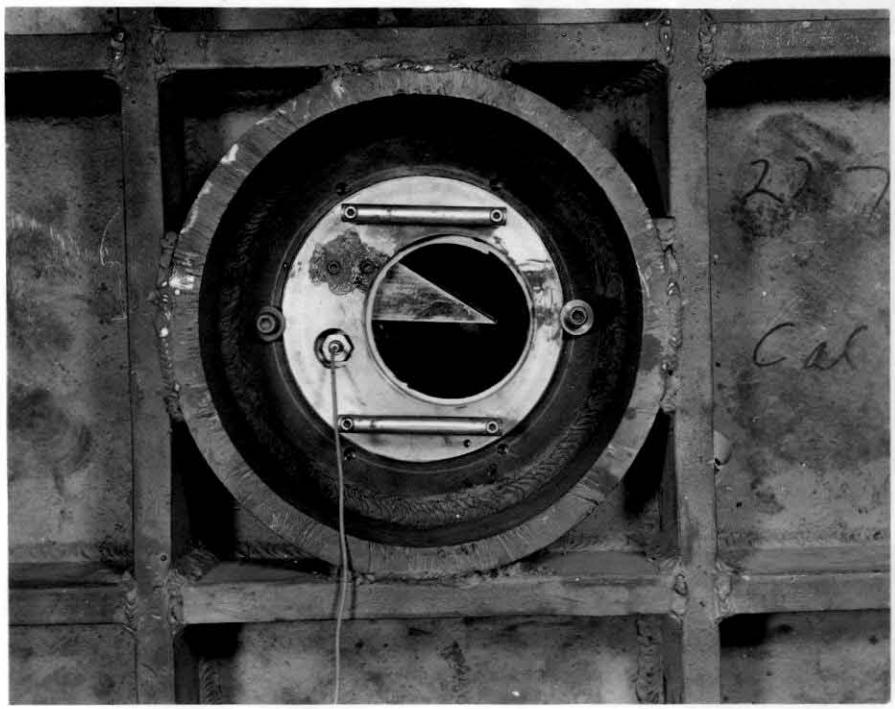

PLATE 3b - THE TEST SECTION SHOWING THE MODEL AND THE PRESSURE PICKUP MOUNTED ON THE WINDOW

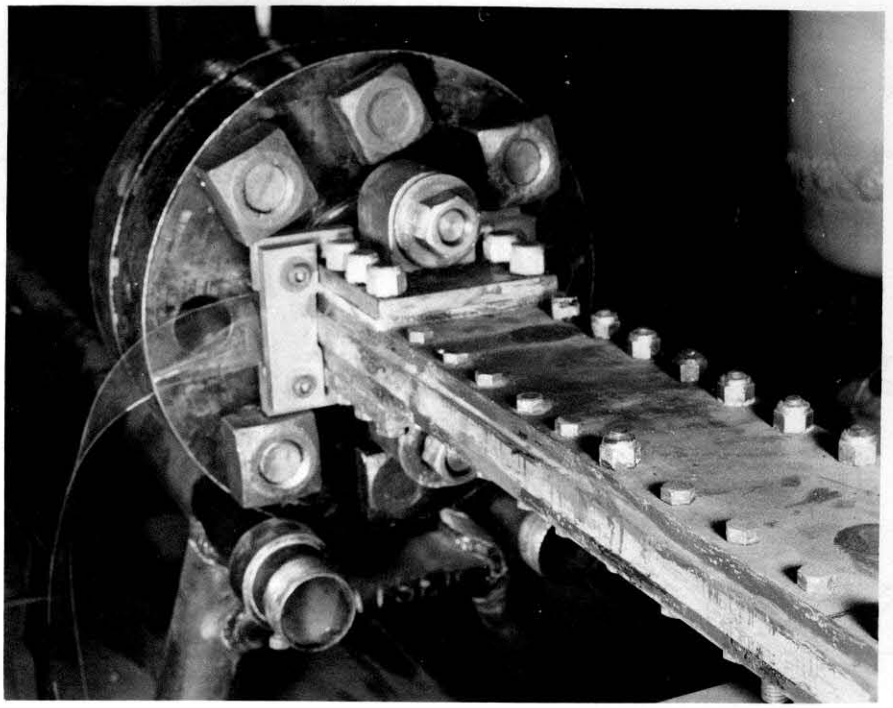

PLATE 4a - THE DIAPHRAGM SECTION

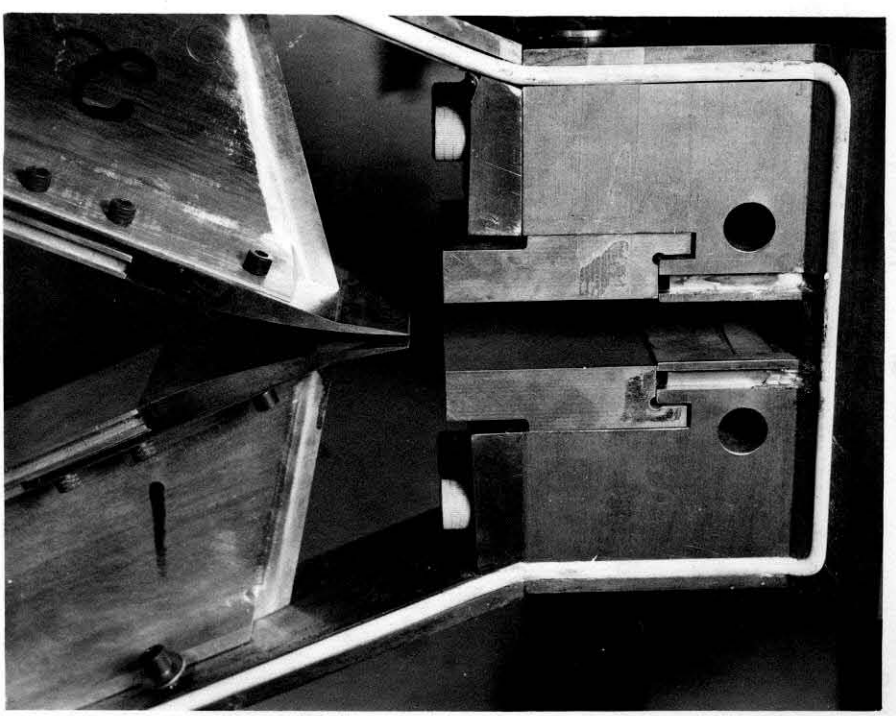

PLATE 4b - THE INLET TO NOZZLE NO. 2 WITH THE SIDEWALLS REMOVED

FIG. II a – NOZZLE NO. 1

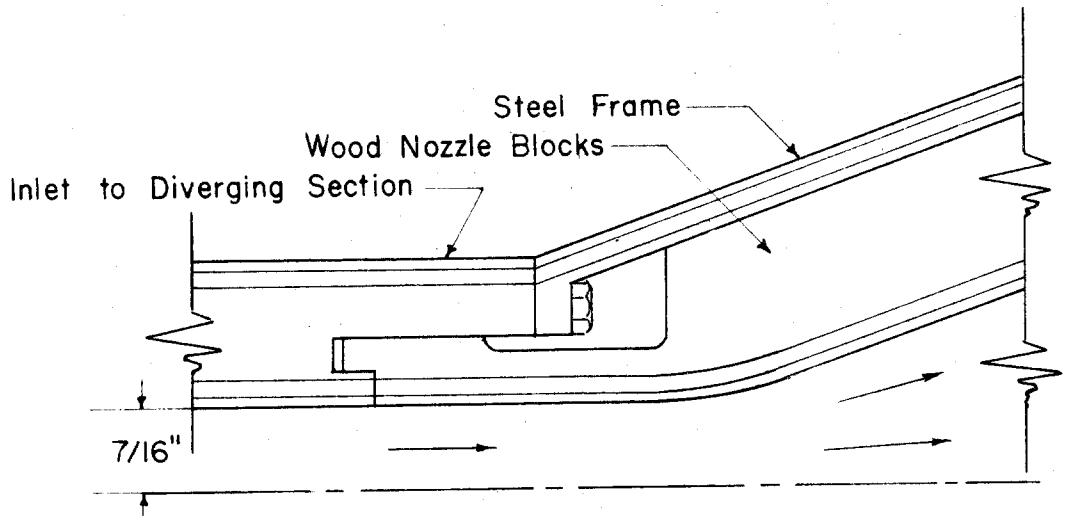

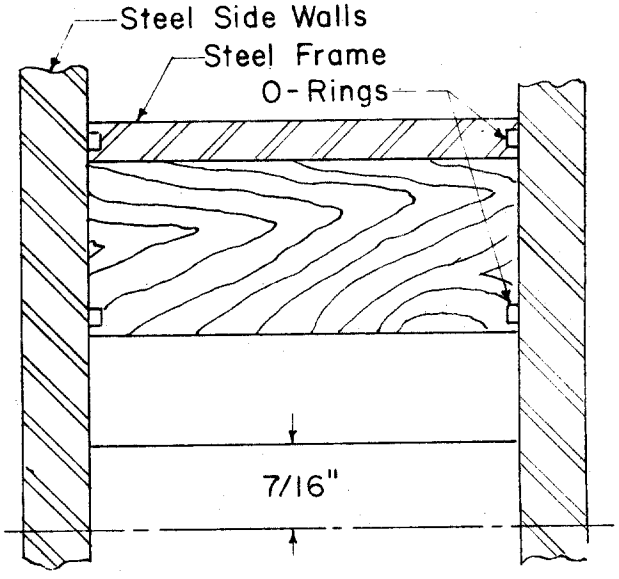

FIG. II b – NOZZLE NO. 3

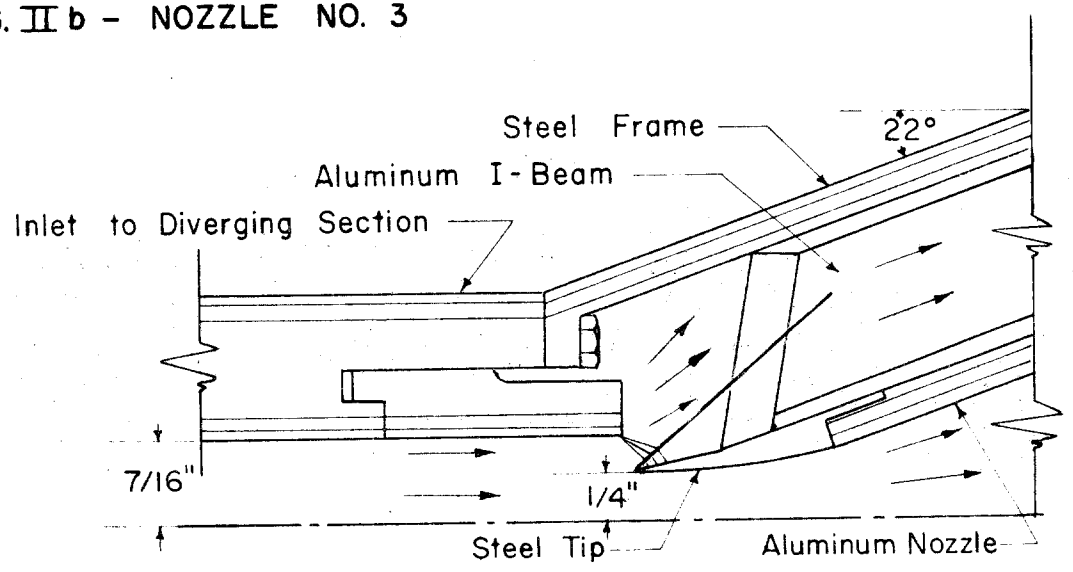

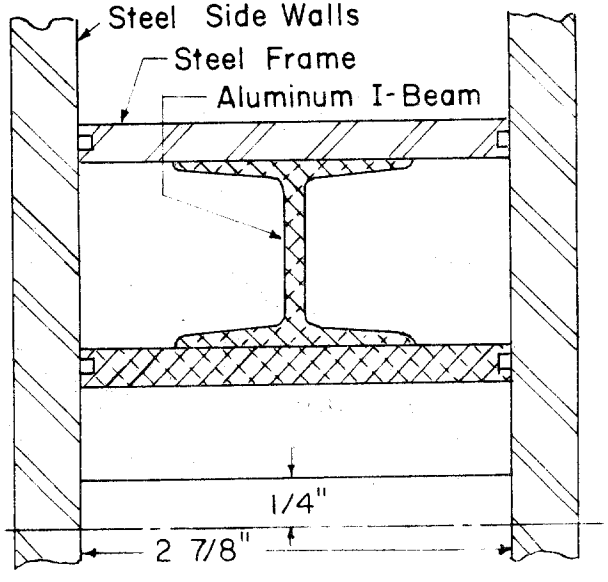

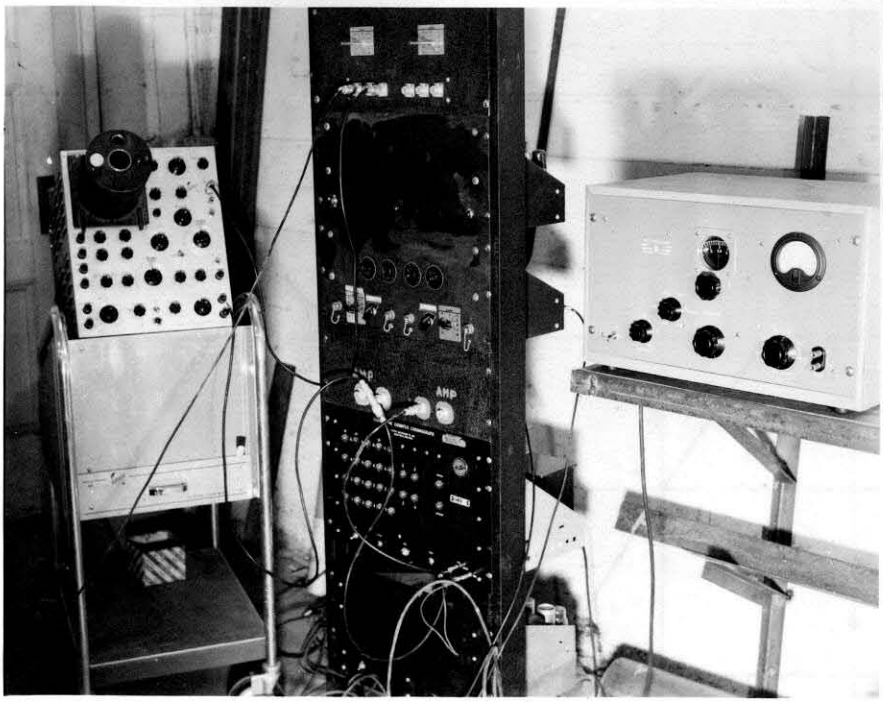

PLATE 5a - ELECTRONIC INSTRUMENTATION

PLATE 5b - QUARTZ PRESSURE PICKUP MOUNTED
ON THE UNIFORM EXPANSION TUBE

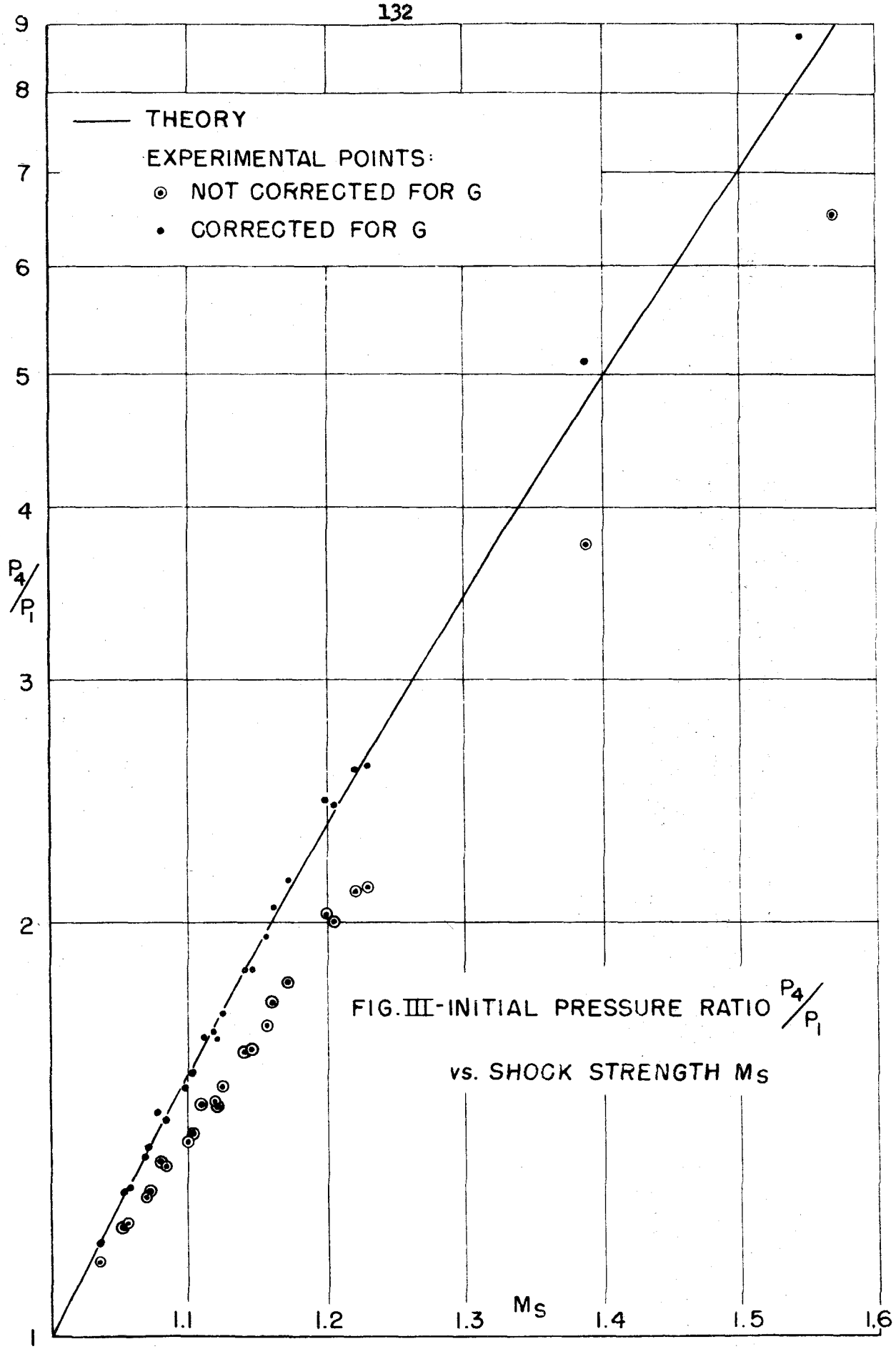

FIG. III - INITIAL PRESSURE RATIO P_4/P_1 vs. SHOCK STRENGTH M_S

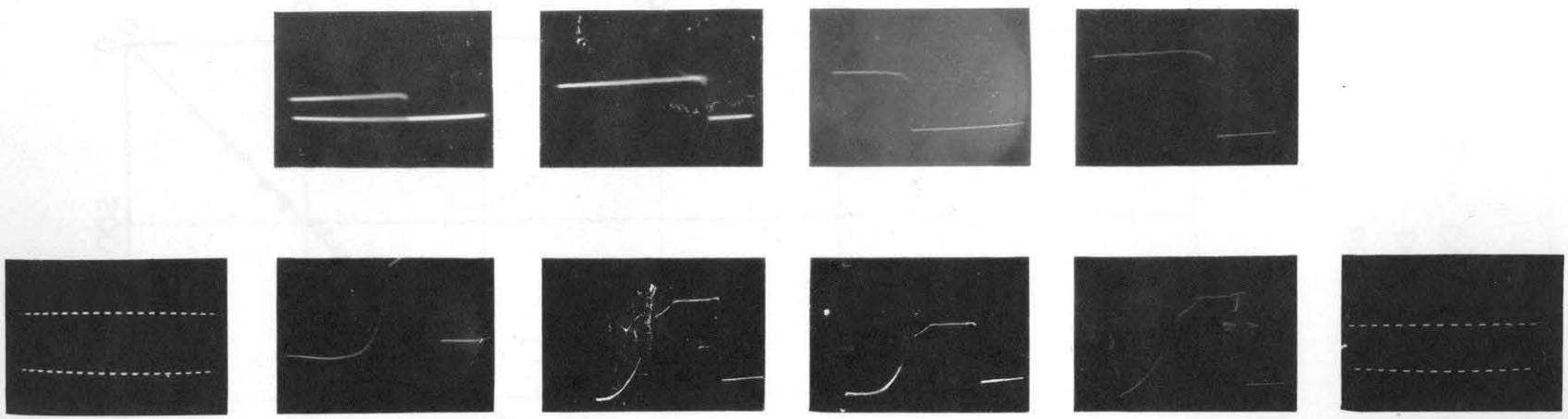

a) QUARTZ CRYSTAL PICKUP

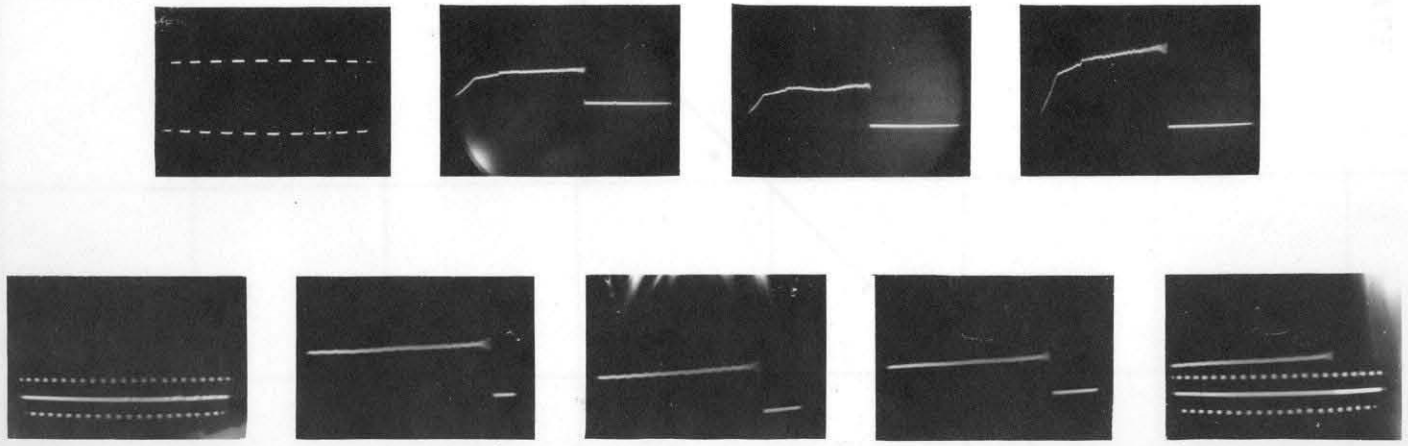

b) BARIUM TITANATE PICKUP

PLATE 6 - TYPICAL CALIBRATION TRACES

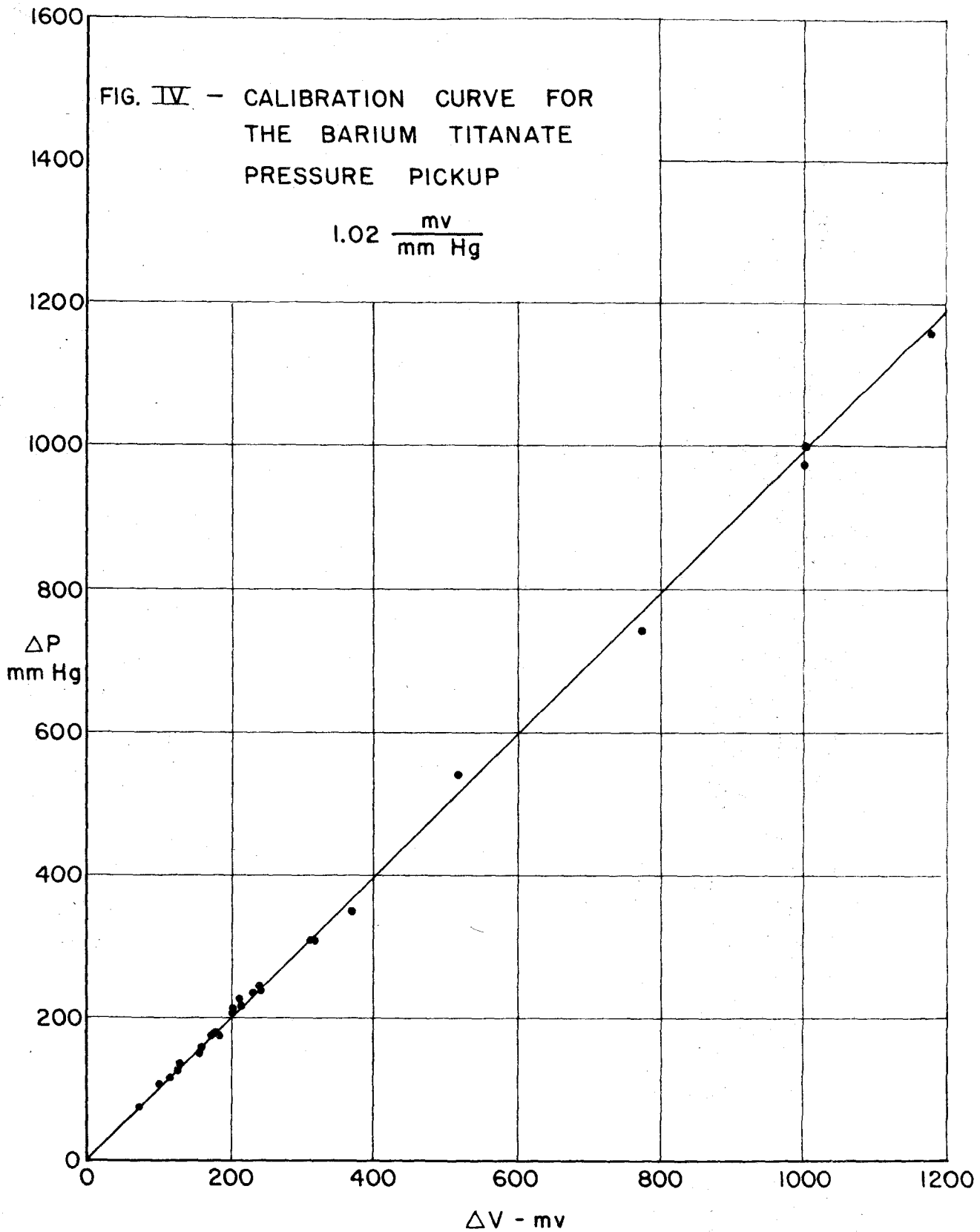
FIG. IV – CALIBRATION CURVE FOR THE BARIUM TITANATE PRESSURE PICKUP
1.02 mv / mm Hg
1600
1400
1200
1000
800
600
400
200
0
ΔP mm Hg
0
200
400
600
800
1000
1200
ΔV - mv

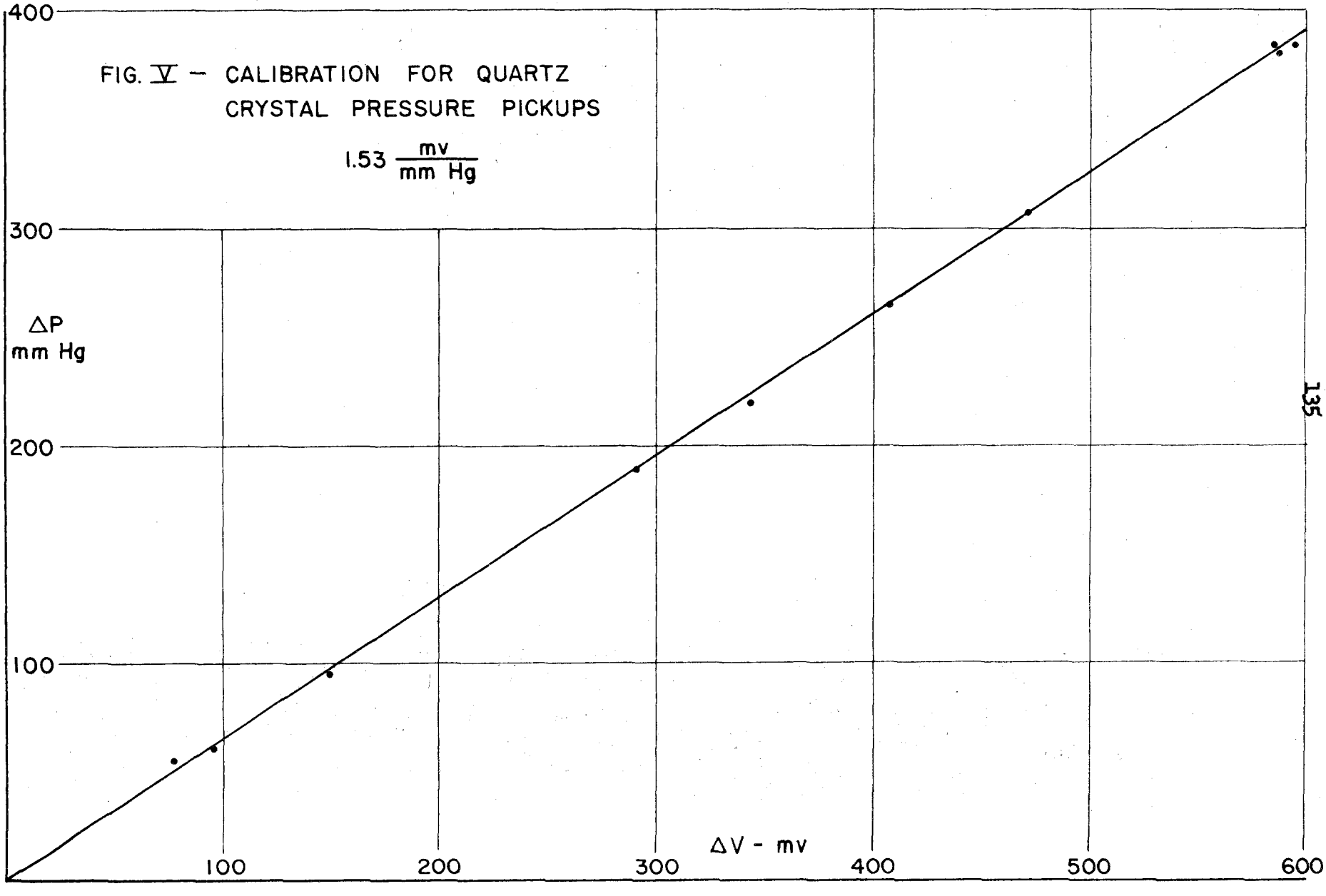
FIG. V – CALIBRATION FOR QUARTZ CRYSTAL PRESSURE PICKUPS
1.53 mv / mm Hg
400
300
200
100
ΔP mm Hg
100
200
300
400
500
600
ΔV - mv

FIG. VI - INITIAL PRESSURE RATIO P_4/P_1 VS. STRENGTH OF SHOCK WAVE

N_2-AIR

(FOR $P_4/P_1 \leq 10$, SEE FIG. III)

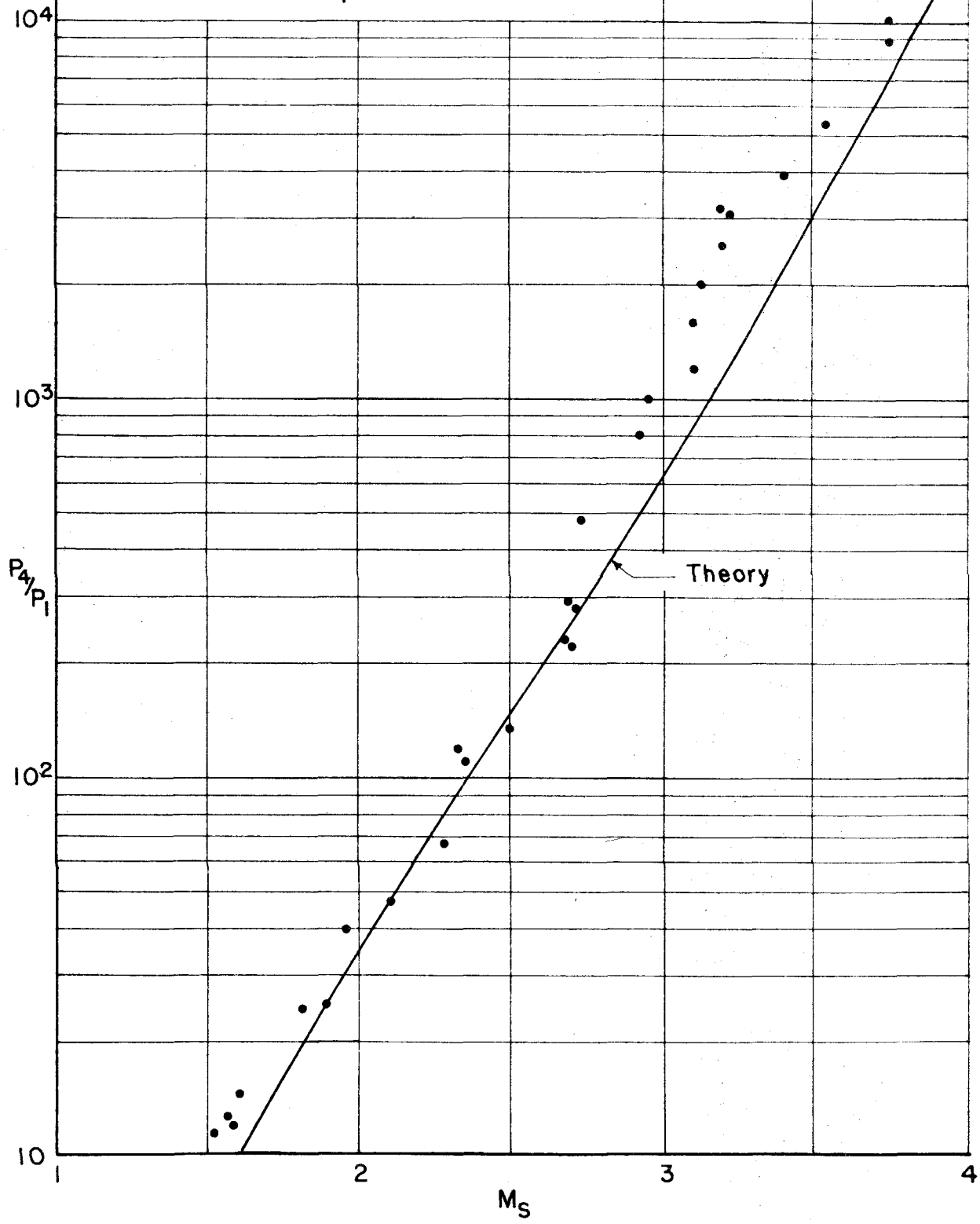

a) $p_4/p_1 = 3.0$
$p_1 = 744$ mm Hg

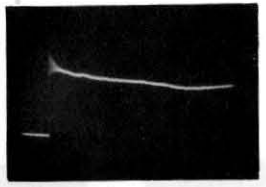

b) $p_4/p_1 = 9$
$p_1 = 80$ mm Hg

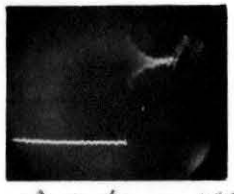

c) $p_4/p_1 = 480$
$p_1 = 71$ mm Hg

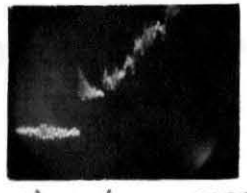

d) $p_4/p_1 = 3220$
$p_1 = 9$ mm Hg

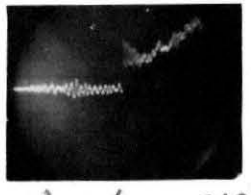

e) $p_4/p_1 = 3400$
$p_1 = 8$ mm Hg

ABOVE: BARIUM TITANATE GAGE

BELOW: QUARTZ GAGE

f) $p_4/p_1 = 2.2$
$p_1 = 746$ mm Hg

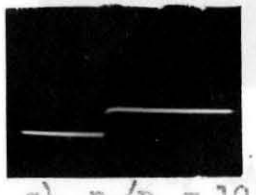

g) $p_4/p_1 = 10.0$
$p_1 = 746$ mm Hg

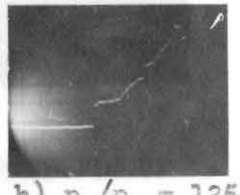

h) $p_4/p_1 = 13500$
$p_1 = 2.7$ mm Hg

i) $p_4/p_1 = 12000$
$p_1 = 2.9$ mm Hg

PLATE 7 - EFFECT OF DAMPING ON THE PIEZOELECTRIC GAGE RESPONSE

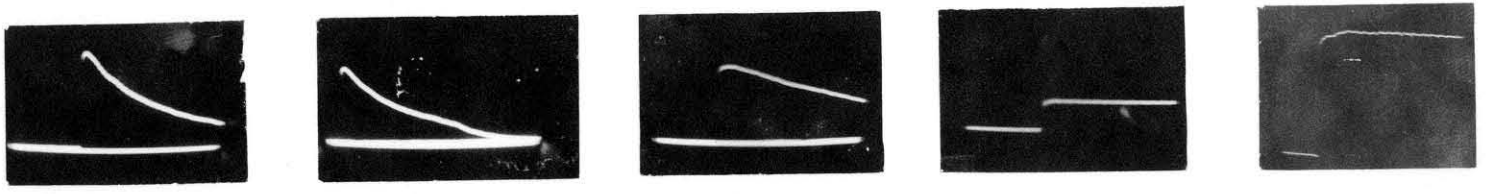

a) QUARTZ PICKUP

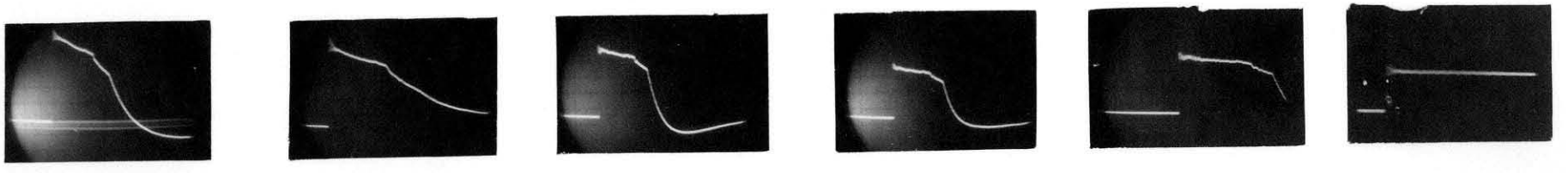

b) BARIUM TITANATE PICKUP

PLATE 8 - EFFECT OF ELECTRONIC TIME-CONSTANT ON THE GAGE RESPONSE

a) $p_4/p_1 = 5700$
$p_1 = 3$ mm Hg

b) $p_4/p_1 = 7200$
$p_1 = 2.8$ mm Hg

c) $p_4/p_1 = 13100$
$p_1 = 2.8$ mm Hg

d) $p_4/p_1 = 10300$
$p_1 = 2.7$ mm Hg

e) $p_4/p_1 = 9500$
$p_1 = 3.1$ mm Hg

f) $p_4/p_1 = 12500$
$p_1 = 2.8$ mm Hg

PLATE 9: PRESSURE TRACES AT THE NOZZLE INLET QUARTZ PICKUP, N_2 - AIR

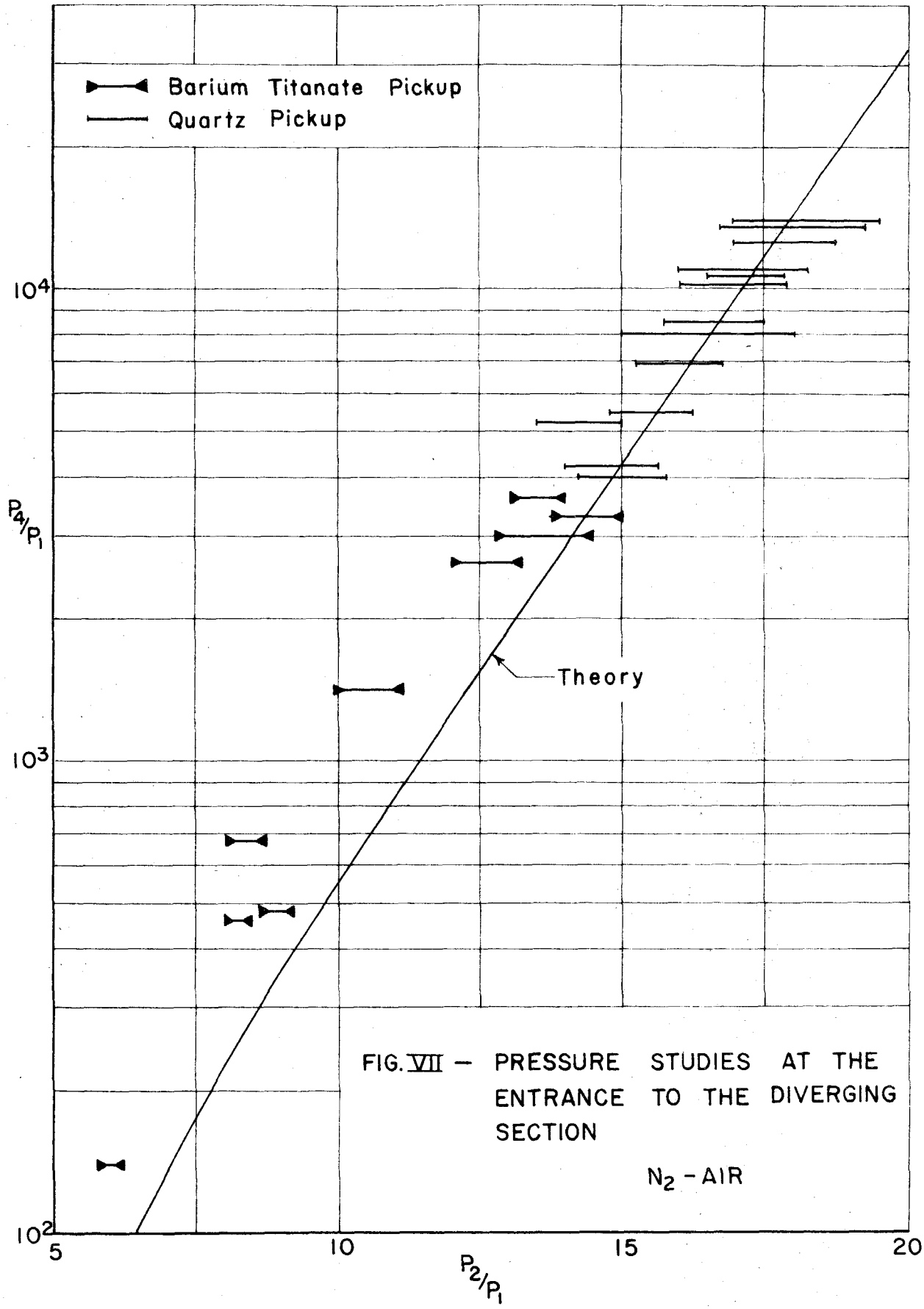

FIG. VII — PRESSURE STUDIES AT THE ENTRANCE TO THE DIVERGING SECTION

N_2 - AIR

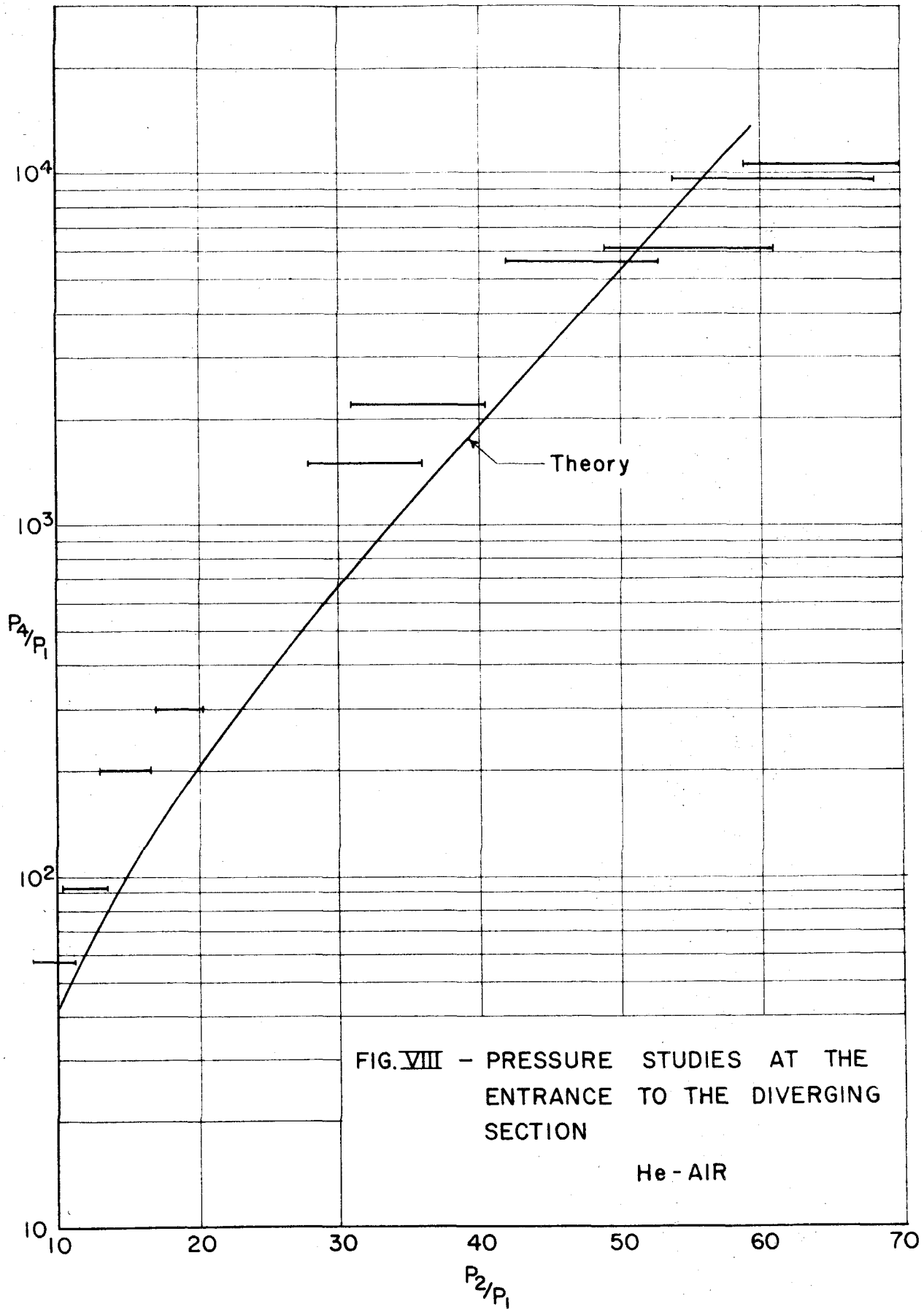

FIG. VIII – PRESSURE STUDIES AT THE ENTRANCE TO THE DIVERGING SECTION

He - AIR

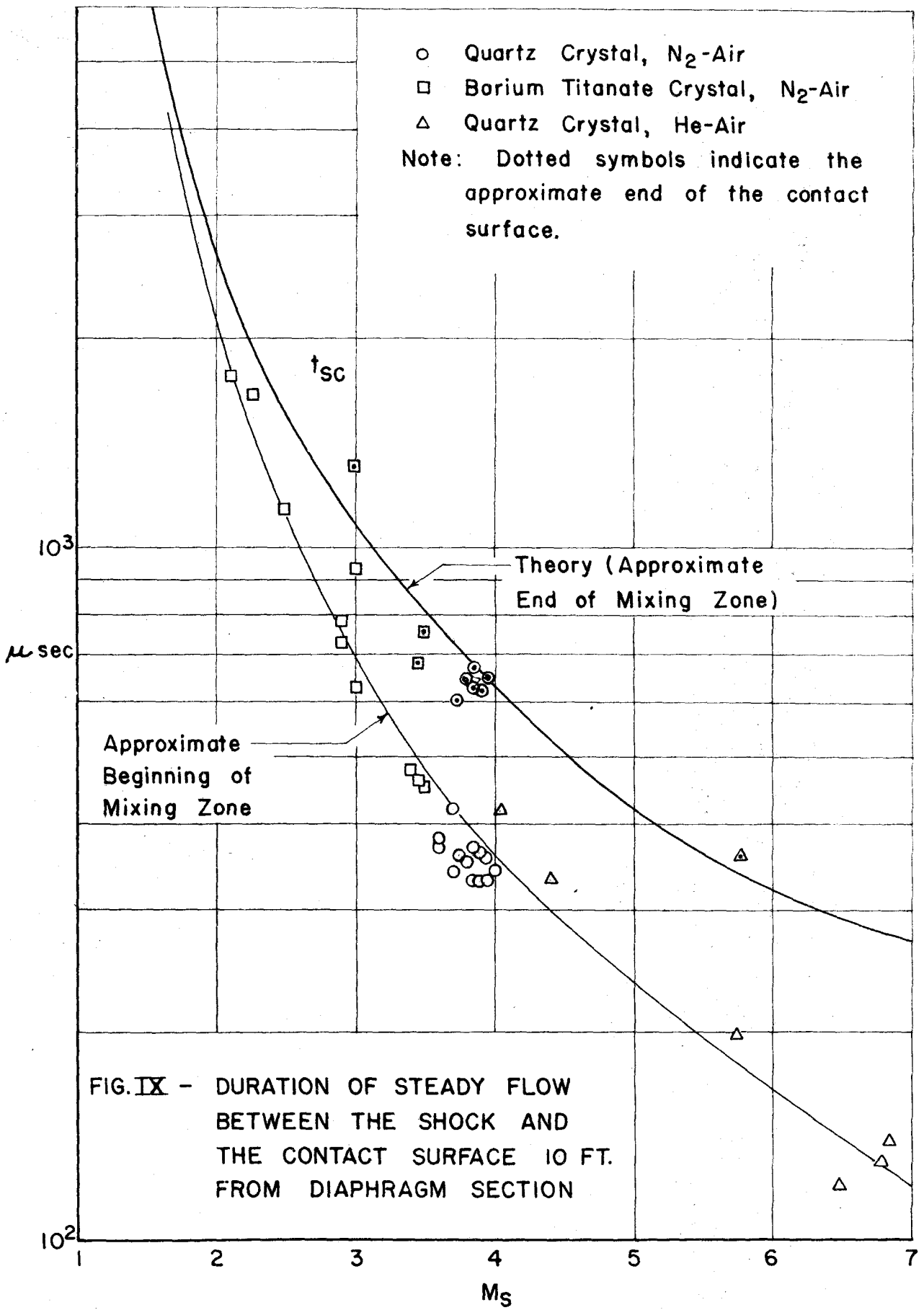

FIG. IX – DURATION OF STEADY FLOW BETWEEN THE SHOCK AND THE CONTACT SURFACE 10 FT. FROM DIAPHRAGM SECTION

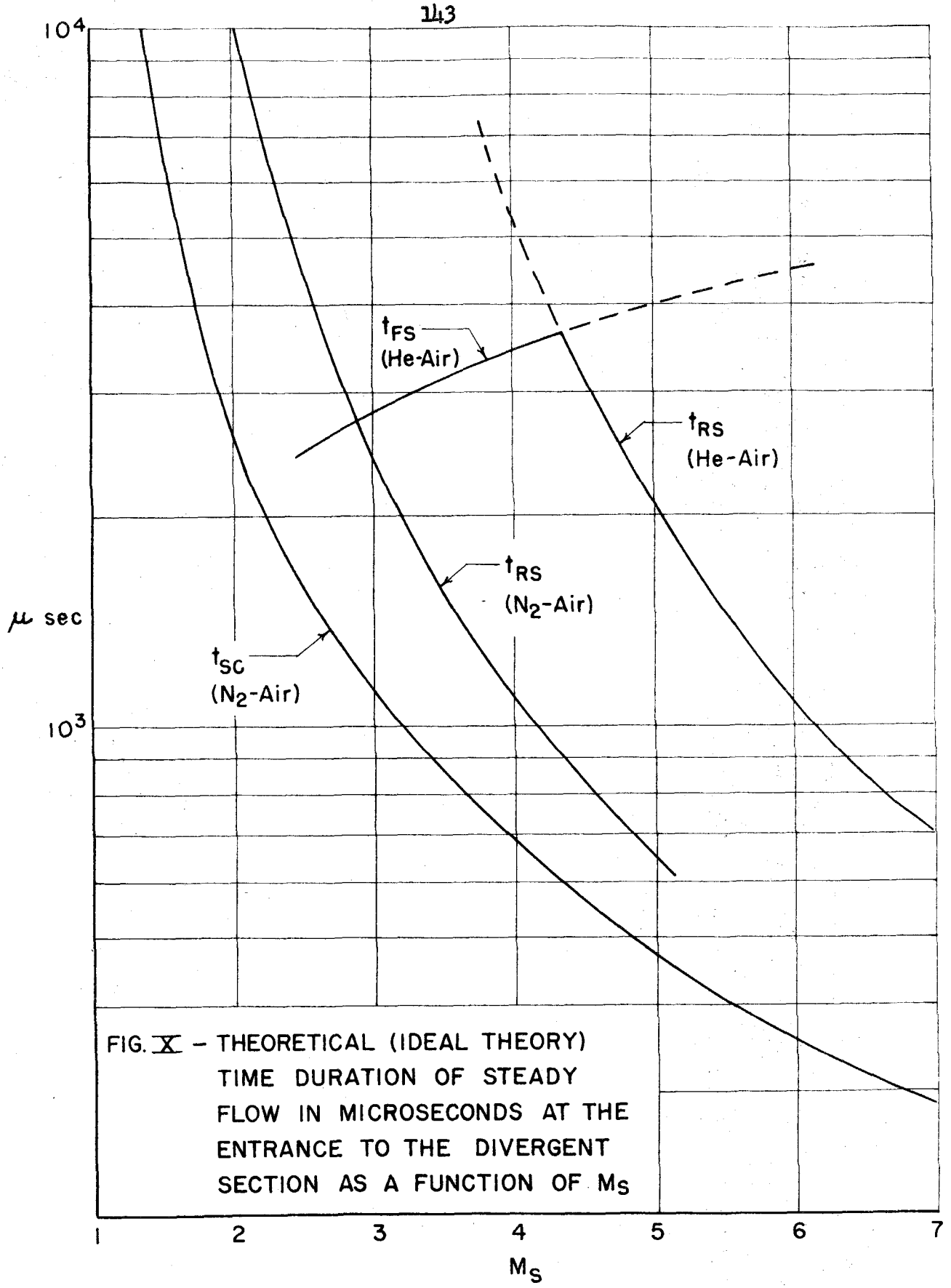

FIG. X – THEORETICAL (IDEAL THEORY) TIME DURATION OF STEADY FLOW IN MICROSECONDS AT THE ENTRANCE TO THE DIVERGENT SECTION AS A FUNCTION OF M_S

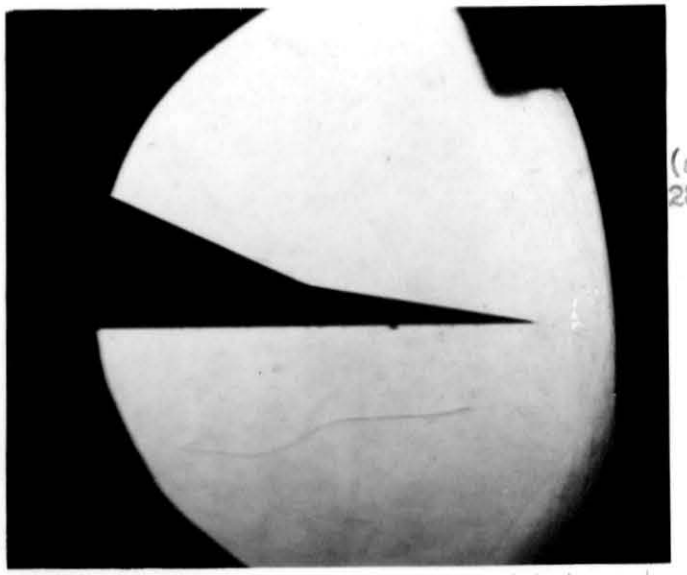

(a) 2800

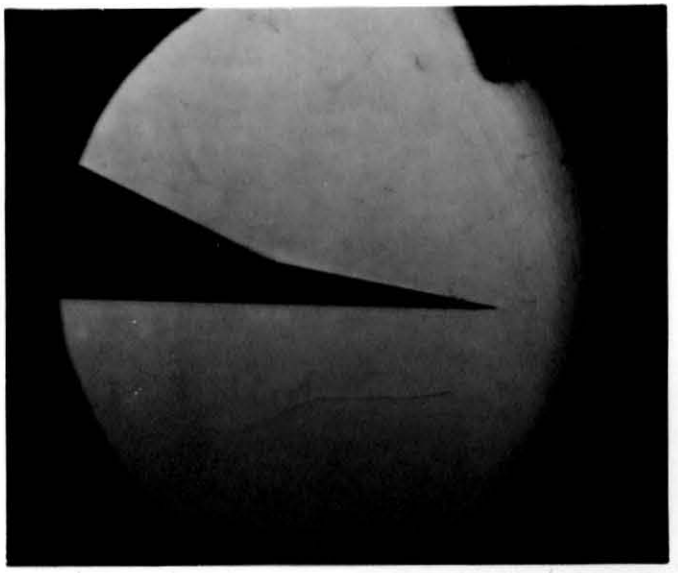

(b) 2900

PLATE 10 - ESTABLISHMENT OF FLOW AT THE TEST SECTION AROUND A 10° WEDGE, N_2 - AIR, $p_4/p_1 = 9000$
FIGURES INDICATE DELAY TIME IN MICROSECONDS

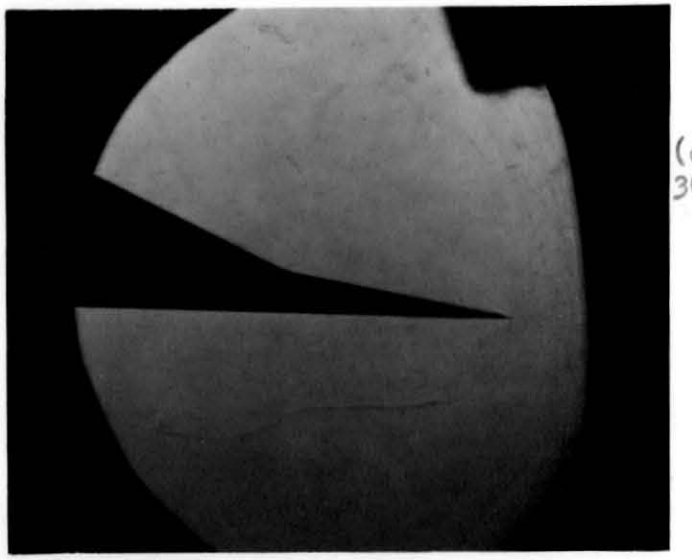

(c) 3000

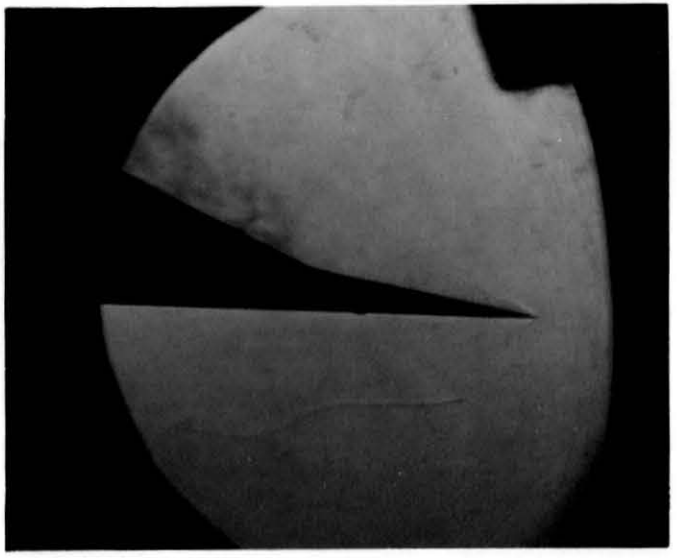

(d) 3100

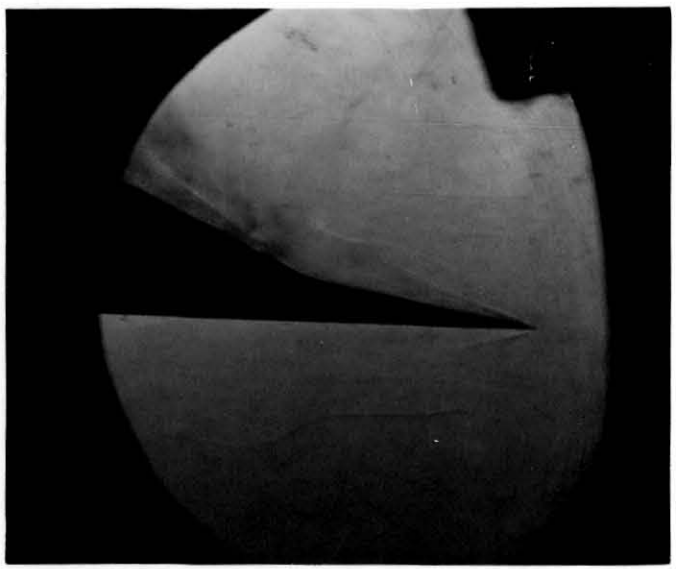

(a) 3200

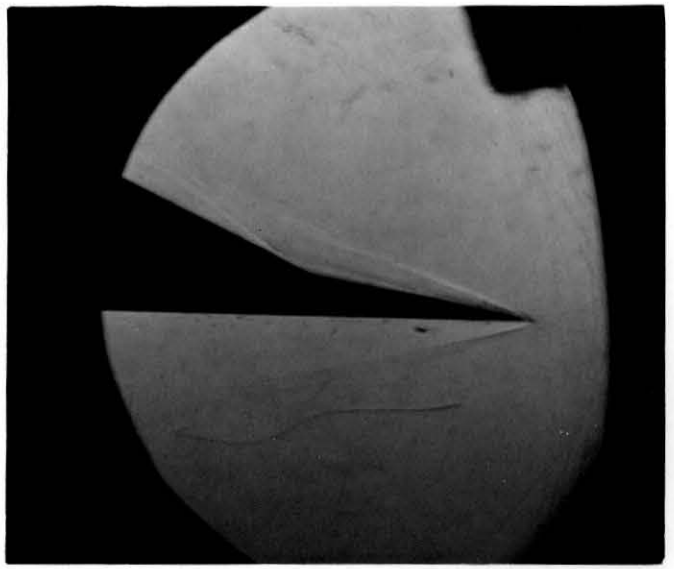

(b) 3300

PLATE 11 - FLOW IN PLATE 10 CONTINUED

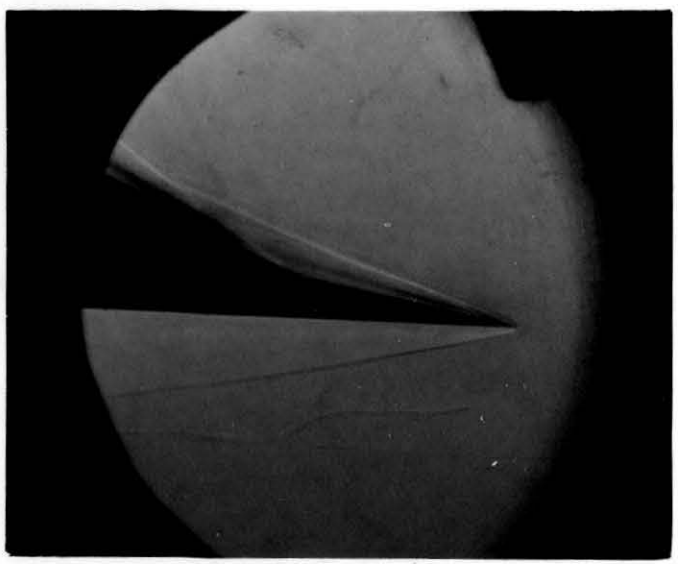

(c) 3500

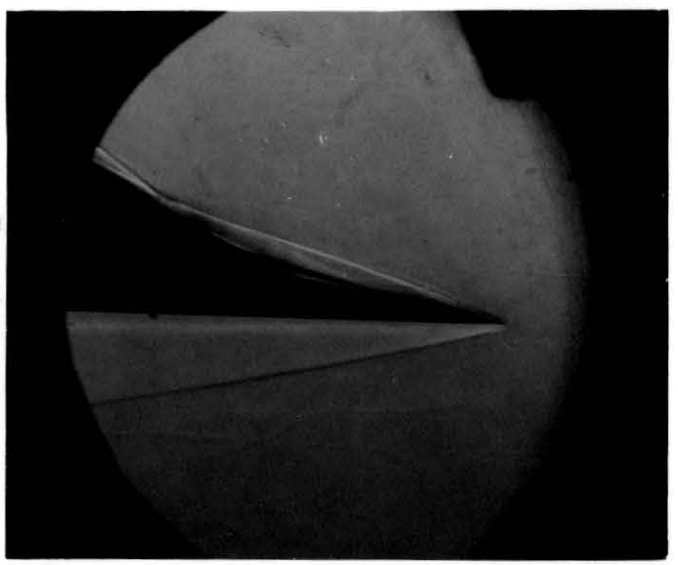

(d) 3600

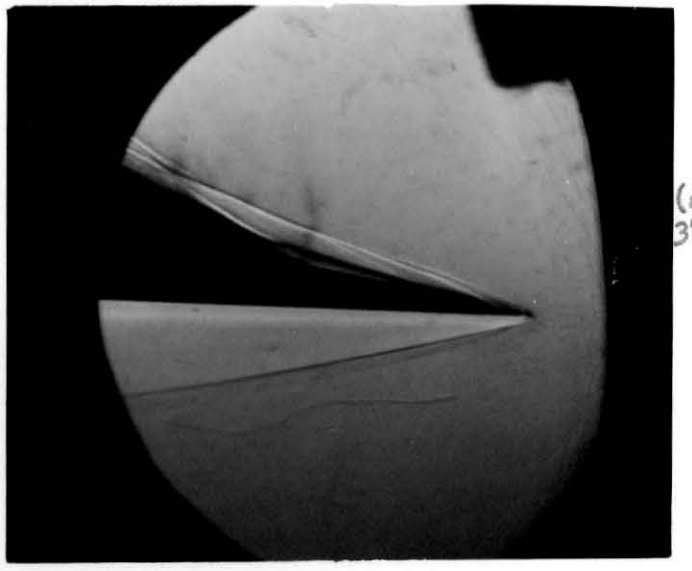

(a)
3700

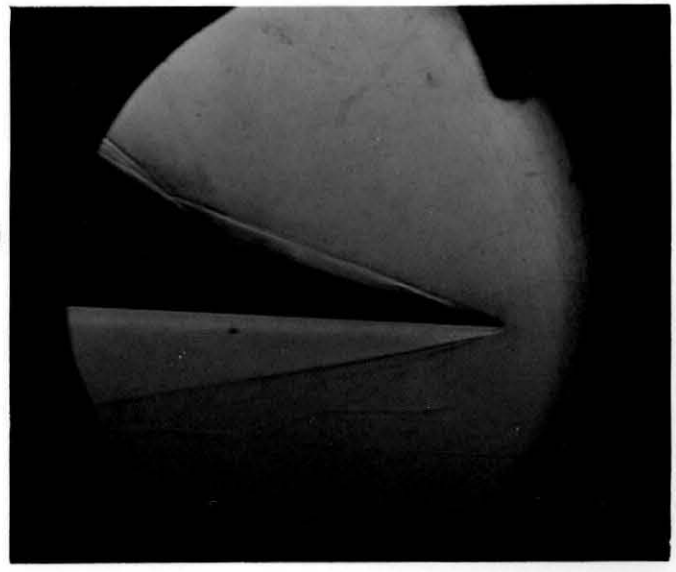

(b)
3900

PLATE 12 - FLOW IN PLATE 11 CONTINUED

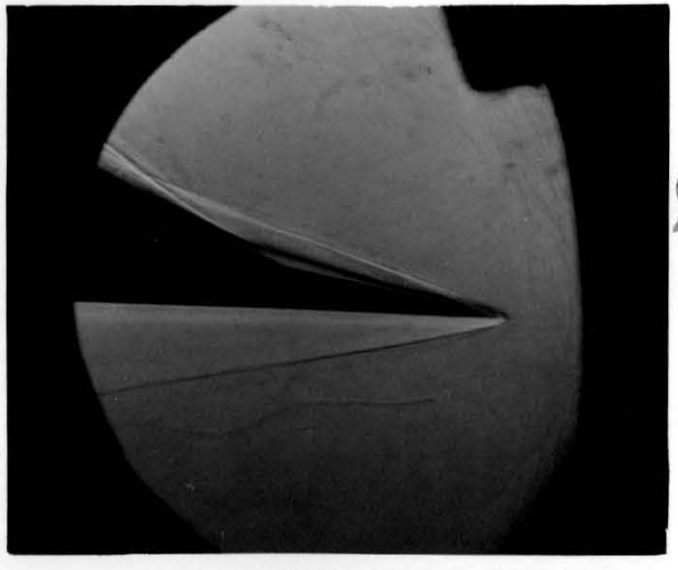

(c)
4100

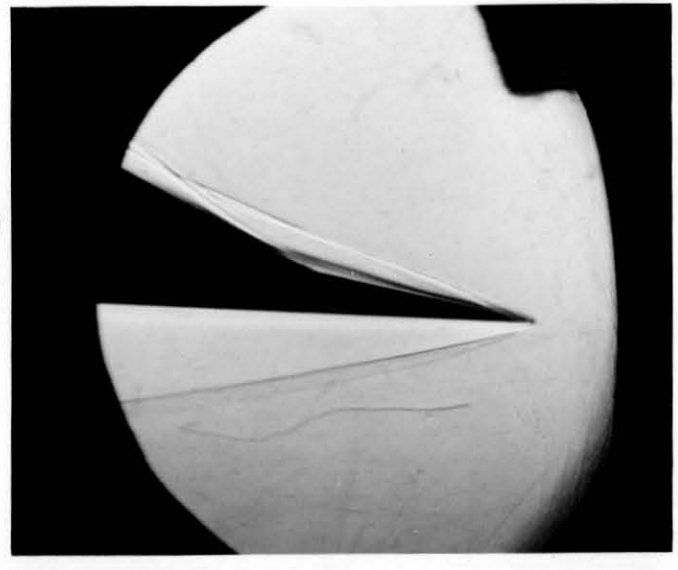

(d)
4300

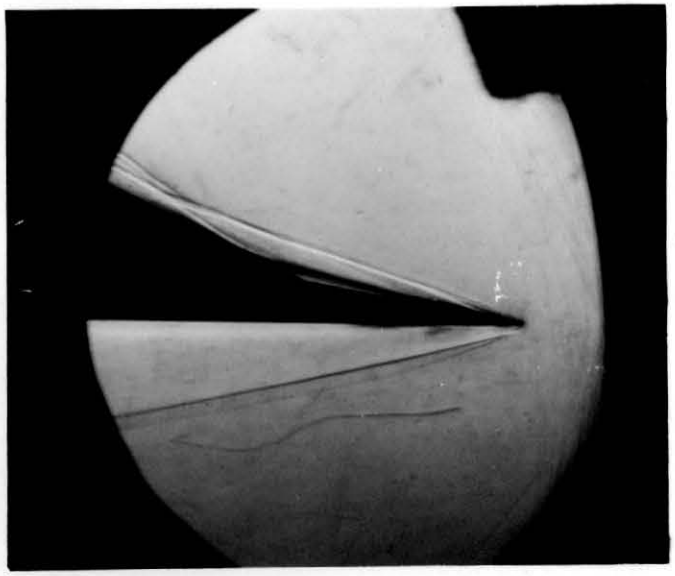

(a)
4500

(b)
4600

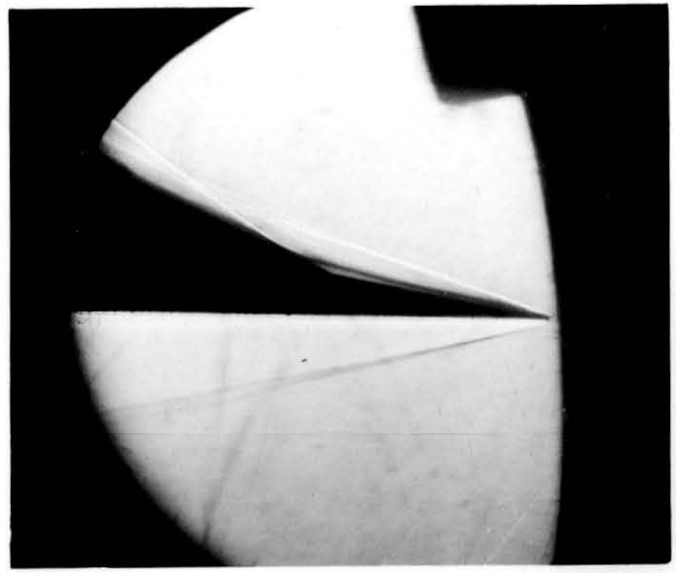

PLATE 13 - FLOW IN PLATE 12 CONTINUED

(c)
4700

(d)
4750

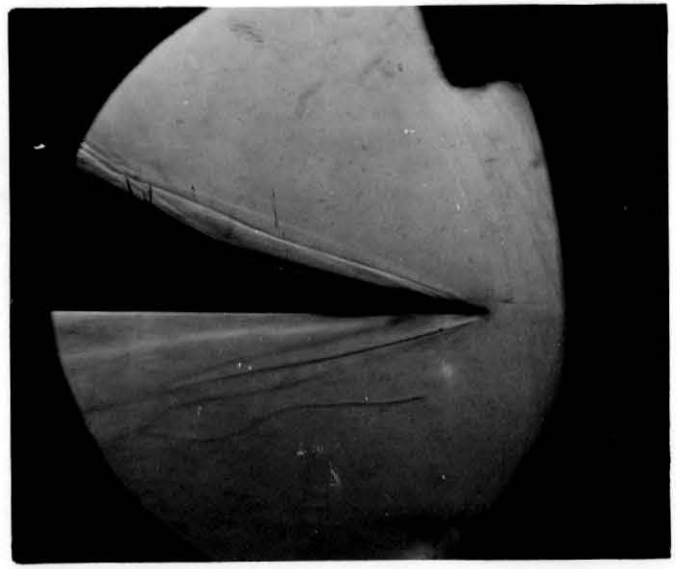

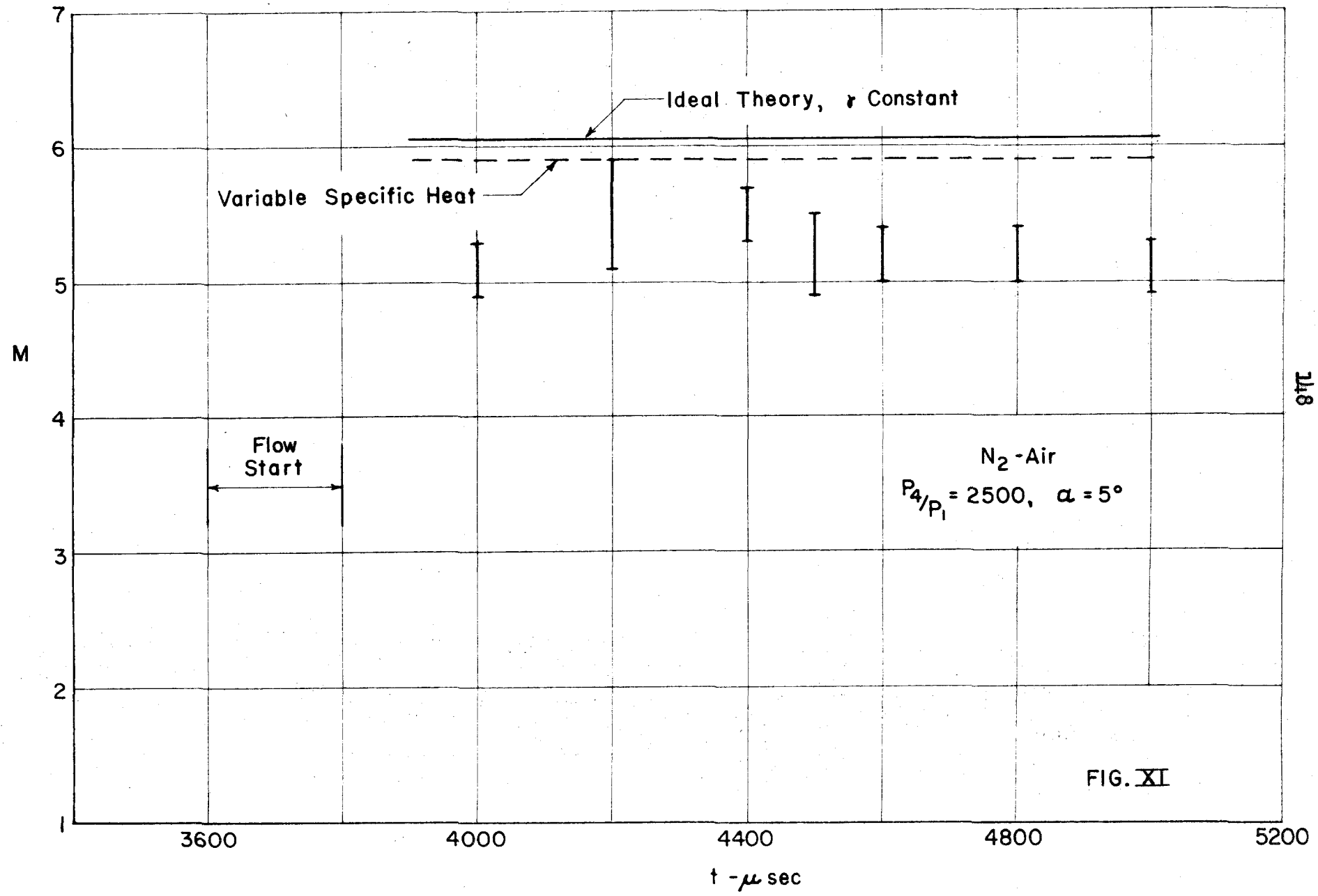
Ideal Theory, γ Constant
Variable Specific Heat
Flow Start
N2 - Air
P4/P1 = 2500, α = 5°
M
t - μ sec
7
6
5
4
3
2
1
3600
4000
4400
4800
5200

FIG. XI

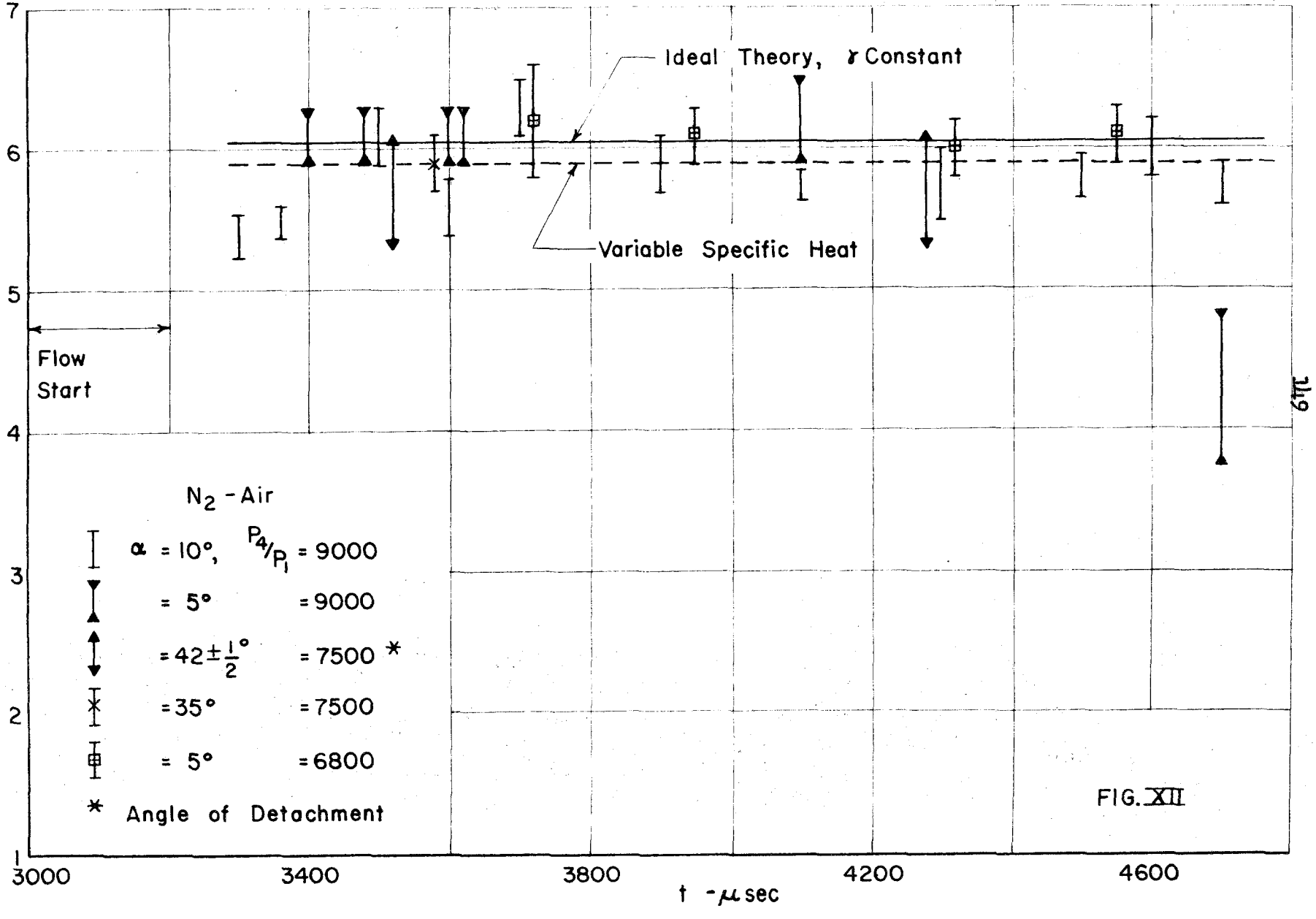
Ideal Theory, γ Constant
Variable Specific Heat
Flow Start
N2 - Air
α = 10°, P4/P1 = 9000
= 5° = 9000
= 42 ± 1/2° = 7500 *
= 35° = 7500
= 5° = 6800
* Angle of Detachment
FIG. XII
7
6
5
4
3
2
1
3000
3400
3800
4200
4600
t - μ sec
ρ/ρ1

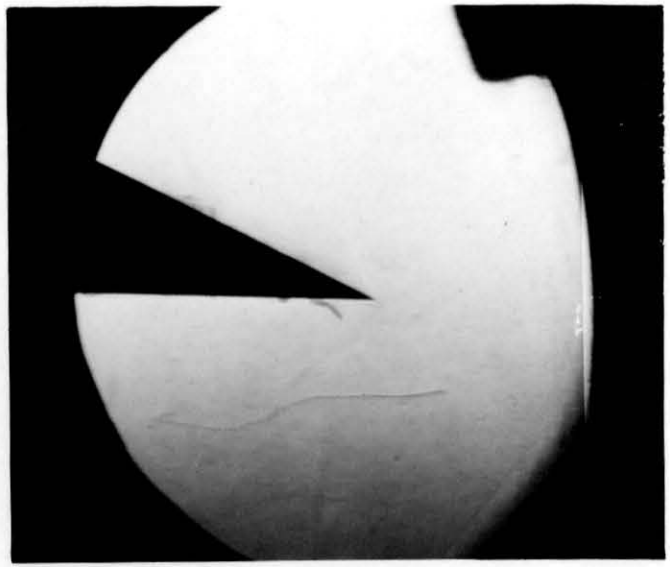

(a)
1500

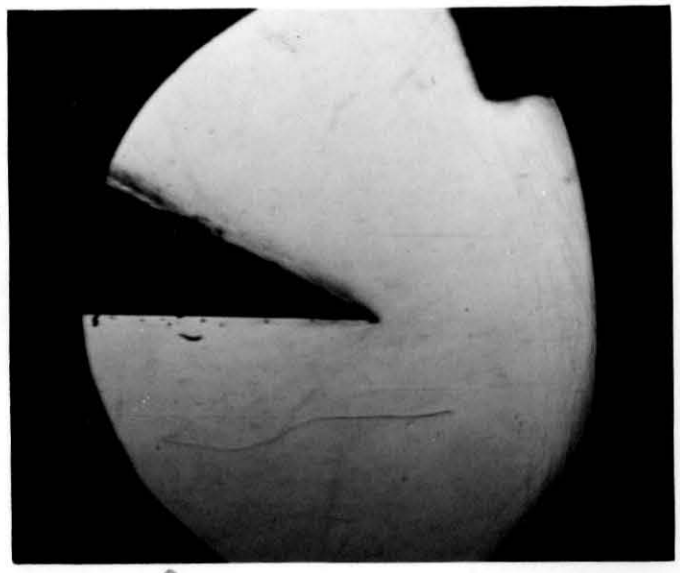

(b)
1600

PLATE 14 - ESTABLISHMENT OF FLOW AT THE TEST SECTION AROUND A 25° WEDGE, He - AIR, $p_4/p_1 = 9500$
FIGURES INDICATE DELAY TIME IN MICROSECONDS

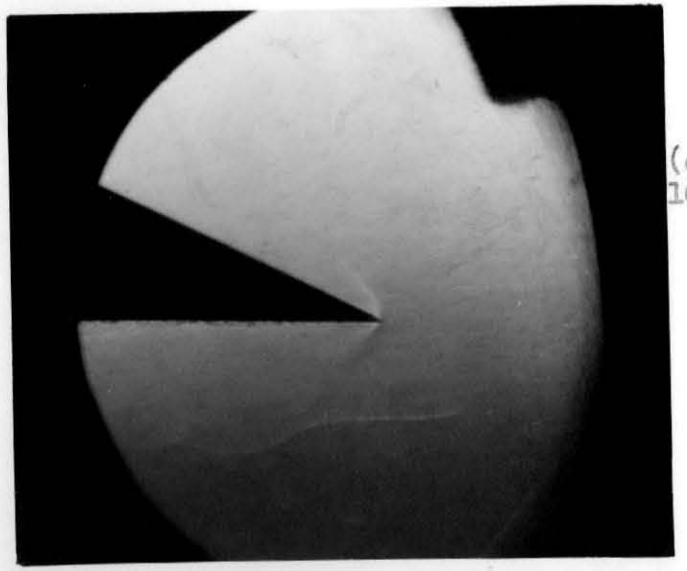

(c)
1650

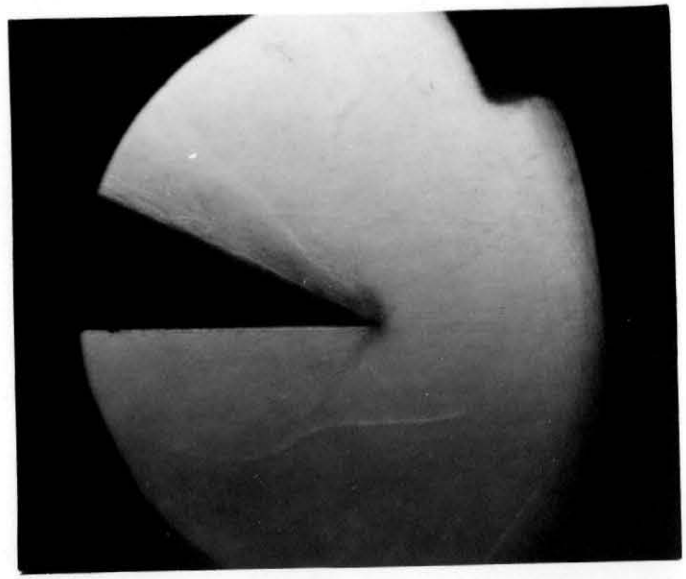

(d)
1700

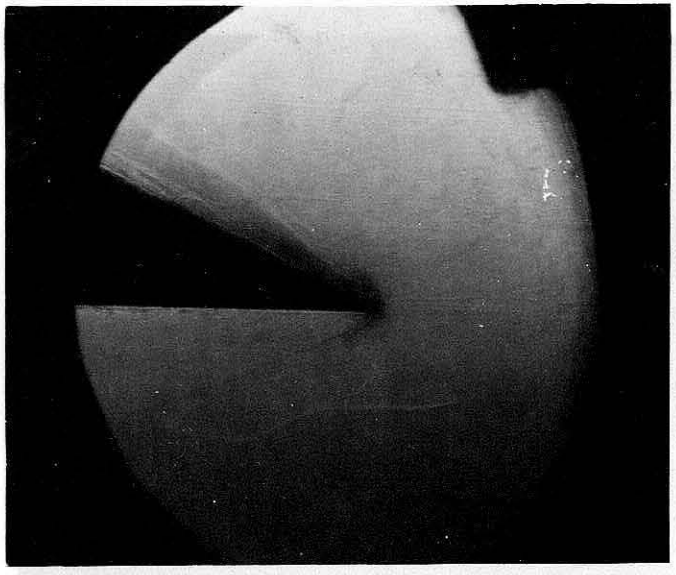

(a)
1900

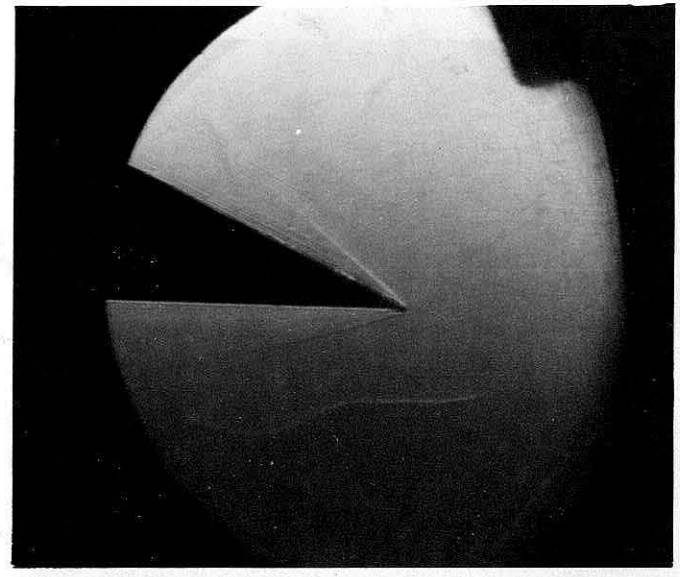

(b)
2000

PLATE 15 - FLOW IN PLATE 14 CONTINUED

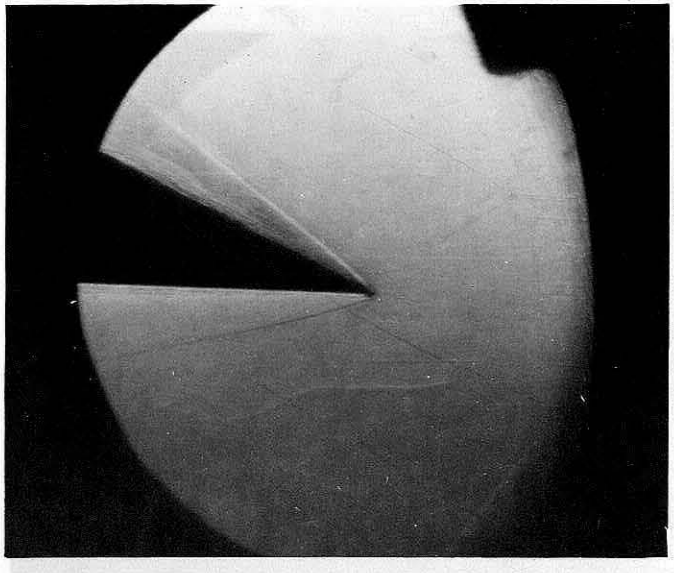

(c)
2100

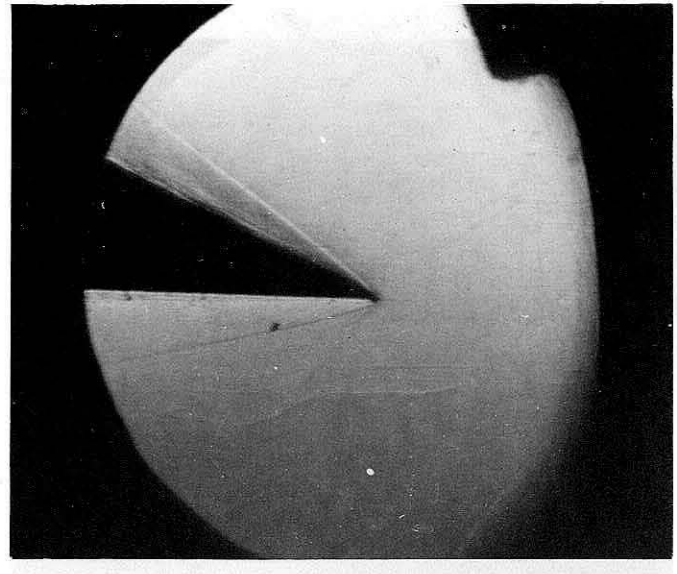

(d)
2200

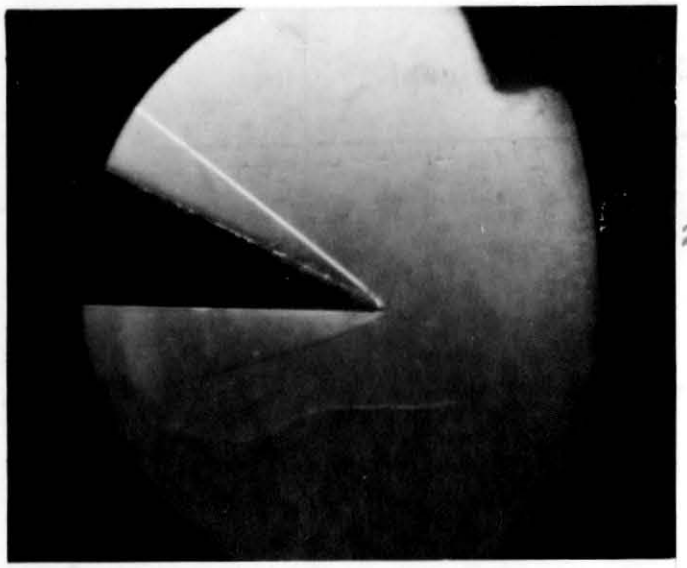

(a)
2400

(b)
2500

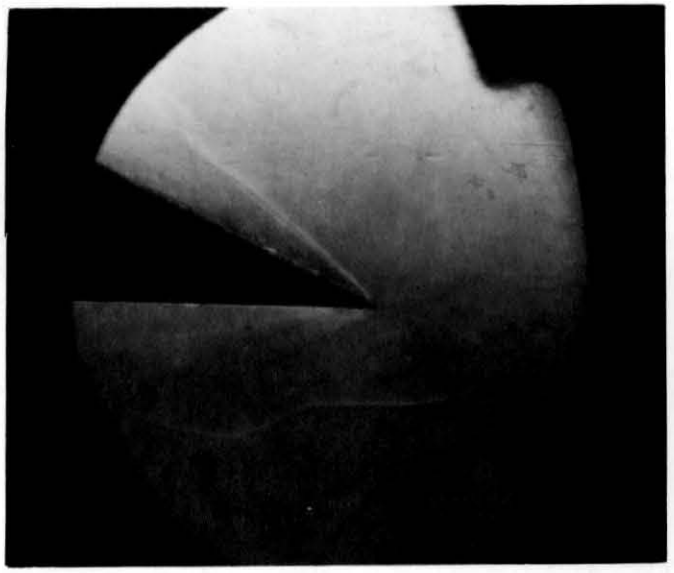

PLATE 16 - FLOW IN PLATE 15 CONTINUED

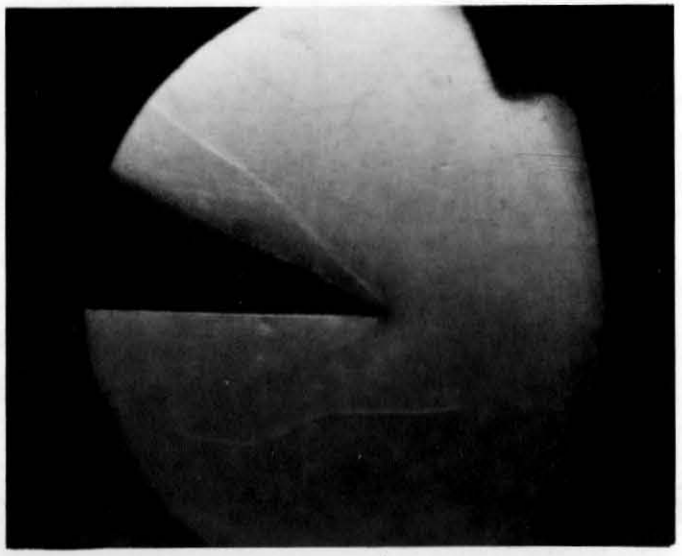

(c)
2600

(d)
2800

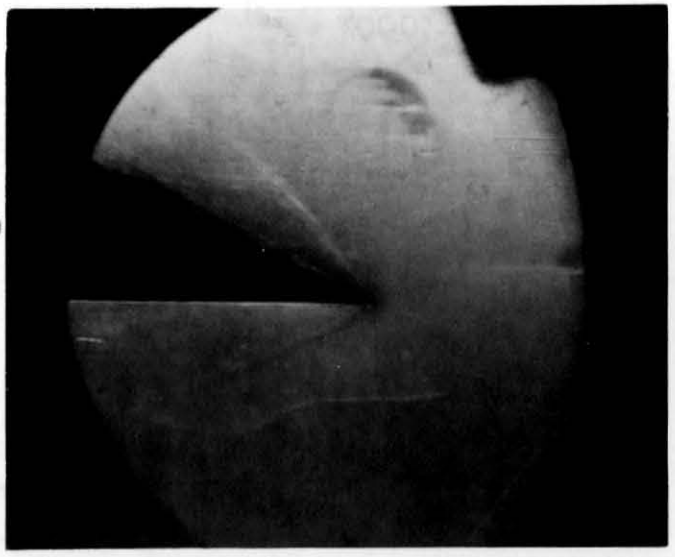

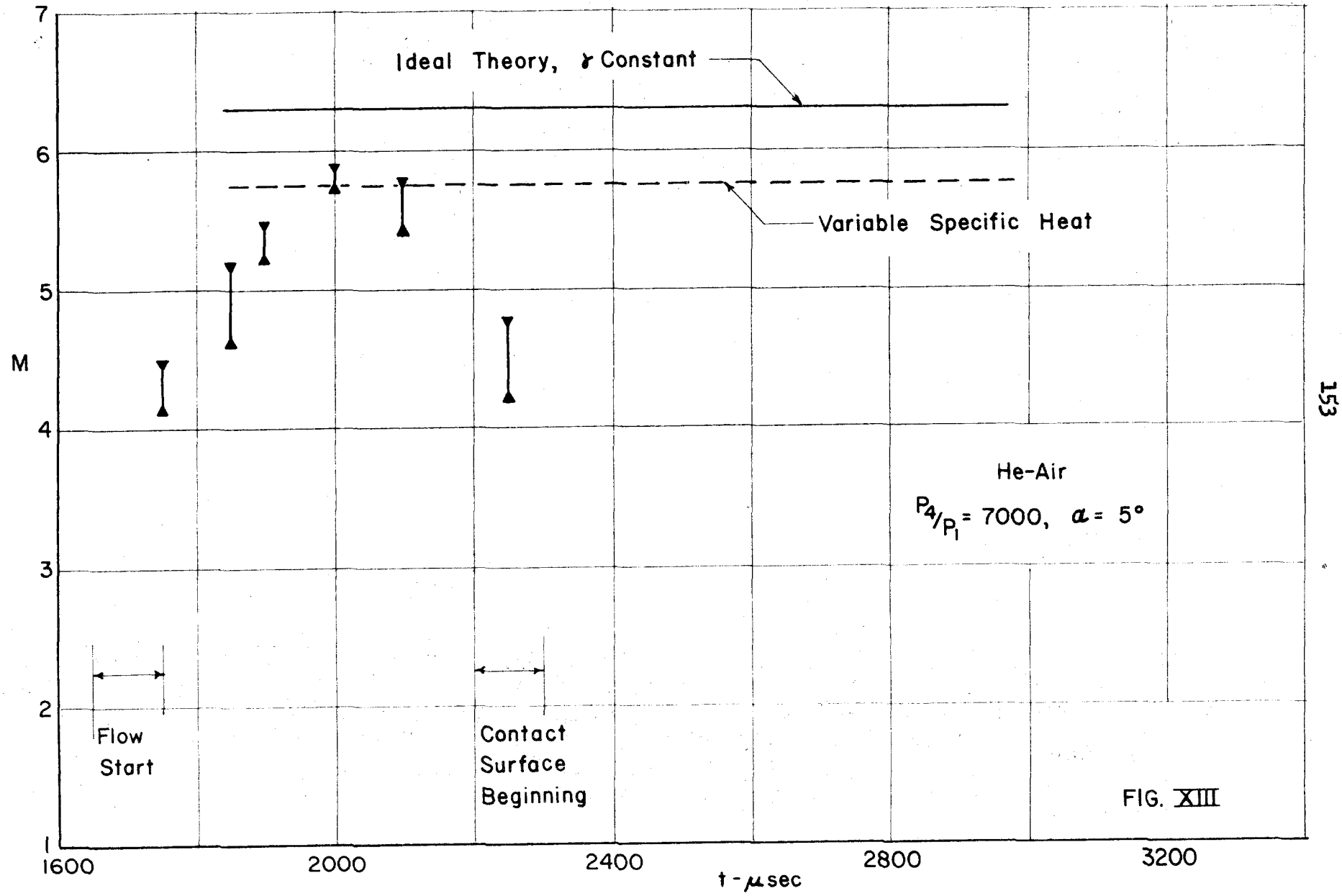
Ideal Theory, γ Constant
Variable Specific Heat
He-Air
P4/P1 = 7000, α = 5°
Flow Start
Contact Surface Beginning
M
t - μsec
1
2
3
4
5
6
7
1600
2000
2400
2800
3200

FIG. XIII

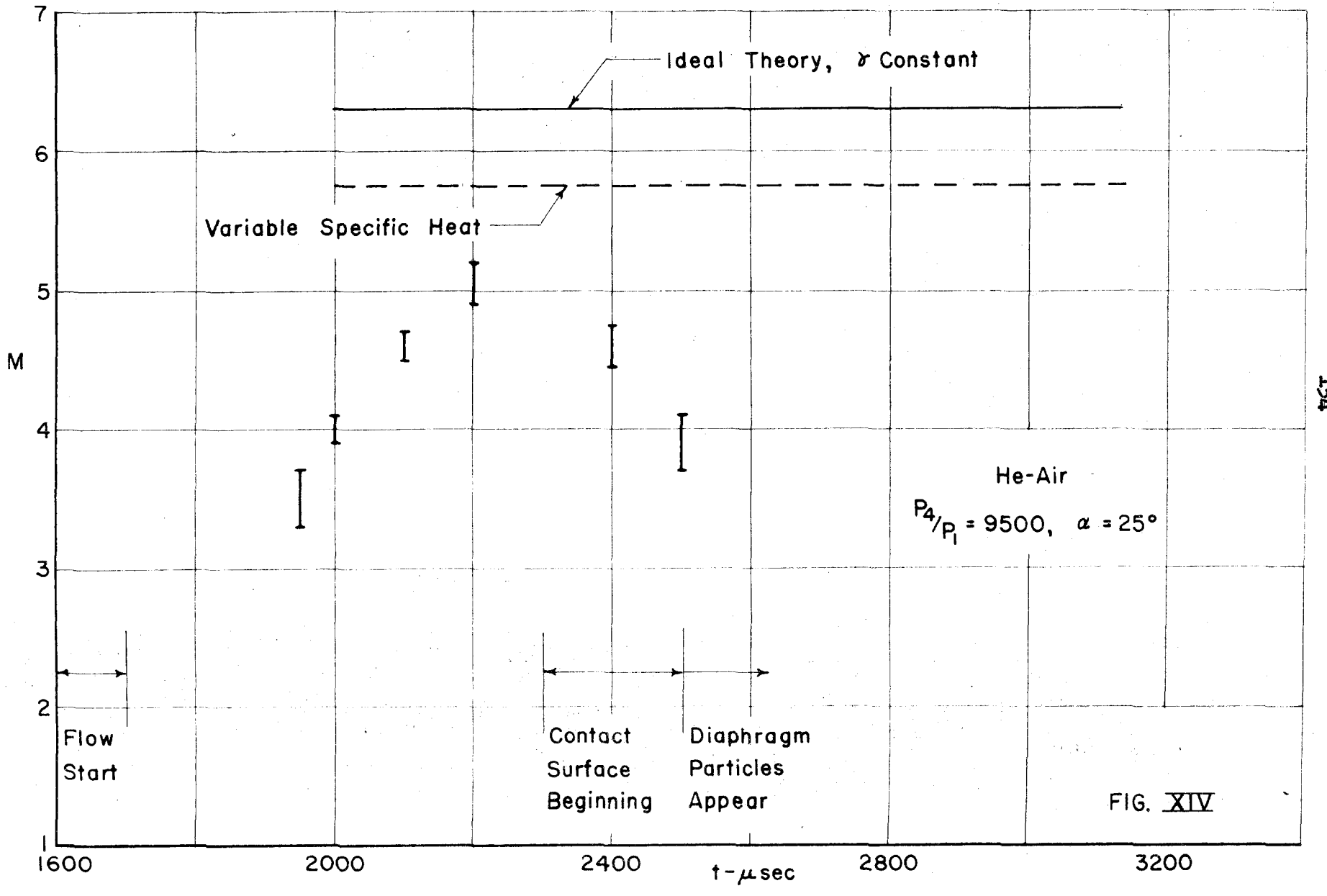
Ideal Theory, γ Constant
Variable Specific Heat
M
7
6
5
4
3
2
1
He-Air
$P_4/P_1 = 9500$, $\alpha = 25°$
Flow Start
Contact Surface Beginning
Diaphragm Particles Appear
1600
2000
2400
2800
3200
t-μsec

FIG. XIV

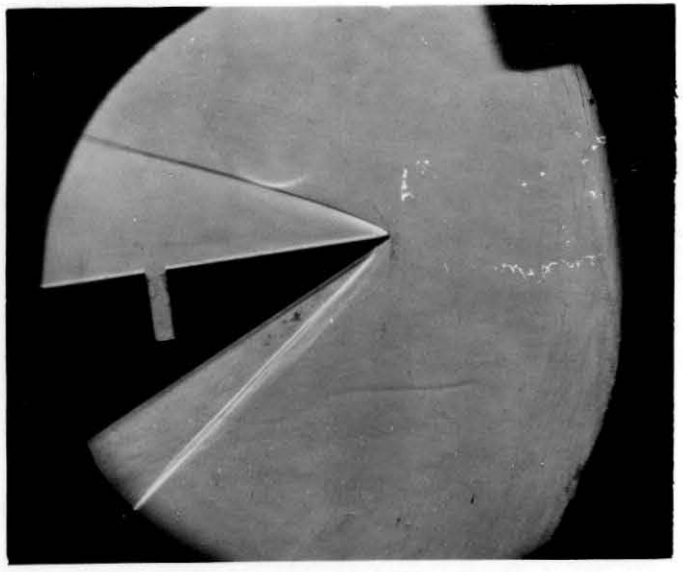

(a)
3600

(b)
2900

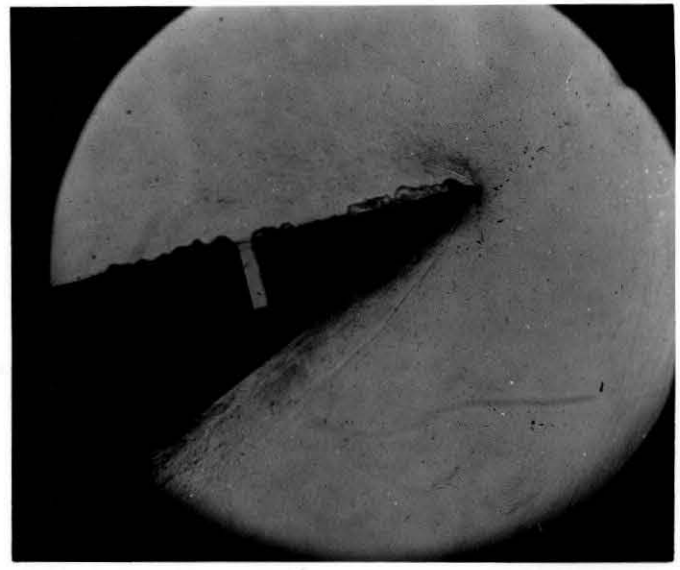

PLATE 17 - a: FLOW OVER A 35° WEDGE, N_2 - AIR AT p_4/p_1 = 7500
b,c,d: FLOW OVER A 41 1/2° WEDGE, N_2 - AIR AT p_4/p_1 = 7500

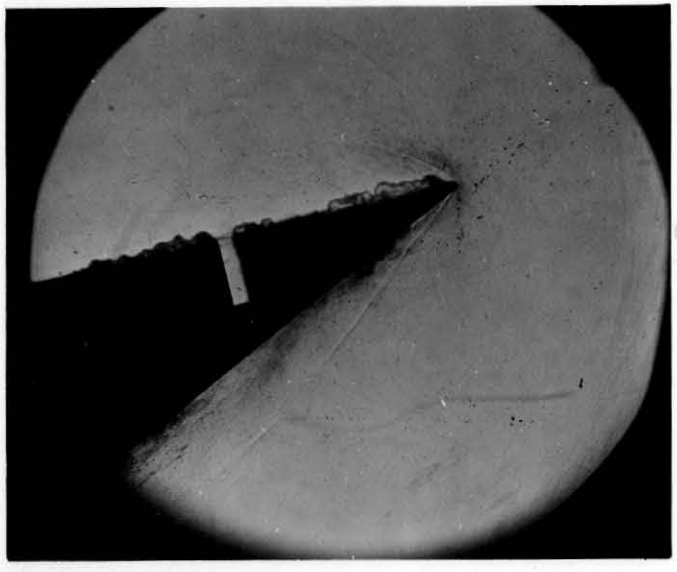

(c)
3200

(d)
3900

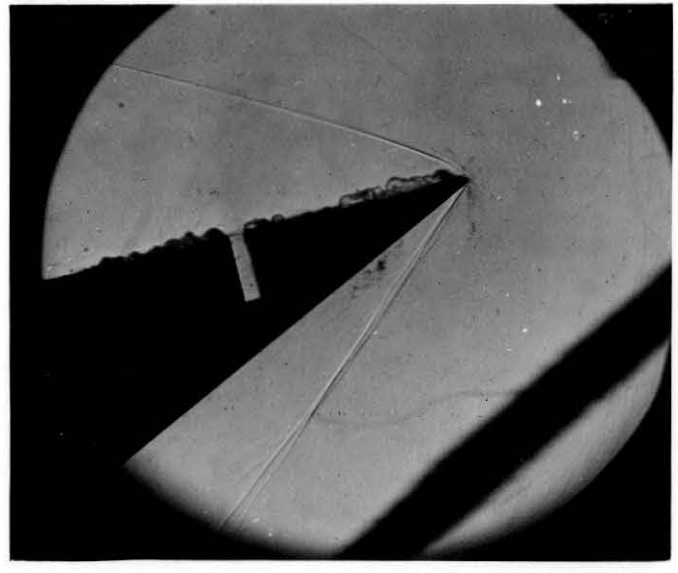

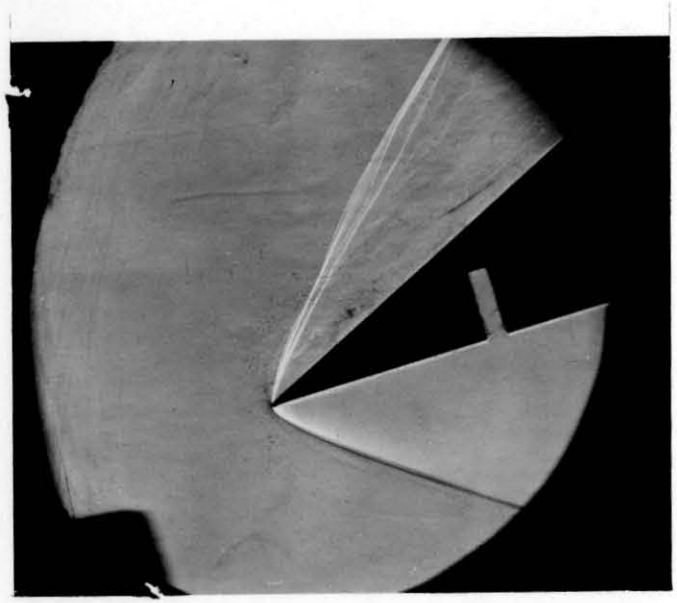

a) 3500

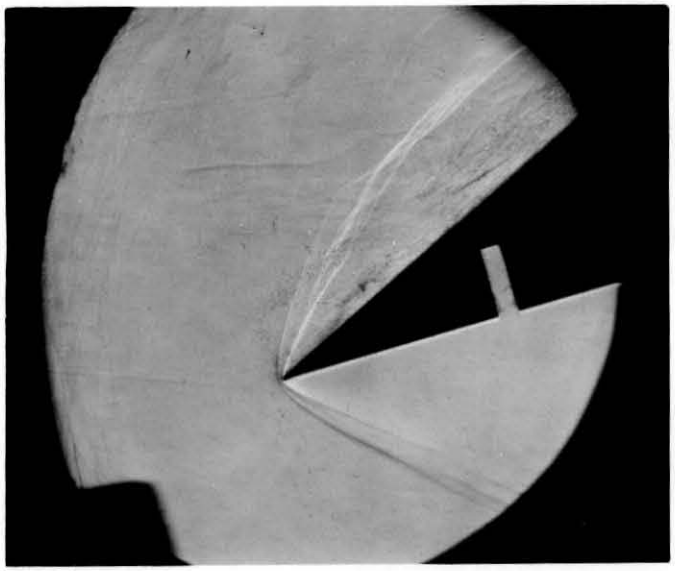

b) 4300

PLATE 18 - FLOW OVER A 42 1/2° WEDGE, N_2 - AIR AT $p_4/p_1 = 7500$

FIGURES INDICATE DELAY TIME

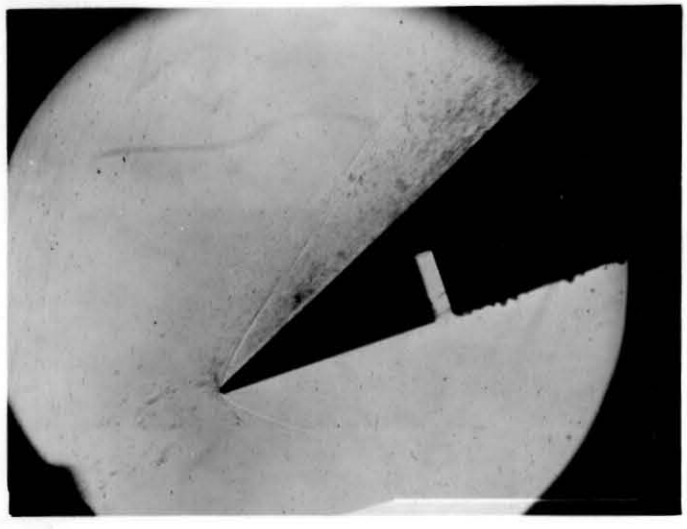

(a)
2900

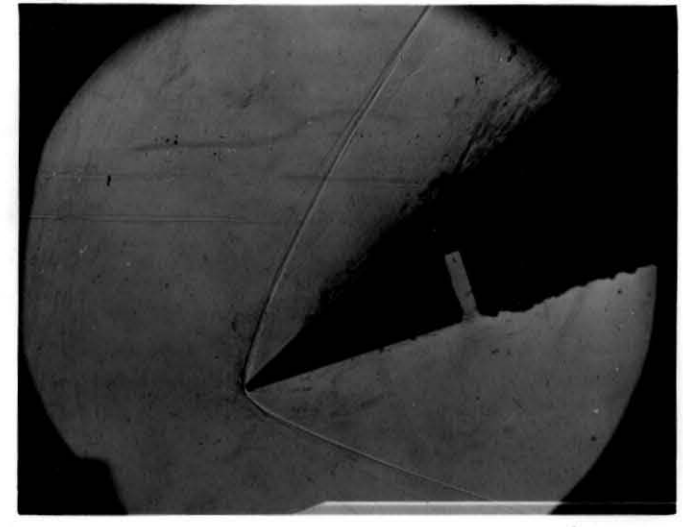

(b)
3900

PLATE 19 - FLOW OVER A 44° WEDGE, N_2 - AIR AT $p_4/p_1 = 7500$
FIGURES INDICATE DELAY TIME IN MICROSECONDS

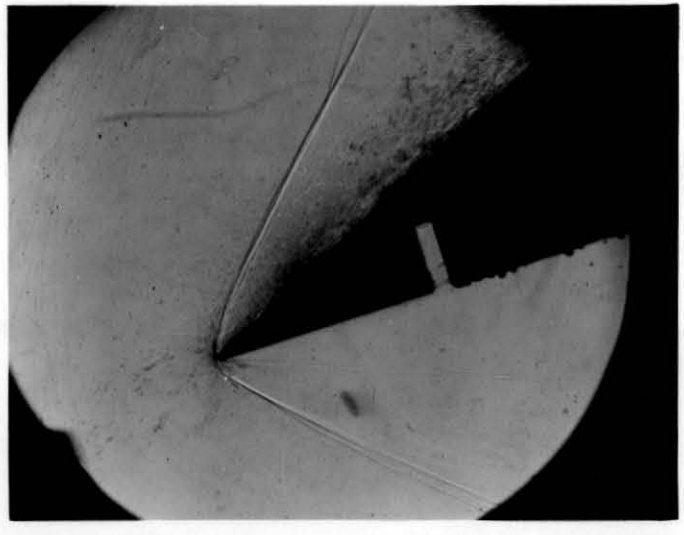

(c)
4400

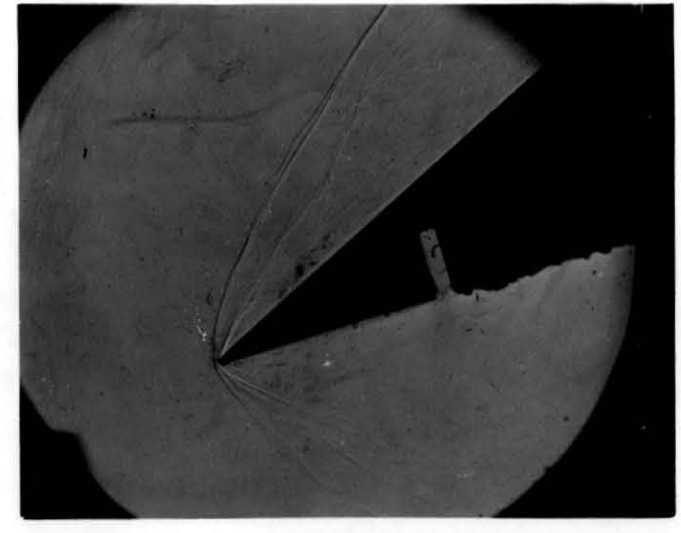

(d)
5000

a) 450 b) 700 c) 850 d) 1000 e) 1300

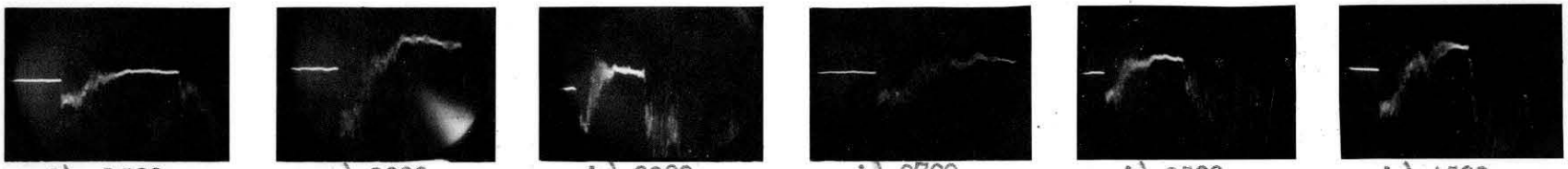

f) 1500 g) 2000 h) 2300 i) 2700 j) 3500 k) 4500

l) 6100 m) 7000 n) 8000 o) 8700 p) 9500

PLATE 20 - STATIC PRESSURE TRACES AT THE TEST SECTION WITH N_2 - AIR
FIGURES INDICATE p_4/p_1

a) $p_4/p_1 = 2600$

b) $p_4/p_1 = 3500$

c) $p_4/p_1 = 5700$

d) $p_4/p_1 = 10250$

PLATE 21 - STATIC PRESSURE TRACES AT THE TEST SECTION WITH He - AIR

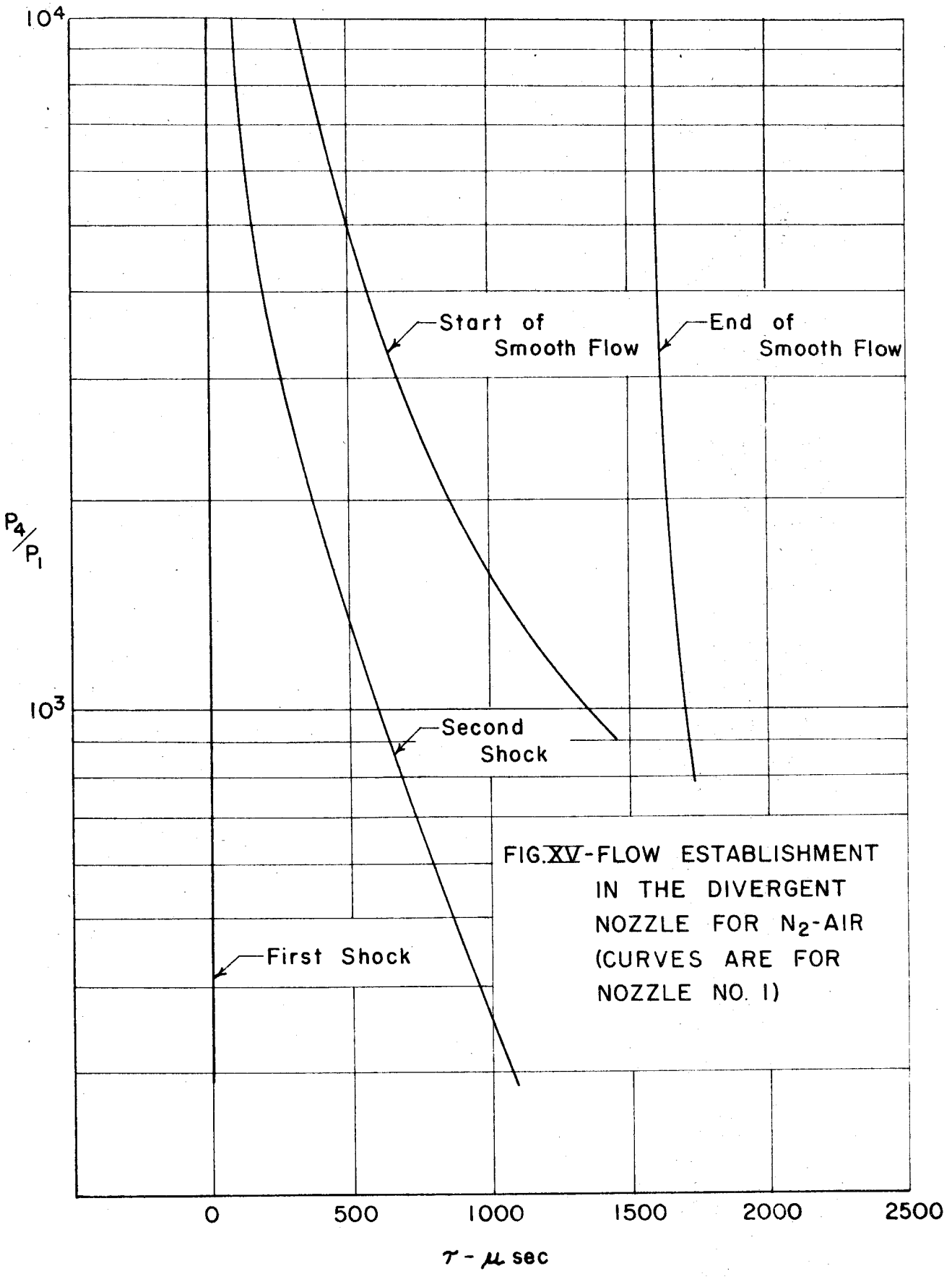

FIG. XV - FLOW ESTABLISHMENT IN THE DIVERGENT NOZZLE FOR N_2-AIR (CURVES ARE FOR NOZZLE NO. 1)

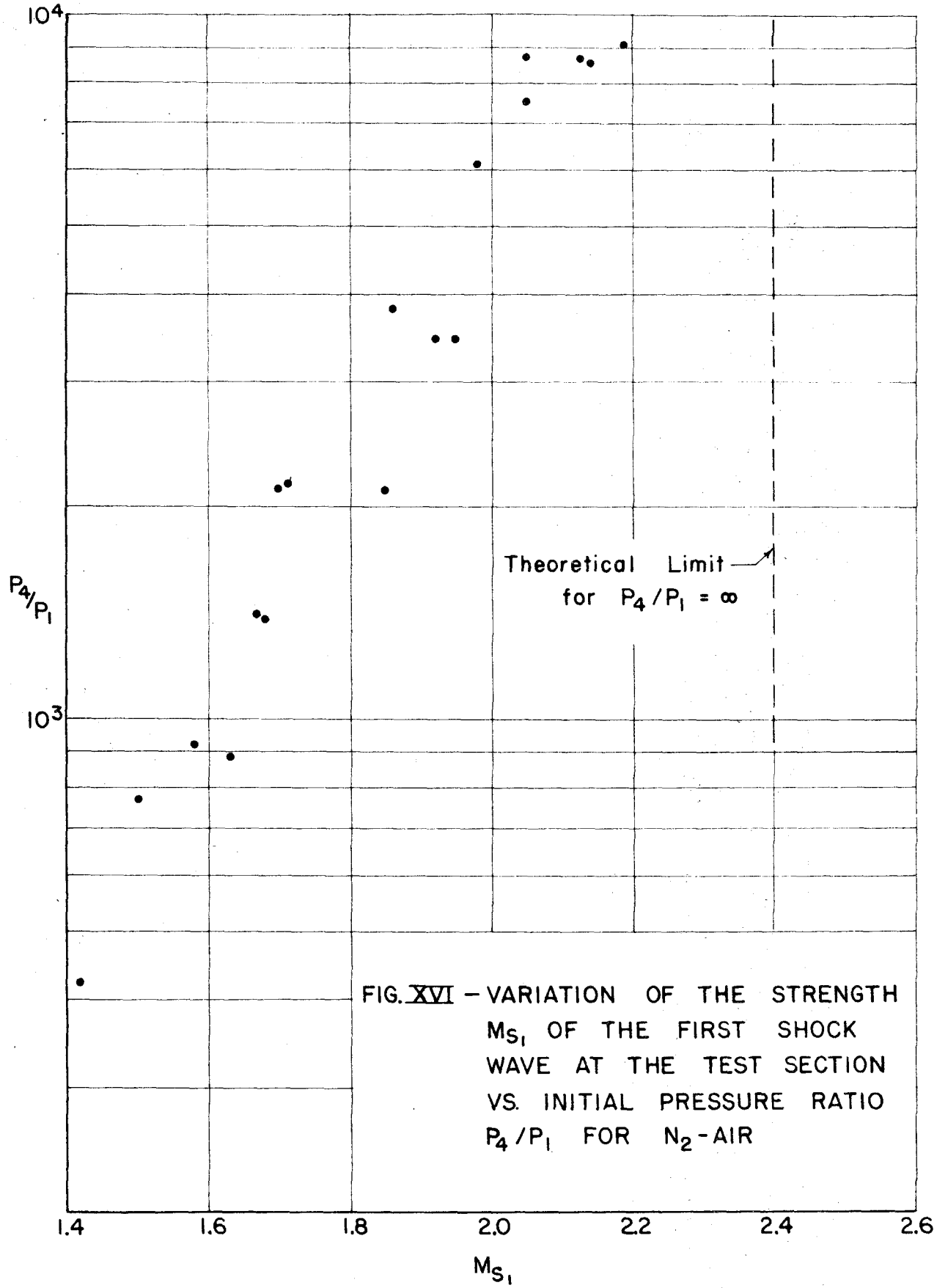

FIG. XVI – VARIATION OF THE STRENGTH M_{S_1} OF THE FIRST SHOCK WAVE AT THE TEST SECTION VS. INITIAL PRESSURE RATIO P_4/P_1 FOR N_2-AIR

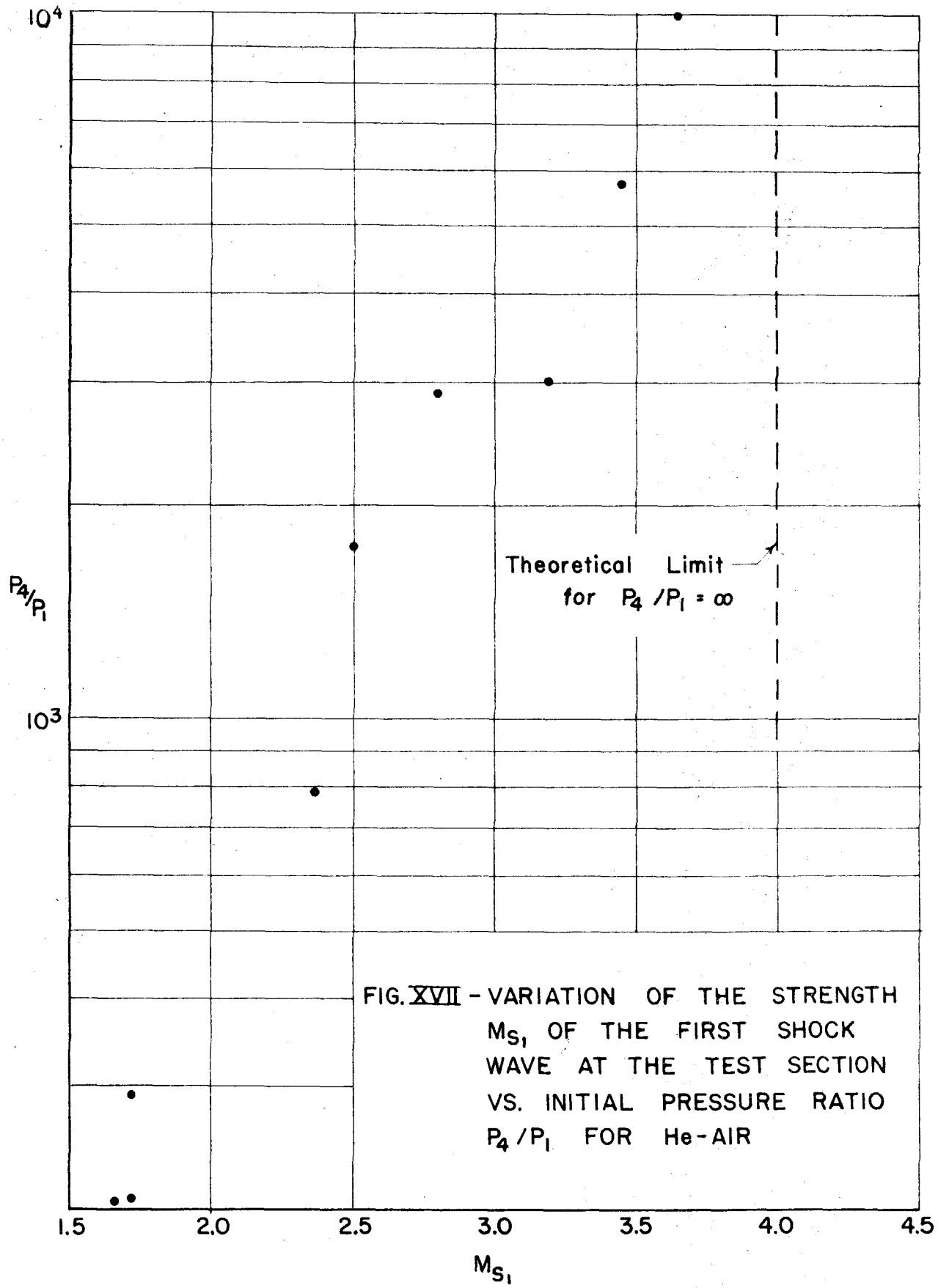

FIG. XVII - VARIATION OF THE STRENGTH M_{S_1} OF THE FIRST SHOCK WAVE AT THE TEST SECTION VS. INITIAL PRESSURE RATIO P_4/P_1 FOR He-AIR

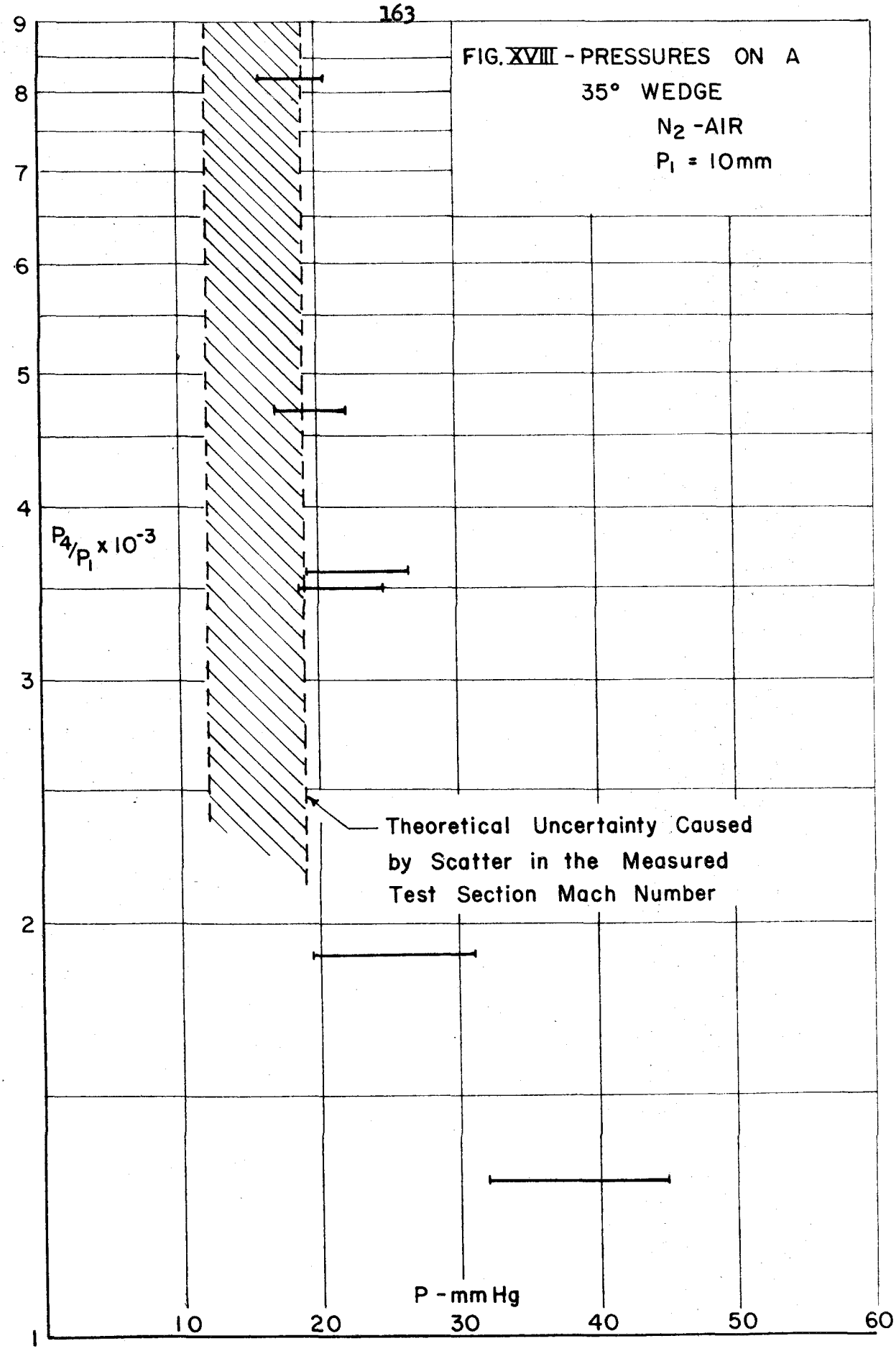
FIG. XVIII - PRESSURES ON A 35° WEDGE
N_2 - AIR
P_1 = 10mm
$P_4/P_1 \times 10^{-3}$
Theoretical Uncertainty Caused by Scatter in the Measured Test Section Mach Number
P - mm Hg
9
8
7
6
5
4
3
2
1
10
20
30
40
50
60

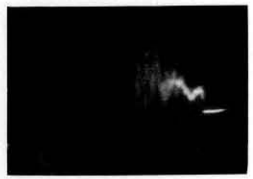

a) $p_4/p_1 = 1300$

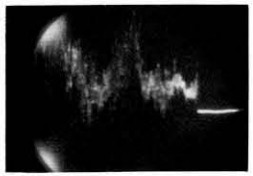

b) $p_4/p_1 = 1900$

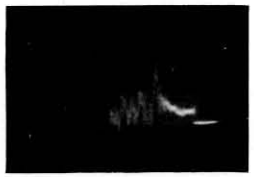

c) $p_4/p_1 = 3500$

d) $p_4/p_1 = 3600$

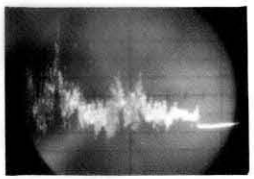

e) $p_4/p_1 = 4700$

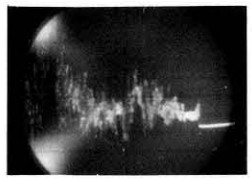

f) $p_4/p_1 = 8150$

PLATE 22 - PRESSURE TRACES ON A 35° WEDGE AT THE TEST SECTION, N_2 - AIR

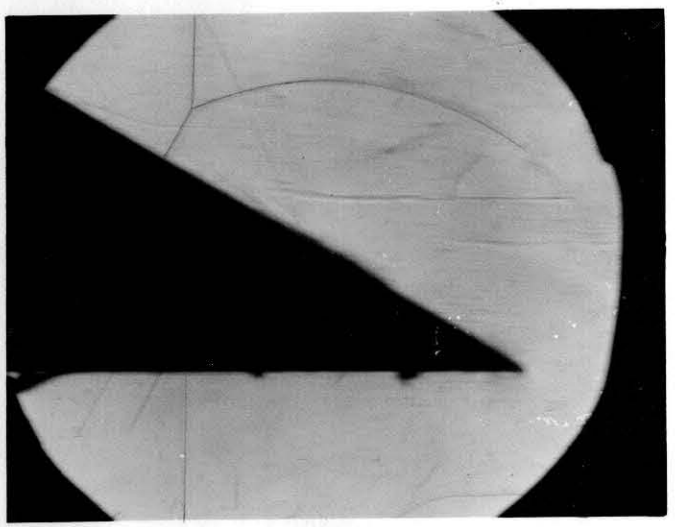

(a)
1500

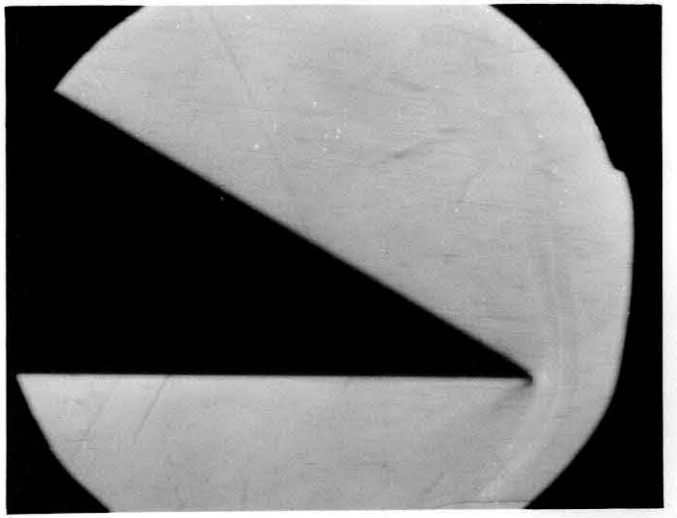

(b)
1700

PLATE 23 - FLOW ESTABLISHMENT AT THE TEST SECTION WITH NOZZLE NO. 3, He - AIR, $p_4/p_1 = 5000$

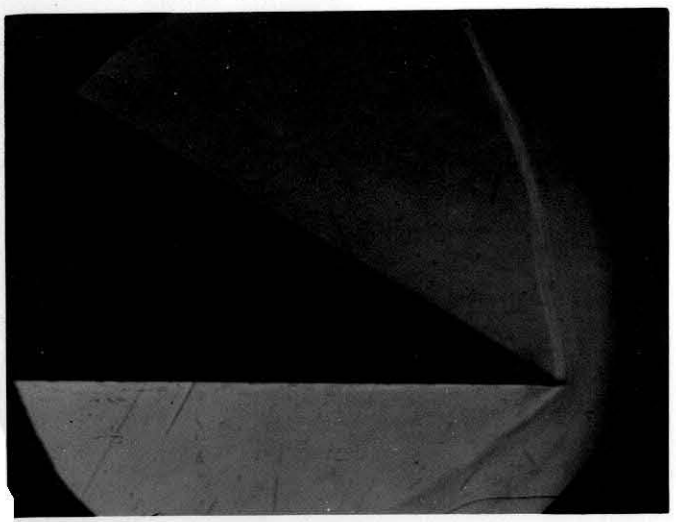

(c)
1800

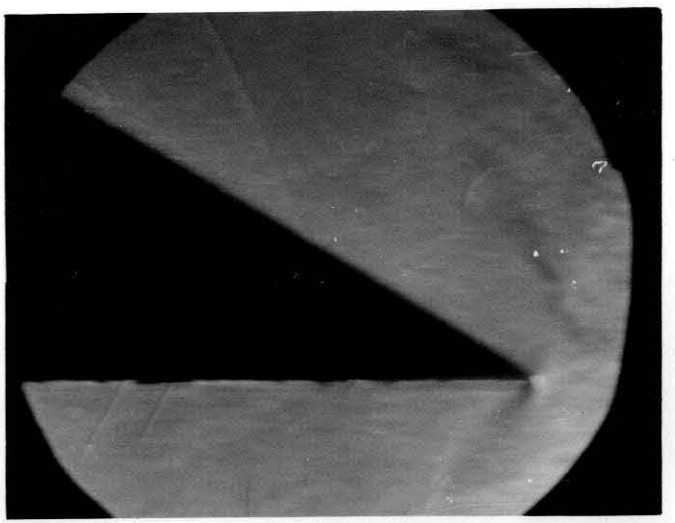

(d)
2000

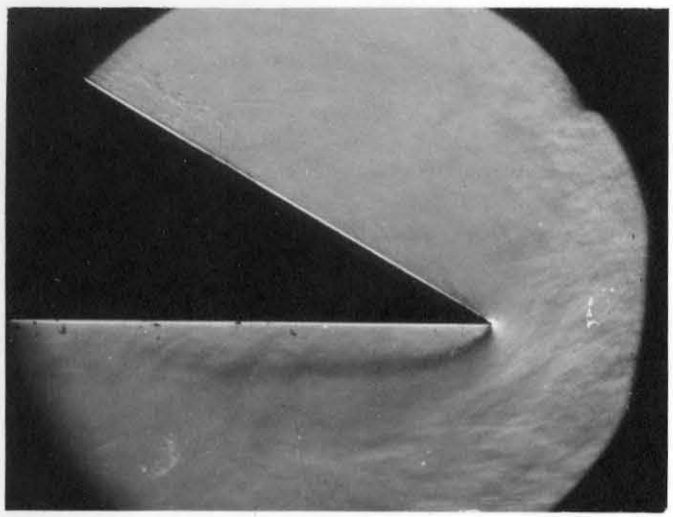

(a)
2200

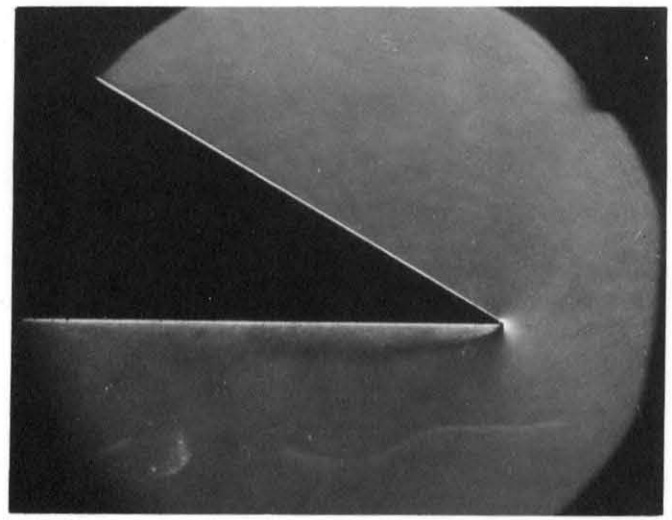

(b)
2400

PLATE 24 - FLOW IN PLATE 23 CONTINUED

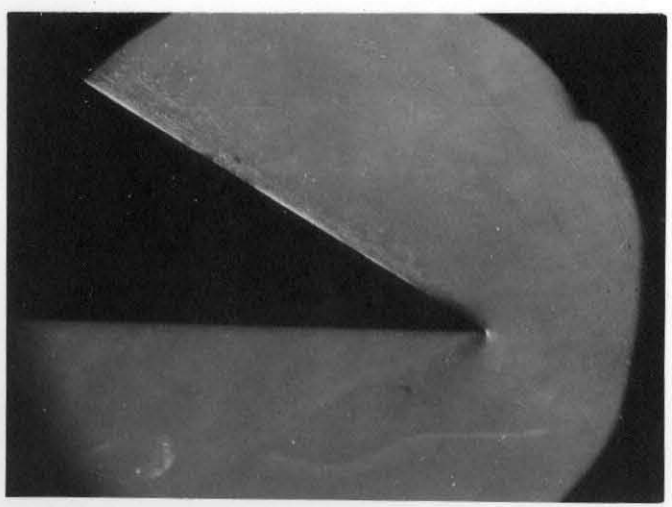

(c)
2600

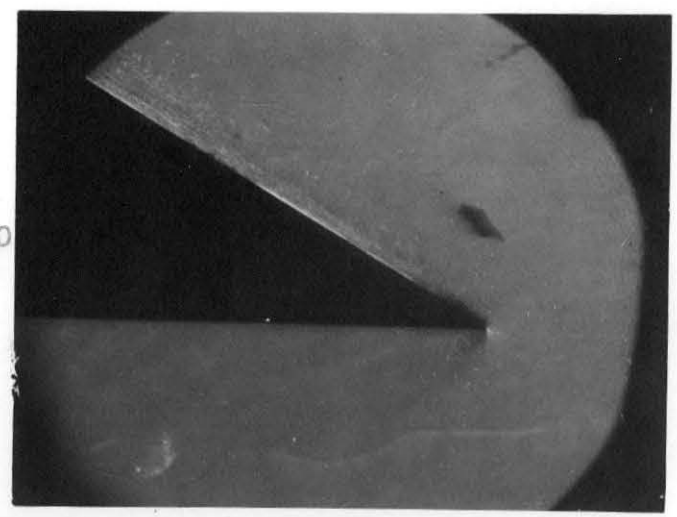

(d)
2800

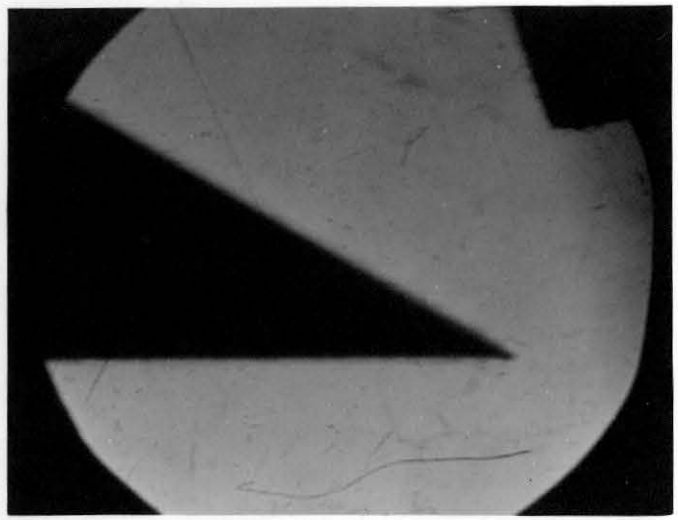

(a)
3400

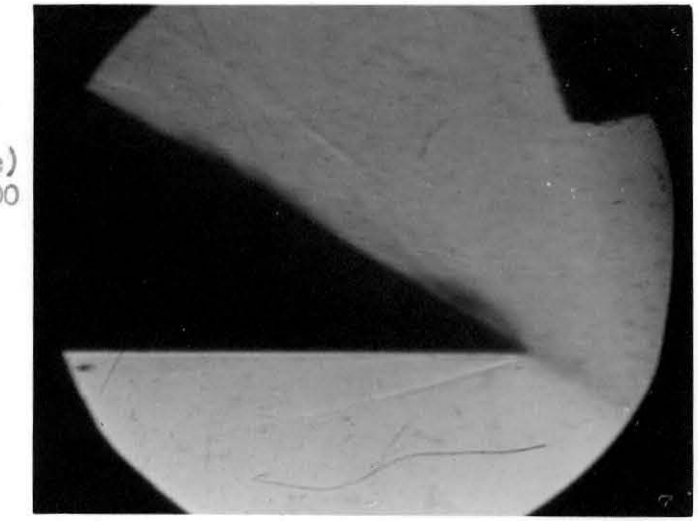

(c)
3800

PLATE 25 - ESTABLISHMENT OF FLOW AT THE TEST SECTION WITH NOZZLE NO. 3, N_2 - AIR, $p_4/p_1 = 3000$

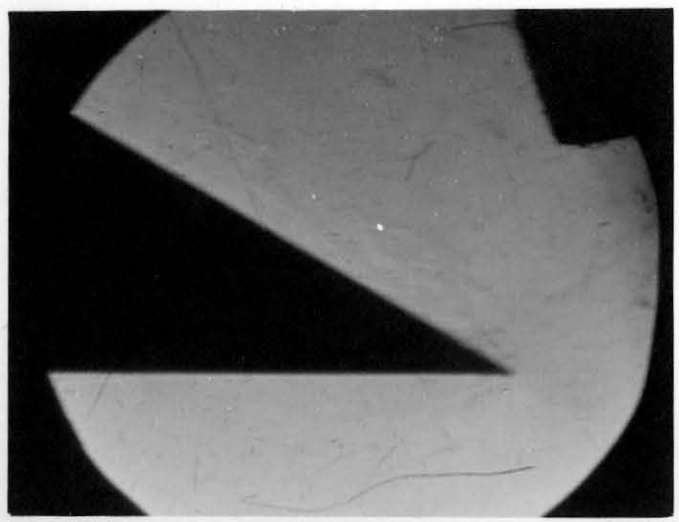

(b)
3600

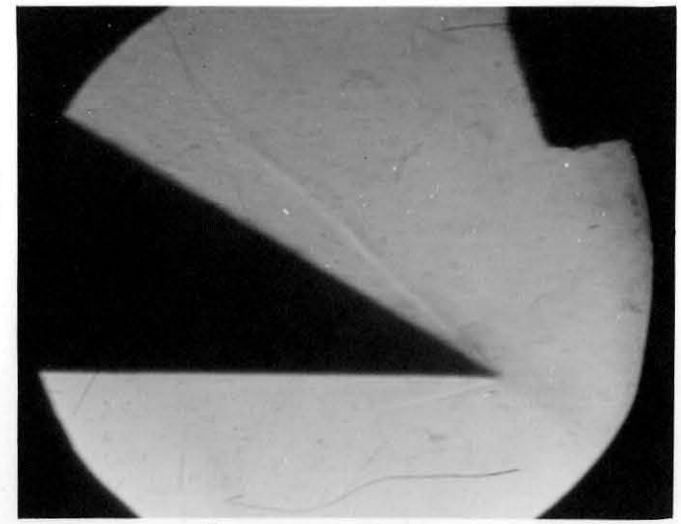

(d)
4000

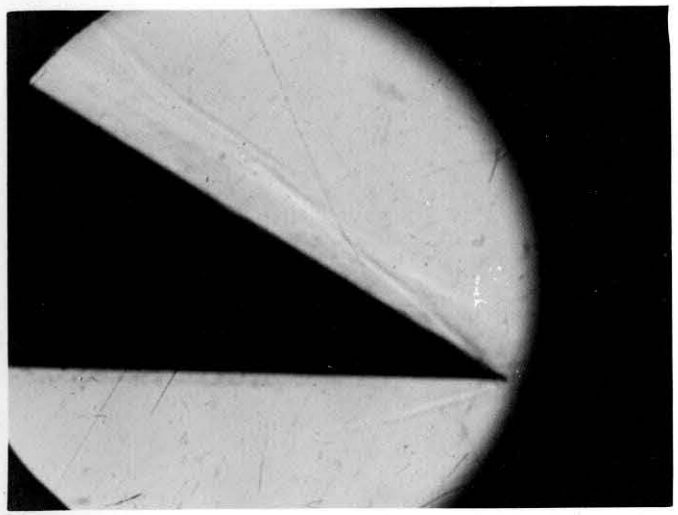

(a)
4200

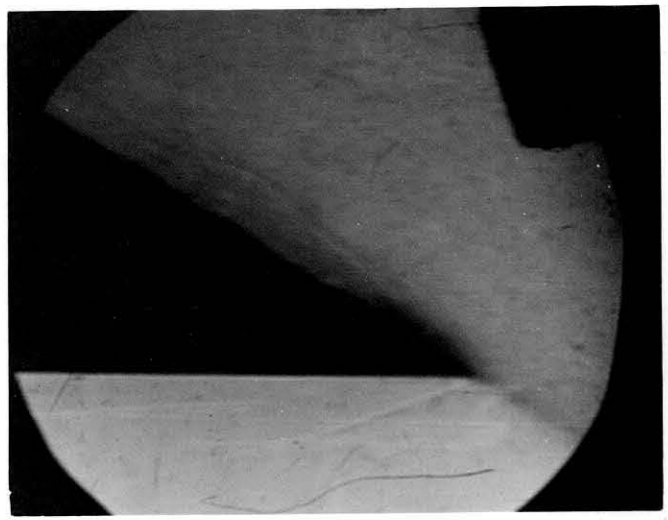

(b)
4400

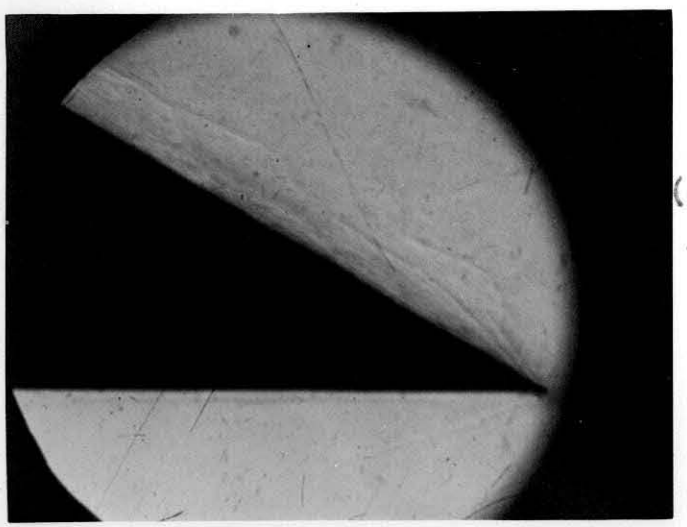

(c)
4500

PLATE 26 - FLOW IN PLATE 25 (CONTINUED)